DEVELOPMENT OF MICROWAVE NDT INSPECTION TECHNIQUES FOR LARGE SOLID PROPELLANT ROCKET MOTORS

CONTRACT NAS 7-544

FINAL REPORT 1117_____15 JUNE 1969

AEROJET
GENERAL TIRE
GENERAL

FINAL REPORT

DEVELOPMENT OF MICROWAVE NDT INSPECTION TECHNIQUES FOR LARGE SOLID PROPELLANT ROCKET MOTORS

FINAL REPORT 1117
CONTRACT NAS 7-544
15 JUNE 1969

M. W. STANDART
PROGRAM MANAGER

A. D. LUCIAN
CONSULTANT

T. E. ECKERT, B. L. LAMB
PRINCIPAL INVESTIGATORS

LIQUID ROCKET DIVISION
AEROJET-GENERAL CORPORATION
SACRAMENTO, CALIFORNIA

ABSTRACT

This is the final technical progress report on work performed under Contract NAS 7-544 for the development of microwave nondestructive testing techniques for large solid-propellant rocket motors. A Frequency Domain Microwave Interferometer has been developed. The device may be described as a near-field radar with high resolution, or as a standing-wave-ratio and reflectometry instrument capable of separating the reflected signal into components according to the location of the reflector along the line, making it, in effect, a time domain reflectometer for waveguide. The microwave technique has been evaluated and successfully demonstrated to detect flaws in full-scale large solid-rocket motor sections, motors, large liquid-rocket, non-metallic nozzle components, and jet-aircraft tires.

Experiments include the effect of target geometry, measurements on defect standards and the inspection of full-scale hardware in the range of 12.4 to 40 GHz. Other applications such as material properties determination and microwave component testing are considered.

All work under the scope of Contract NAS 7-544 has been completed successfully. The microwave frequency-domain interferometer has been developed into an established nondestructive test instrument.

This interferometer is an outgrowth of work done under NAS 7-367, and during the course of the two successive phases of NAS 7-544 there have been separate but parallel efforts to actually apply the instrument to inspection. Since the outcome of these efforts is of importance in evaluating the success of the present project, it has become customary to include accounts of their progress in the 7-544 reports in addition to the progress of tasks identified in the original proposal. This final report includes an account of related application efforts with particular emphasis upon the Titan Ablative Nozzle Skirt inspection fixture.

TABLE OF CONTENTS

APPENDIXES

FIGURE LIST

FIGURE LIST (Cont.)

NAS 7-544 Final Report 1117

DEVELOPMENT OF MICROWAVE NDT INSPECTION TECHNIQUES FOR LARGE SOLID-PROPELLANT ROCKET MOTORS

I. INTRODUCTION

This report describes the accomplishments completed under Contract NAS 7-544. NAS 7-544 is the continuation of the work performed under Contract NAS 7-367[1]. The objective of the program is the development and evaluation of a microwave testing technique capable of detecting and discriminating the location of defects in a propellant grain and propellant bond system. Observations and measurements pertinent to this objective have been documented and, as a result of the observations, the scope of the investigation was broadened and generalized to cover the expanding class of high-performance, high-reliability articles made principally of non-metals. Such items are becoming more common in aerospace industries, and are exceedingly difficult to inspect by ordinary methods. The instrument used for the feasibility demonstration under NAS 7-367 has been elaborated and refined to produce several interesting variants and a number of promising designs. The versions actually constructed have been extensively evaluated both on the test bench and in the inspection of full-scale POLARIS motor sections, POLARIS fleet-motors, TITAN-family ablative nozzle skirts and large jet-aircraft tires.

The complete description of the instrument's ultimate capability and behavior is beyond the scope of this Contract. Improvements in performance are highly anticipated in very promising applications to the inspection of non-metallics. Nevertheless, the objective of the instrument-evaluation phase of the project and the development of an inspection device, placed into production utilization have been accomplished successfully. Even though the instruments do not yet represent the best that can be done with present technology, the latest versions are applicable to the inspection of a wide variety of aerospace components. In fact, a concealed unbond-type flaw was located by microwave inspection in a TITAN ablative nozzle skirt, and this flaw was verified by X-ray inspection. Further, flaw propagation was recorded by alternate dynamic testing and microwave inspections. Excellent correlation was established among microwave,

[1] Development of Microwave NDT Inspection Techniques for Large Solid Propellant Rocket Motors, NAS 7-367, Final Report 0948, Phase I, Cribbs, Lamb, Lucian dated 6 May 1966.

X-ray and visual inspections conducted during this TITAN III MOL advanced-design ablative skirt development program.

Special tooling was fabricated and the microwave instruments were adapted to the nozzle socket sections of POLARIS A3P first-stage motors. This system was tested on a full-scale aft section having built-in defects. Both a 1-mil metal shim and a 3-mil mylar shim introduced between the insulation and propellant were detected by microwave inspection but could not be detected by a betatron inspection. The geometry of this four-nozzle aft section precluded the betatron detection of the 3-mil mylar shim. In an attempt to determine the minimum separation that can be detected between insulation and propellant, the detection of an unbonded region produced by a thin wax layer in the nozzle socket section was questionable by microwave inspection.

The Titan ablative skirts are now being inspected with a microwave frequency domain interferometer. This device is part of an automatic microwave/acoustic impact system. The design for the microwave system is an improved version of the one contained in the final report of NAS 7-367. The system is installed at Aerojet Sacramento and is inspecting all Titan III B/C/D ablative skirts. Results have been most satisfactory to date and interior defects have been located in the ablative liner, and at the inside of the liner where it joins the honeycomb shell. Overall, the inspection seems superior to any of the conventional methods. Shakedown problems were considered to be very minor since the system was designed, fabricated, installed and placed in production operation in a period of about 3 months. The overall performance of this instrument has been well up to expectations. The adaptability of the instrument to other representative inspection problems is still in progress and further successful applications are expected.

At this stage, then it may be said with confidence that:

1. Microwave inspections can achieve sufficient sensitivity to detect flaws in solid propulsion systems and other aerospace components. As this report is prepared for final publication, a microwave system for in-process propellant inspection is completing bench tests and is about to be installed on an inspection fixture. Another system will be built for inspection of cured propellant

samples. These instruments are being built to designs developed under Contract NAS 7-544. This work is being done under Contract NAS 3-12036 (NASA-LeRC) whose purpose is to perfect Non-destructive Test techniques for eventual use in inspecting a 260-in. solid propellant rocket motor.

2. The problems of actually conducting an inspection can be solved, and are no more forbidding than those which attend conventional inspection operations, provided there is some agency to provide the first users with the necessary technical back-up, and to encourage the development and maintenance of adequate standards.
3. Further developments and applications other than nondestructive testing are extremely promising.

II. TASK SUMMARY

The objective of the program was the development and evaluation of a microwave testing technique capable of detecting and discriminating the location of defects in a propellant grain and propellant bond system. This objective has been achieved and, in the execution of this contract, observations and measurements pertinent to this objective and to other applications which might contribute to the advance of general technology have been documented. A summary of the work performed is presented by task.

Task I - Construction of an Improved Signal Processing System (Single-Channel Type)

The single-channel processing system was completed, fully evaluated, and performance is exactly as theory predicted. The improved signal-processing system is a single, self-contained unit. Its suitability for field tests has been demonstrated. Front panel controls have been provided for routine operation. System stability over long periods of time greatly exceeds that of the original signal-processing system developed under NAS 7-367. The improved system is compatible with commercial microwave sweep generators over a wide range of frequencies. However, its design capability can only be realized with the fastest sweep-rate generator that is commercially available from E-H Laboratories. The depth-range scanning speed has been increased from one scan per ten sec to four scans per sec and sensitivity has also been improved. When operated by a trained NDT inspector, resolution of 0.5 mm can be achieved in Ku band. In K-band, engineering-operator resolution is demonstrated to be 0.01 mm for detecting target motion.

Task II - Construction and Evaluation of a Multichannel Signal Processing System

Circuitry for a two-channel signal processing system has been completed successfully. The second channel electronics is quite similar to that developed in Task I. The two channels were tested and proved adequate to evaluate the multichannel concept. A multichannel unit was found to be feasible and useful, and it was found that additional readout equipment is required to make full use of multichannel data. Designs for this equipment, as well as a more

practical method of duplicating channels, have been established.

Task III - Design and Fabrication of a Grain Defect Model

A means of constructing good models has been developed using laminated plastic sheet for separations and a sandbox filled with sand or other powder in which various defects may be simulated. A model constructed with Plexiglas and silica sand proved successful for simulating defects in materials of low refractive index and low loss. To simulate other materials one merely selects a different powder from published microwave properties of materials. Several powders may be mixed for fine control.

The task has been greatly enhanced and expanded by defect models made available from the POLARIS and TITAN programs.

Task IV - Ridge-Waveguide Probe and Circuit Development

Some ridged waveguide was manufactured from Plexiglas to determine if operation over octave microwave bandwidths was feasible. They were not completed because of the difficulty in achieving a suitable copper coating on the Plexiglas. In discussing this problem with microwave engineers at Westcon seminars, it was concluded that operating rectangular waveguide beyond its high frequency limit would provide a more tractable solution to the problem. This solution was originally rejected because of double moding of waveguide for frequencies beyond its band. Most engineers felt that relatively simple precautions would result in the elimination of double moding. Furthermore, theoretical considerations show that dispersion in a rectangular waveguide would allow operation over a greater depth of field. For these reasons work on ridged waveguide was terminated.

Some preliminary experiments were performed by operating K-band signals in Ku-band rectangular waveguide. Because this was outside the scope of the contract and the time required for other tasks, these experiments were not carried to the point that firm conclusions could be drawn.

Task V - Evaluation of Defect Detection Capability

Investigations on the capability of the system to detect defects were conducted. It was noted that for a single spherical void, detection is good when the radius of the sphere is equal to or greater than lambda/2 pi. Laminar defects cause pronounced signals. Reflected signals are detected from areas

whose dimensions approximate 1/2 wavelength. The exact minimum size for various materials has not been precisely determined. In K-band, and using phenolic composite material, an area measuring 1/16 sq in. is readily detectable. In Plexiglas, with a refractive index of 1.6, separations 1-1/2 x 2 in. are detectable down to a thickness of 0.005 in. The resolution improves at higher frequencies and is proportional to wavelength.

Task VI - Development of Readout and Data Interpretation Systems

The development of readout and data interpretation systems was successfully completed. The microwave inspection system developed under this contract is compatible with standard off-the-shelf, commercially-available recorders. An oscilloscope with a memory tube was found to be very satisfactory when the interferometer is depth-range scanning. With the faster electronics, a persistence scope was used. Permanent recording can easily be accomplished with a camera or tape recorder.

For rapid scanning, while gating at a predetermined depth, commercially available X-Y recorders can be used. The selection of a recorder depends upon the speed required for a particular application.

Task VII - Development of Suitable Defect Standards

Standards of known microwave attenuation and cross section have been completed. Typical of these standards is a 7 x 4 x 1-3/8 in. Plexiglas block constructed of Plexiglas sheets with a built-in delamination. The area of the delamination is 3/4 x 3/4 in. and its thickness is 0.030 in. The delamination is located approximately in the center of the block and at one-third the depth. Another is 12 x 12 x 8 in. Plexiglas with 14 2 x 1-1/2 in. separations at a depth of 4 in. The separations vary in thickness from 0.005 to 0.5 in.

Task VIII - Analysis of Results in Preparation of Interim Report

In addition to reporting the information obtained on the previous tasks, a considerable amount of data are presented that is considered appropriate to the advancement of general technology. Work performed on TITAN family ablative skirts has been highly successful demonstrating that microwave inspection is applicable to composite thermo-setting plastic materials. The testing of waveguide components has been demonstrated and its application to

the testing of waveguide systems and waveguide components is highly promising.

Another very promising application is considered to be the inspection of military and commercial aircraft tires and efforts are now being made to parallel the development of this inspection technique with the development of filament-wound advanced-design aircraft tires and filament-wound advanced-design aircraft structures.

Another very significant development is the capability of the microwave system to measure refractive index directly, and very rapidly. The materials do not have to be cut to precise dimensions and inserted in a waveguide. The major advantage is the elimination of the risk of gross errors that can occur when making such measurements by conventional methods because of the complexities of these methods.

Upon completion of the original eight tasks, work commenced on additional tasks to develop the microwave technique to a state where it can be utilized in NDT inspection and process control operations. Instrumentation and techniques have been established that can be applied to production inspection without undue delay for special electronic design and testing. This continued development effort has established the design of microwave FM interferometry to a state comparable to that of ultrasonic test techniques. In the case of laminated composites and elastomers, microwave techniques were shown to be far superior to those available in ultrasonics.

Work performed in achieving the second set of tasks is presented in the subsequent discussion and these newer tasks are differentiated from the earlier set by the use of a letter suffix.

Task IA - Phase Insensitive Analyzer

The basic problem of visually interpreting defect indications has been that the form of the indication varies cyclically with range. Several methods of eliminating this feature were studied. Since the cyclic variations (phase sensitivity) are sometimes useful, it was desirable that phase insensitivity be a selectable, alternate display mode. A circuit which does this has been designed and built, and the feature can easily be included in previous designs by adding another 4" x 6" circuit card.

Tests indicate that this feature is useful where operator confusion is a problem. It is not recommended, however, as the sole display mode. It

cannot contain more information than the original display mode, and probably loses some sensitivity.

Task IIA - Multiplex Signal Analyzer

For experimental work, and manual inspections, a CRT display of reflected power vs. depth, similar to that of an ultrasonic tester is used. For automatic inspection it has been customary to inspect at a fixed depth. When several depths were to be examined at once, duplicate signal analyzers have been required. The multiplex analyzer permits four selected depths to be inspected at the same time and recorded. The maximum speed with which the horn can be moved over the specimen is reduced by a factor of four, which is tolerable in many applications. The multiplex analyzer was not completely successful. It turned out to be more complicated than expected, while the conventional single-channel design has been greatly improved. At present, then, multiple independent channels are to be preferred unless a very large number of channels are required.

Task IIIA - Hand-Held Probes

By eliminating some of the bulkier components present in the earlier waveguide systems it has been possible to reduce the size and weight enough to permit hand-held operation. It was found that using flexible waveguide between the microwave tube and waveguide system, combined with removing the microwave tube from the sweep generator gives adequate flexibility. Ku-, K-, and Ka-band hand probes have been built. The source of microwave signals is a Backward Wave Oscillator tube, usually called BWO. The BWO and detector/mixer diode are the only tubes or semiconductors which actually operate at microwave frequencies. The BWO has a wider electronic tuning range than klystron or magnetron tubes more commonly used as microwave generators and its relatively low power is sufficient for this application. The latest miniature Backward Wave Oscillator tubes permit even smaller units. A Ka-band unit with the tube rigidly mounted on the waveguide has been built small enough for one-hand pistol-grip operation.

Task IVA Modified Sweep Generator

Several methods were investigated for obtaining more satisfactory sweep generators than the presently available commercial units which are

not designed for nondestructive testing applications.

Designs of circuits for driving backward wave oscillators were studied, simplified and modified. Components were assembled to produce a breadboard stage of a Ka-band sweep generator. Testing and further component packaging were completed to conclude that a Ku- K- Ka-band sweep generator can be incorporated into one sweep-generator/signal-analyzer package that eliminates all unused features. The BWO is kept out of the package and becomes an integral part of the waveguide probe as shown in some of the hand-held probe designs. The combined generator-analyzer and probe design should form the basis for successful commercial NDT units.

Task VA Applications Guide

The entire experience with the Frequency Domain Interferometer has been summarized in an Applications Guide. This guide explains the general principles of operation of the instrument, and offers some suggestions as to experimental techniques and setting up inspections. It is written for the Nondestructive Test engineer who might contemplate using one of the existing designs for inspection purposes, and this guide assumes no particular familiarity with microwave technology. This Applications Guide was prepared concurrently with this final report as a separate publication.

III. INSTRUMENTATION

A. SIGNAL ANALYZER DEVELOPMENT

The original schedule included two tasks which have been considerably modified. These were an improved signal analysis unit and a multichannel instrument. Two signal analysis units have been developed; the latest has better characteristics than the first. The latest unit started as the multichannel signal processor. It was to have consisted of more than one channel similar to the first one. Some components would be common to different channels. When the first channel of the second analyzer was operational, it was planned to combine this single channel with the existing analyzer for some preliminary tests. By this time, however, experience with both specimens and production parts showed that something more than two or three channels of the same type would be needed. At the same time, the variety, availability and price of integrated circuit modules had so dramatically changed that the design

contemplated for the multichannel unit would have been obsolete. For this reason, the intended multichannel signal analyzer was completed as another single-channel unit. The two single-channel units were tested as a two-channel system. This proved adequate to evaluate the multichannel concept which was found to be feasible and useful. A single horn was used to simultaneously scan at two different depths. Of course, additional readout equipment was required to make full use of multichannel data.

Knowledge and experience in the use of new integrated circuit modules had progressed to the point that the development of a more satisfactory design for a multichannel unit could proceed. The use of the new integrated circuit (IC) modules allowed a large number of operational amplifiers, flip-flops, shift registers, and the like, to be put into a small space at a low cost, and without too much labor and design effort. It thus appears that analog and digital computing functions, previously considered beyond the resources of this laboratory, could be included in the design. This is required to make full use of the multichannel data.

B. WAVEGUIDE INSTRUMENTATION DEVELOPMENT

The development of ridged waveguide components has been investigated and found impractical at this time. The sweep characteristics of microwave generators now available make it difficult to compensate for dispersion in rectangular waveguide. The problems with ridgeguide proved even more severe, especially with the hybrid waveguide-and-coaxial system. However, theoretical considerations show that dispersion in a rectangular waveguide would allow operation over a greater depth of field. Therefore, it has been concluded that the use of ridgeguide does not warrant further effort for the applications now in sight.

C. DEVELOPMENT OF PHASE-INSENSITIVE SIGNAL ANALYZER

The original method of eliminating phase sensitivity visualized the combination of two channels of the type already in use. If Channel A and Channel B have a phase difference of 90° than $A^2 + B^2$ will be a signal similar to those of the basic analyzer, except that the display form would not change with target position. It will be recalled that the phase involved here is the relative phase of the detected microwave signal and the analyzer's local oscillator. As the work proceeded, it became apparent that the square and

square-root circuits would be more expensive and troublesome than expected, whereas, the remainder of the system seemed to be going in the opposite direction. A search was therefore made for a less expensive and more reliable method. The first candidate method involved eliminating the ase sensitivity by a change in the timing sequence of the existing analyzer. P evious work had established that the phase changes in the display as the target moves coincide with the initial phase of the microwave signal, i.e., in the case of Ku-band swept from 12.4 - 18 GHz, there is a 360° phase shift each time the reflector moves one-half the wavelength of 12.4 GHz, the starting frequency. If the starting frequency were zero, an infinite wavelength would result, and infinite target motion would be required to produce any phase change in the display. The microwave sweep cannot actually be started at zero frequency, but if it could be, the linear sweep of 18 GHz would have to start about 2 milliseconds before it actually does. If the local oscillator sweep were started 2 milliseconds earlier than normal, when the microwave sweep actually did start, the result would then be the same as if both sweeps had started from zero frequency and in phase. Typically, a microwave band has a bandwidth of about one-third of its highest frequency, so that the detected signal for the case just described is quiescent for the initial two-thirds of the extrapolated sweep period, and a frequency ω_o for the remainder. Analysis shows that the display is:

$$D(\omega) = \int_{\frac{2T}{3}}^{T} [\mathrm{Sin}\ (\omega t)\ \mathrm{Sin}\ (\omega_o t)]\ dt \simeq \frac{1}{2} \frac{\mathrm{Sin}\ (\omega-\omega_o)\ T - \mathrm{Sin}\ \frac{2}{3}\ (\omega-\omega_o)T}{\omega-\omega_o}$$

This function is illustrated in Figure 1. The frequency ω_o represents a reflecting target at a particular range, and ω is the local oscillator frequency. Since the latter frequency is a linear sweep it corresponds to the horizontal scale on the display oscilloscope whose horizontal sweep is driven by the same signal that sweeps the local oscillator. Thus, Figure 1 is what would be seen on the oscilloscope. As a matter of fact, this is exactly what is seen. The circuit had been built by the time the analysis had been checked out, so that the result just presented was quickly verified and the effort immediately abandoned.

Fortunately, another way of circumventing the $A^2 + B^2$ complications

has been found, and since the complete analysis was favorable, a phase-insensitive unit was constructed. The circuit is similar to those built previously except between the chopper and sampling bridge. A tuned circuit, rather than integrator, is used. In typical operation, the detected microwave signal is 40 KHz and the tuned circuit is resonant at 70 KHz. The chopper signal is swept through 110 Kc to produce a sideband of 70 KHz. A chopper frequency of 30 KHz also hetrodynes the 40 KHz to 70KHz and could be used, but there would be interference from harmonics of the 30-KHz signal.

After each microwave sweep, a tuned circuit charges a capacitor. The charge on the capacitor is the amplitude of the ringing and is independent of phase. After this signal is sampled, circuits damp the resonant tuned circuit, close the gate, and discharge the detector capacitor.

D. MULTIPLEX SIGNAL ANALYZER

The multiplex signal analyzer has four channels and is designed to examine a specimen at four different depths. Rather than construct four duplicate channels it was decided to use four successive sweeps of the microwave generator. This will, of course, reduce maximum inspection speed but not seriously. In the normal depth scan mode, the depth is swept slowly so that in effect each microwave sweep signal (they are repeated at 1000/sec) is analyzed at a slightly different depth. In fixed depth scanning the instrument always examines one depth. In multiplex scanning with the present system four depths are analyzed. For test purposes only, a CRT readout is used and, in this case, four dots are displayed on the screen. These are generated in succession by supplying four different pairs of voltages to the signal analyzer controlling the phase and depth of each of the channels. Figure 2 shows what is done schematically. An ordinary phase sensitive display could be set to display any of the four traces at the right. By means of the manual scan any of the points marked by * could be monitored continuously. The multiplex unit has provision for monitoring four points in rotation and displaying them at the appropriate horizontal position.

The performance of this circuit was disappointing. Satisfactory reliability was not obtained during the time available, and it is probable that when finally in working order, the multiplex unit would be little more compact than a unit with four separate channels. The most recent design for a con-

ventional signal analyzer is much more compact than those in existence when this task was planned. Earlier designs employed commercial function generators which were bulky. These have since been eliminated, and independent channels are competitive with a multiplex unit except where a very large number of channels is required. Also, the independent channel does have some advantage in very rapid inspections and is somewhat more versatile. At present independent channels are recommended for practical application particularly since the applications involving relatively thin specimens are not likely to require many channels. Thus, multiplexing would be of little value. In the case of thick specimens it is probable that some sort of holographic technique is destined to be the ultimate answer. Thus it does not appear worthwhile to devote further effort to development of multichannel instruments. Independent channels will probably serve most needs at present, and a very reliable design exists.

E. HAND-HELD PROBES

The development and construction of the hand-held probes proved to be surprisingly simple and gave far better results than had been expected. In previous work with the waveguide systems, either there was a lack of components leading to the design shown in Figure 3 which was unsatisfactory, or a concentration of effort on other tasks which led to the designs used until recently. These followed conventional microwave practice, more or less, and had been inspired by observing how similar functions were performed in conventional systems. This led ultimately to Systems A and B shown in Figure 4. These work quite well, although they are heavy and bulky. In fact, the two-horn system is probably still the best available when size and weight are not critical, and when sensitivity very close to the horns is not needed. The advantage of high-quality couplers is that they split the signals without producing large reflections. These reflections are a problem, because two reflectors close together cause the detector to receive signals both directly, and after multiple reflections. This gives the same indications as multiple targets, and is quite confusing. Detector mounts themselves cause reflections, especially the shorted-guide type, whose impedance cannot be matched to that of the waveguide over a full band. This type of mount is shown in Figure 4E. It is rugged, gives a large signal and is desirable except for the large reflection.

The probe-type detector mount of Figure 3 will give small reflections, but only with a fine probe, shallow probe penetration into the guide, and resultant fragility and weak detected signal. Thus, if one reflecting element must be improved upon, it is best to use a more elaborate coupler. Experience has shown, however, that placing a ferrite isolator between the coupler and the detector gives very good results. (The isolator has very high attentuation in one direction, very low attenuation in the other). There are other pairs of reflecting discontinuities, but in practice they cause little trouble. For this reason, the arrangement of Figure 4C is best for most purposes when the slightly better performance of the systems in Figure 4A or B is not absolutely necessary. In 4C, the simple E-plane Tee is an adequate substitute for the larger, heavier, and more expensive directional coupler, and can divert both outgoing and incoming signals down the same waveguide to the detector. This allows a single ferrite isolator to absorb reflections from the single detector, and results in the compact units shown in Figures 5 and 6. Note that only the horn, isolator, and detector mount are beyond the capability of a simple machine shop. The remainder of the units can be easily fabricated from waveguide tubing and flanges which are not expensive. Twists and bends are made by filling the guide with sand to prevent collapse and softening it by heating with a torch. The Tee is made by milling a slot in a broad face of the guide and silver brazing a carefully squared piece of waveguide tubing into the slot. Thus, custom fabrication to fit available space is quite feasible. This is fortunate because microwave components are not easily obtained without long delays.

Discontinuities in waveguides give rise to reflections which are, fotunately, composed of many higher order modes, as a rule. Most of these are attenuated rapidly in the waveguide so that discontinuities far from the detector are not so troublesome. For this reason, flexible guide can be freely used between the microwave source and the hand-probes shown in Figure 6. Provided the rigid-guide section is kept in good condition, rather severe damage to the flexible guide can be tolerated without serious consequences. Although the flexible guide is fragile and rough handling will eventually sever it completely, it can be field-repaired by a soldered butt joint and the repaired segment splinted. This does no great harm beyond making a couple of inches quite rigid,

but it would be advisable to enclose the flexible guide in some sort of limited flexure tube to prevent sharp bends and tension. Twistable guide will survive longer in this application. Because of its dispersion characteristics and the fact that its characteristics change slightly with flexing, the use of flexible guide should be limited to the source side of the Tee. A short piece can be tolerated at the horn if absolutely necessary provided it is not allowed to flex very much or very rapidly.

For use as a hand-held probe, one of the new waveguide systems is connected to the backware wave oscillator (BWO) by an arm's length of flexible waveguide. The oscillator is itself removed from the sweep-generator cabinet and attached to the latter by a twenty-foot cable. The eight-pound oscillator can then be carried on the operator's hip, comfortably supported by a Sam Browne belt. The operator then has his hands free to handle the probe. The cable from oscillator to sweep generator also carries the detected signal so that the analyzer and sweep generator can be mounted in a single rack. This arrangement proved quite satisfactory for hand-probing inspections. The weights and dimensions of the probes are given in Table I.

TABLE I

Band	Frequency	Wt. BWO	Wt. Probe	Length	Width	Height
Ku	12.4 - 18 GHz	8 lb	3.8 lb	36 in.	2 in.	5 in.
K	18 - 26.5 GHz	8 lb	1.6 lb	19 in.	4 in.	3 in.
Ka	26.5 - 40 GHz	8 lb	1.2 lb	11 in.	1.5 in.	5 in.

The Backward Wave Oscillators are Varian series VA160 and VA400, the standard and miniature "O" type shielded BWO respectively. Their characteristics are:

Standard	Wt	Size diam x Length	Power in MW
VA 162M	8 lb	4 in. x 6 in.	50
VA 163M	8 lb	4 in. x 6 in.	25
VA 164M	8 lb	4 in. x 6 in.	10
Miniature			
VA 470M	4 lb	3 in. x 6 in.	20
VA 480M	4 lb	3 in. x 6 in.	10
VA 490M	4 lb	3 in. x 6 in.	5

All units actually built have used standard BWO's except the most recent Ka-band version. It employs a miniature BWO. The convenience of the smaller size and weight is greater than would be expected from examining the figures, whereas the 50% power decrease is not particularly significant. Sensitivity is spurious-signal limited rather than noise-limited, and both spurious and useful signals are reduced in the same proportion as BWO output. Doubling the gain of the detected signal amplified thus compensates for the power loss when the low powered miniature tube is used. With the very small Ka-band waveguide probe, the BWO/waveguide combination can be reduced to 5.2 lb. This is not too heavy to manipulate by hand and can be operated with one hand. It is possible to handle either K- or Ka-band units with one of the miniature BWO's rigidly coupled to the waveguide if flexible guide must be avoided. Of course, this assumes very careful handling. The BWO's cost from $1000 to $3000 depending upon frequency and, in practical use, it would probably be unwise to depend completely upon operator caution to protect them. In that case, some kind of case and padding would be required, and the size and weight would be increased; but it is still safe to say that Ku-, K-, and Ka-band hand probes have proved exceptionally satisfactory.

In order to test the feasibility of a hand probing operation, an inspection was made on a 3-ft Polaris A3 chamber section cast with live solid propellant. This cylindrical section has a variety of built-in defects. K-band (18 - 26.5 GHz) equipment was used to determine how well the hand-held probes would perform. In order to simulate the most unfavorable inspection conditions scanning was not permitted; the inspection being strictly point-by-point. One operator handled the probe, the other operated the analyzer and recorded data. The analyzer was set to examine the depth corresponding to the insulation-propellant interface and no depth scan was used. Data readout was by means of a galvanometer in place of the oscilloscope since the display output is a DC signal when depth scan is not used. The defects were not difficult to recognize from the galvanometer indications. First, the indication for a defect-free point was determined. The galvanometer reading was noted for twenty randomly selected points in defect-free regions. The average reading was 22.4 arbitrary

scale units.[1] The maximum was 28, the minimum 17. This gives a standard deviation of 1.7 so that the 2σ limits (95% confidence) are 19 to 25.8 arbitrary units. Next, randomly selected points within known defect areas were examined. The results are given in Table II.

TABLE II

RELATIVE DEFECT INDICATIONS FOR VARIOUS KNOWN SEPARATIONS ON A PROPELLANT DEFECT SPECIMEN

0.002 in. Sep.	0.008 in. Sep.	0.015 in. Sep.	0.020 in. Sep.	0.025 in. Sep.
19	21	-2	7	-10
18	4	5	11	9
12	-5	1	-2	0
5	18	0	2	-4
19	17	2	11	6

The separations were not of sufficient area to allow more points. If one calls a point defective whenever the galvanometer reading falls outside the 2σ limit regions of the specimen, the results are quite good. All points in the 0.015, 0.020 and 0.025 in. separated areas are identified as defective; four out of five for the 0.008 in. separation, and three out of five for the 0.002 in. separation. Furthermore, a check revealed that the "good" indications obtained in the 0.002 in. and 0.008 in. separations were near the center, and the defect indications invariably were found near the edges. Previous inspections of this specimen with scanning systems indicate that the separations have closed up in the center somewhat, and visual examination and probing with shims indicate that the 0.008 in. and 0.002 in. separations are probably open only at the edges. On the whole then, the results of this experiment were most encouraging, and suggest that the hand probes will prove useful whenever automatic scanning is not possible. It might be noted that none of the separations examined here would be classified as serious in a production A3 Polaris first-stage motor, and indeed the standard radiographic inspection presently used would hardly reveal all the separations in this specimen.

---

[1] The galvanometer had a series resistor which was adjusted to give convenient deflections. It was not calibrated since only relative values are important. The DC signal which was monitored is adequate to drive a recorder such as the Mosley 135 X-Y Plotter.

F. MODIFIED SWEEP GENERATORS

The use of commercial sweep generators has been satisfactory but is somewhat expensive as the desirable units cost from three to seven thousand dollars. Much of this cost is due to the presence of features not required of a sweep generator which is part of a frequency domain interferometer. It was therefore of interest to know whether simpler ones could be constructed. The purpose of Task IV was to answer this question. The existing units use a Backward Wave Oscillator tube (BWO) as the microwave source. An obvious approach to the problem is to accept the BWO and build simpler circuitry around it. This, of course, limits the economy since the BWO is expensive itself and the economics of production make it difficult for a special unit to be much cheaper. There are still, of course, the advantages of smaller size, fewer controls, and the possibility of making one circuit capable of sweeping several BWO's so that Ku-, K- and Ka bands could be covered by one unit, with only the BWO's being changed along with the waveguide system when shifting bands. This would save the cost of two sweep generators (less BWO) when three-band coverage is desired.

In addition to this method there were several less probable but more desirable approaches. Very small, solid-state, voltage controlled microwave generators are being developed. There is good reason to hope that there will eventually be matchbox-sized units weighing less than a pound which can replace present units. None is now available in the higher bands with adequate performance, but X- and Ku-band units are a distinct possibility in the near future. A search of available equipment forced the rejection of this approach at present.

Another solid-state technique involves the use of some of the new diodes designed for generating high harmonics. These are used for frequency multiplication at microwave frequencies, and offer the possibility of slightly modifying the signal analysis with some prospect of improving performance. The original instruments use a linear sweep across an entire band as indicated in Figure 7.

The two signals reaching the detector are separated in time by Δf, depending upon target distance. When they are mixed at the detector, there is present in the output the beat frequency, Δf, which persists throughout the sweep.

Analysis of the frequency spectrum of the output thus identifies reflections from targets at different distances, as each target gives rise to a single frequency in the detector output.

One could generate such a linear sweep, for example, from 1/2 to 1 GHz where a variety of sources are available. By 8X frequency multiplication, a sweep of 4-8 GHz would result, provided adequate multiplication factors and bandwidth were possible. Such multipliers which require only a diode and its waveguide mounting could cover several bands with one generator. The construction of diode mounts with adequate bandwidth was outside the scope of the program and well beyond the present capabilities of this laboratory. With improvised mountings, the signals obtained were not very clean, and although some rudimentary range sensitivity was obtained, performance was poor.

The idea originally conceived for this type of sweep generator was somewhat different from the one just described, which generates a linear sweep as do the ones now in use. Instead of this, the original plan had been to generate a "comb" of discrete frequencies covering the band. Each "tooth" of the comb would be harmonic of a single master frequency. This master frequency could then be swept over a rather narrow band. The signal analysis in this case would be quite simple. When such a signal is used in the present interferometer, the result should be that only for certain frequencies of the master signal could all harmonics (the teeth of the comb) be in the same phase at the detector after being reflected from a target at a particular range. Thus analysis would consist of simply displaying the detected signal on an oscilloscope whose horizontal sweep was synchronized with the sweep of the master signal. Preliminary consideration of the method led to the expectation that the unambigous range, depth of field and general resolution and sensitivity would be roughly comparable to the performance of the present units.

Unfortunately, the complexity of constructing such an instrument was under estimated and it was soon apparent that this approach would not lead to an instrument of practical use for some time. Since investigation had shown that sweep generators would be a problem it was decided to explore the redesign of existing units. While it was not economical to construct a single sweep generator to replace a commercial unit, if frequency domain interferometers are ever to be produced in quantity for nondestructive test purposes, it will be necessary to

know some of the design requirements of the sweep generator. For this reason a breadboard BWO sweep generator was constructed.

Figure 8 shows the block diagram of the breadboard unit. Figure 9 shows the relationships of the signals generated by the unit. This is quite similar to the circuitry in the E-H generators now in use. The low voltage sweep is generated by solid-state circuitry, amplified by tube circuits to the high voltages required by the BWO. Experiments with the breadboard unit indicate that a single circuit can be made so that, by a selector switch, it can operate a Ku-, K-, or Ka-band BWO. All that would need to be duplicated would be the diode network which shapes the sweep sawtooth. This must be adjusted to each particular BWO and waveguide probe as a rule. The reduction in volume of circuitry is not great, but a fair amount of hardware could be eliminated in the form of controls which are not used.

In another experiment, the sweep repetition rate was raised from the 1,000/second, typical of theE-H Laboratory's unit, to about 3,000 with the breadboard model. This works quite well; the limitation encountered was in the signal analyzer's sampling bridge but the microwave signal remained good. It had been feared that some subtle changes might make very high repitition rates unsuitable for this application but it appears that the Varian BWO's can be driven up to the maximum sweep rate quoted in the manufacturer's literature which corresponds to a repitition rate of 15,000/second for a linear, full-band sweep. This should allow several multiplex channels to be operated with the same inspection speed which is now possible with a single channel (the limiting speed for multiplex channels is 1/n times the speed for a single channel where n is the number of multiplex channels).

No great improvement in the quality of the sweep signals seems likely with circuits of this general type. The diode network in the breadboard version was built with 15 pots for adjusting the sweep sawtooth as compared to the 10 in the E-H unit. The sweep sawtooth is not linear but adjusted to compensate for non-linearities in the BWO. The extra pots did not allow better adjustment, and this operation remains rather delicate as it always has been. Fortunately, it does not show much tendency to drift from the proper adjustment.

Figure 10 shows the indication obtained from a single plane, metal

reflector in tests. The breadboard sweep generator, and a Varian VA 490M BWO were used. This shows good symmetry and peak-to-side lobe ratio. Here the sweep is the full Ka band, 26 - 40 GHz.

The conclusion from this entire investigation of the sweep generator is that replacement of the E-H laboratories 5 series is not yet to be recommended in all cases. Solid state generators will no doubt eventually become available but none have all the required feature s yet, a least not at the higher frequencies. Constructing one would still be a rather formidable task. The construction of a simplified BWO generator would not be economical for single unit construction or even limited production unless an extremely compact unit were needed, or there were some reasons for operating BWO's of several frequency bands with one sweep generator. The signal analyzers, it will be recalled, work with microwave systems in any band, and only the sweep generators and waveguide probes are restricted to one waveguide band.

Thus for general purpose inspection use the EH 560 series is still the best choice, with the only easily made change being the removal of the BWO from the sweep generator, to which it can be connected by a long cable. This allows the sweep generator and signal analyzer to be placed in a single enclosure, and is quite satisfactory where only one frequency band is used. The BWO weighs only 4-8 pounds and is much easier to attach to the waveguide than the entire sweep generator. As manufactured, the Ku, K, and Ka-band sweep generators deliver the microwave signal from a front panel waveguide outputs, which must be coupled to the interferometer's waveguide system.

If an extremely compact unit in one package is required, it would be possible to construct a special sweep generator of the type just described. The one actually constructed is considerably larger than the E-H instrument because of the commercial modular power supplies used, but with careful design a reduction of the total volume of the frequency domain interferometer could be achieved.

G. APPLICATIONS TO LARGE PROPELLANT GRAINS

Because of the great expense of preparing large propellant samples, no full scale models with extensive defects have been available for testing under this contract except for the block used to demonstrate penetration under Contract NAS 7-367. Another problem has been the lack of any definite accept/reject

criteria; indeed there has scarcely been an order of magnitude estimate. For these reasons, the present contract has yielded more general development of the frequency-domain interferometer than practical evaluation to propellant inspection. Also, it was more economical to do experimental work with Ku-, K-, and Ka- bands, which do not give as much penetration in propellant as do the bands below X-band. While not allowing direct evaluation of propellant inspection, this work has developed the technique to a point from which design of an inspection fixture for large grains is relatively straight forward; such an instrument is, in fact, now under construction.

Contract NAS 3 12036 (NASA, Lewis Research Center) "Development of NDT Techniques for Large Solid Propellant Grains" is now under way. This contract, due for completion about August 1970, will include full scale evaluation of microwave grain inspection. There will be specimens of the 260" motor grain which measures 72" along the motor axis, and which will be approximately 42° Sectors. Tests scheduled include an in-process inspection with an X-band (8-12.4 GHz) microwave Frequency Domain Interferometer. The in-process inspection it intended to detect bubbles and folds in the propellant during casting, when penetration requirements are limited to the depth to which the bayonet tube is submerged in the propellant. It is this relaxed penetration requirement which permits the use of X-band, which does not give great penetration although resolution is good. The X-band equipment has been constructed and bench-tested. Performance is about as expected on the basis of work with Ku-, K- and K_a- bands. The prospect of an in-process inspection is most encouraging since another completed part of NAS 3-12036, the failure mode analysis, suggests that voids of approximately 4.2" diameter might be quite serious. An X-band unit should be able to detect such voids, but will not penetrate very deeply. Lower frequencies would not have adequate resolution. Because of the slow casting, it is quite feasible to scan the entire propellant surface in a time during which the propellant level will not rise significantly. Thus, at least some defects might be detected while they are near the surface, and while corrective action is feasible.

Also scheduled are tests involving cured propellant specimens to evaluate inspection techniques for cured motors. The specimens will be sectioned, and also inspected by other techniques for comparison. Although

not strictly part of NAS 7-544, the studies just described are a direct result of NAS 7-544, and thus merit discussion here. The final report of Contract NAS 3-12036 should contain the definitive evaluation of microwave inspection of large solid propellant grains. At the time of this report, the status of microwave NDT is accurately indicated by its inclusion in the group of techniques selected for evaluation under NAS 3-12036. It is one of the techniques which will actually be applied to the defect specimens along with established methods such as radiography.

IV. EXPERIMENTS

A. GENERAL PROCEDURES

Before considering experiments, it is necessary to describe the variants of the basic system, and the several readout modes available. The forms of the waveguide system are shown in Figure 11. Forms A, B, and C are in order of ascending performance, generally, but also of decending convenience. B is bulky compared with A, but is more sensitive and has better resolution. B gives a large front surface reflection, but does not mix the strong outgoing signal with the weak reflected signal since the signal diverted to the mixer by the first coupler is 10 db down from the main line. The second coupler, however, only diverts half of the returned signal to the mixer. Form C represents the best in sensitivity. Only one coupler is used, all of the returned signals intercepted by the horn goes to the mixer, and with the horns against the specimen, there is no front surface reflection. The disadvantages, of course, are that the complete antenna assembly is larger, and the instrument cannot see objects very close to the horns. One must be more careful in aligning the horns, but this form would be useful where one wishes to examine surfaces at such angles that the reflection is not straight back toward the transmitting horn, since the receiver could be placed to receive the reflection.

Data readout systems vary considerably with the application. For such operations as the measurement of refractive index, where there is no need to scan across the specimen, the oscilloscope of the signal analyzer is used for readout. In making accurate measurements of reflected signal strength with any of the waveguide systems of Figure 11, an attenuator can be placed in the waveguide between the horn and the remainder of the circuit. With a two-

horn arrangement it can be in either branch. In the one-horn arrangement, the attentuation value read from the attenuator dial must be doubled, as it attenuates both outgoing and incoming signals. With the attenuator in place, signal amplitudes may be compared by noting the attenuation required to make their indications the same size on the oscilloscope. This eliminates the effect of any non-linearities in the electronics. A metal reflector that provides 100% reflection serves as a reference.

When a specimen is being scanned, there are several other read-out modes which are useful. The basic oscilloscope display obviously cannot be recorded on any of the usual recorders. The signal analyzer, however, has provision for stopping the depth scan. In this case, the basic display ceases to be a reflection strength vs depth curve, and becomes a single dot whose vertical position is a function of the strength of the signal coming from one particular depth. A manual control is provided so that the depth being examined can be varied. In practice one observes the depth scan trace on the oscilloscope, selects the position to be monitored, switches from automatic to manual depth scan, and moves the dot to the desired position on the trace. Figure 12 shows how this operation appears on the primary display. The two traces are depth scans with and without a defect present. The specimen was stationary during both traces. The dot shows the correct setting of the manual depth scan to record the defect. As the horn moves across the defect, the dot will move from the lower trace to the upper one and back. This voltage is usually recorded on an external recorder. The photograph of Figure 12 was made by a triple exposure.

For recording, the primary readout is connected to a recorder. The recorder drive is linked to the scanning motion, and C-scans may be produced which constitute a map of reflection as a function of position on a surface at the selected depth within the specimen. In this way one may, for example, monitor a bond-line for signs of separation. When the bond surface is not at a fixed depth, but varies slightly in its distance from the horn, various problems ensue if this variation is not regarded as a defect. Often dimensional tolerances are loose enough that this is quite normal. In such cases small changes in the position of the reflecting surface will cause the changes shown in Figure 13. Trace A shows the interface in the normal position. Trace B shows it at a slightly greater depth, but otherwise unchanged. Trace C shows the result of re-adjusting the display phase. (See Appendix A for an explanation

of this effect.) It is more apparent in Trace C that a simple position change has taken place with no change in amplitude. If one could convert all indications to the symmetric positive peak form, a multi-channel system would be quite useful. With four channels, for example, one could record on a two-pen recorder (a) which channel had the maximum signal, and (b) the amplitude of the largest signal without regard to the channel in which it appeared. This would allow dimensional changes to be distinguished from separations at the bond line.

At this time, manual rotation of the phase control is the only means of dealing with this problem. The rotation produces a trace typically shown in Figure 14, which greatly reduces operator error. A single reflector at any position produces an indication of the same shape. The terms omniphase and monophase are used to distinguish the types of scan produced with and without changes in display phase. Since the phase control rotation is not yet automatic, this display mode is rarely employed in scanning a specimen. One example obtained by manually rotating the phase control can be found in Section V.C.

B. FUNDAMENTAL MEASUREMENTS

1. Distance

The quantity which is measured is not literally distance, but electromagnetic path length, L, which is related to the actual distance l by

$$L = n\,l$$

where n is the refractive index of the medium through which the waves propagate, and

$$n = \frac{V_o}{V_m}$$

where V_o is the speed of the waves in vacuum, V_m the speed in the medium. Since the refractive index of air is 1.0, for all practical purposes, L and l may be taken as equal to each other in air. A correction is required when measuring distances within dielectric materials.

The electromagnetic distance to a reflector can be determined by two methods. In one method, the location of the reflection peak on the oscilloscope screen may be noted. After suitable calibration, the position along the horizontal sweep can be read as the electromagnetic range of the reflector. This is the method familiar in radar and sonar. The only pre-

caution required arises from the fact that the form as well as the position of a reflection peak changes with the position of the reflector. Since the instrument is provided with a phase control, one can change any of the forms shown in Figure 4, Appendix I, to the symmetric positive form for convenience in determining horizontal position. The range indication is not changed by this phase adjustment.

A second method uses the technique of interferometry. One of the results of the analysis in Appendix I is that the trace goes through the forms of Figure 4, Appendix I once each time the distance from horn to reflector goes through 1/2 wavelength of the initial frequency of the microwave sweep. One may measure distance by counting cycles of the sequence of display forms much as one counts fringes with an optical interferometer; the range is then the number of cycles multiplied by the half-wavelength. For interpolation, one can use the phase control, which has 1000 divisions per cycle; 20 divisions produce a visible effect. This control is linear, so that precision is quite good. Figure 15 shows the calibration curves obtained by these methods. Non-linearities in the sweep circuits of the signal analyzer cause curve A to show some deviations from a straight line. These are minor compared to interferences expected in inspection operations (see Figure 16). The less convenient cycle counting method shown in curve B of Figure 15 will not often be required except for detecting very small changes.

2. Strength of Reflected Signals

The measurement of reflected signal strength still poses problems both in the measurement itself and in interpreting results. The response of the signal processing circuit is not reliably linear. For precise work, the height of the peak on the oscilloscope screen is not measured. A better method is to put an attenuator in the waveguide and note the attenuation required to bring all indications to a standard amplitude. However, the height of the peak on the oscilloscope screen is a useful indication, and is probably accurate enough for inspection purposes. It is, for example, probably as useful as a similar indication from an ultrasonic inspection.

3. Absorption

No satisfactory measurements of absorption have been taken.

Of course, one can always place a sample of a given material in front of the horn, and if several thicknesses are available, get an excellent idea of what thickness of specimen can be inspected. This is quite adequate for many inspection purposes. A real measurement of absorption will require a collimated beam which is not provided with the simple horns now in use. The general problem with signal strength measurements also contributes here. Further work can probably solve these problems.

4. Refractive Index

The method for determining refractive index follows at once from the measurement of distance and electromagnetic length previously discussed. To measure refractive index one requires parallel faces (see Figures 17 and 18). The specimen is placed between the horn and reflector, the reflector far enough from the specimen so its indication does not overlap that of the specimen. The phase and position of the peak produced by the reflector on the oscilloscope are noted. The specimen is then removed and the reflector is moved until the peak returns to its initial position and phase. The distance d through which the reflector was moved is noted. If the original phase and position of the indication have been restored, the electromagnetic distance from horn to reflector must be the same in both cases, i.e., the specimen thickness t through a material of refractive index n is the same electromagnetic distance as t + d through air (n - 1) or $n = (t + d)/t$. This is very convenient, and gives surprising accuracy. Specimens should be about an inch thick, although better results are obtained with thicker ones. If the material is in thin sheets, several may be stacked to form the required thickness. They need not be firmly pressed together, and no great care is required in positioning the specimens except that the beam must pass through them. In practice 2 x 3 in. is a good size. If the faces are not parallel, or are not plane, there will be errors, but surprisingly rough specimens give fairly good results.

The refractive indices of a number of specimens were obtained. All readings were consistent and reproducible. It is difficult to check the accuracy of most measurements but three are well known materials whose dielectric constants are to be found in such references as "Dielectric Materials and Applications," A. R. Von Hippel, editor; John Wiley, New York/MIT Press, 1954. Teflon, polystyrene, and Plexiglas furnish a good

check of accuracy as their absorption is small, their magnetic properties negligible, and thus the refractive index is the square root of the dielectric constant, which is most commonly tabulated. Table III shows the results. The refractive index determined by the FM interferometer is not strictly a single-frequency index, however, few dielectrics show significant variation over a single waveguide band so that these refractive indices should be satisfactory for almost all purposes. If this measurement fulfills its promise of accuracy and convenience it should greatly enhance the usefulness of the FM interferometer as it is undoubtedly easier than preparing a sample which will fit into a waveguide for standing wave measurements as is the general practice. The new method would allow the user of an FM interferometer to perform in an hour, measurements which would otherwise require the services of a well equipped microwave laboratory. Some data from the Stanford Research Institute[1] are included in Table III. Values are comparable. Since we cannot measure the refractive indices of the small waveguide samples used by Stanford, there may be a real difference since the materials are not too uniform. The Stanford report advised that the seven measurements in each band be averaged. They were made at 1 GHz intervals and most of the specimens showed at least one anomalous value in each band. Also, wide scatter was noted. Since our measurements are quite repeatable, this technique for refractive index determination could be one of the better ones available.

C. EFFECTS OF TARGET GEOMETRY WITH SIMPLE REFLECTORS

In order to study the effects of target geometry without having to consider other variables, metallic reflectors were used. They may be regarded as perfect reflectors and do not give reflections from multiple surfaces as do dielectric specimens. The thickness of the metal is of no importance. Cardboard discs covered with foil and steel spheres are convenient as is aluminum adhesive tape. A block of low-density styrofoam provides a good target support. For the tests about to be described, a styrofoam block of 12 x 12 in. was mounted upon a compound carriage taken from an immersion ultrasonic tank and the microwave generator and waveguide were clamped to the table of a vertical milling machine. The Ku-band (12.4 - 18 GHz) micro-

[1] Reference previously cited.

TABLE III

REFRACTIVE INDICES OF SOME MATERIALS

Material	Measured Index FM Interferometer	Calculated From Published Data
Plexiglas	1.62	1.61 (10 GHz)[1]
Teflon	1.44	1.43 (10GHz, 25 GHz)[1]
Polystyrene	1.60	1.59 (10 GHz, 25 GHz)[1]
Plaster of Paris*	1.78	
Plaster of Paris*	1.80	
Plaster of Paris (Aluminum Filled)	1.93	
Glass-Epoxy (POLARIS A3 Case)	2.19	2.15 band average[2]
Brick, Cannon Buff Standard Smooth	2.05	
30-Mesh Masonry Sand	1.63	
Inert Propellant 260-in. formulation	2.29	
Live Propellant		2.60 band average[2*]
260-in. motor formulation	2.50	2.59 band average[2*]

*Two samples

[1]Von Hippel

[2]Stanford Research Institute

wave equipment was used. Data were recorded on an X-Y plotter. The X-axis drive was obtained from a potentiometer geared to the lead screw of the compound carriage. Table motions of the milling machine were used for vertical indexing and horn-to-specimen distance control. The specimen was moved horizontally for scanning. The waveguide system was in the one-horn configuration. This is not the most sensitive arrangement, but is more convenient than the two-horn system, and will probably be more commonly used. Figure 19 shows the results of scanning the styrofoam block with various steel spheres imbedded in it. Since it is not really practical to put too much confidence in quantitative data concerning reflected signal strength, a plot of scattering cross section vs sphere diameter was not completed. Our collection of steel spheres did not represent many points whose circumference-to-wavelength ratio would fall between 1 and 10 for frequencies in Ku-band. Theoretically, the curve should be smooth up to a circumference-to-wavelength ratio of 1.0 (Rayleigh region), oscillate from 1.0 to 10 (resonance region) and be smooth thereafter (optical region) (see Figure 20). Our data cover the Rayleigh region fairly well, and the first maximum occurs at a diameter of 0.312 in. For single frequencies, a 0.312 in. sphere would represent a maximum point for 12.4 GHz. It is difficult to calculate a curve corresponding to Figure 10 for a swept frequency; however, the experimental curve, Figure 21, is reasonable. Extension of the data into the optical region would have required diameters large enough that the near-field beam would have been nonuniform over the target to a very significant extent, and for this reason, no large spheres were used. The fact that the experimental curve drops more rapidly after the first maximum is probably due to the non-uniformity of the near-field beam.

The curves of Figure 21 are to be taken as a rough indication of the relative sensitivity to spherical reflecting surfaces. Single frequency theory using the lowest frequency of the sweep will provide estimates of performance as good as can be expected. No indication of reflector size can be obtained from the horizontal scale of the traces of Figure 19. The reflection is like radiation from a point source, and the peak width simply indicates the directional characteristics of the horn.

Figure 22 shows the results of duplicating the previous experiment with metal discs rather than spheres. In this case, the size of the target is

revealed to some extent by taking peak width at one-half maximum. Note, however, that no target gives an indicated width less than 2 in.

Curve A in Figure 23 demonstrates the difference between plane and spherical surfaces more clearly with a 0.75 in. sphere and a 0.75 in. disc. The peak width is approximately the same, but the disc is seen to give a stronger reflection. Trace B in the same figure compares 3 and 4 in. diameter discs at a gain reduced from that of Trace A. The indicated widths are 3 and 3.5 in., respectively. Trace C shows the response to a "semi-infinite" plane, a metal sheet large enough to give the maximum possible response during almost one-half of the scan. The sharp edge is hardly suggested by the trace, but the point halfway between maximum and minimum gives a fairly good indication of the position of the edge.

Figure 24 shows the geometry involved in effective beam width. Note that there is no focusing in the usual sense. With horns that do not produce a convergent beam, or a parallel one in finite length, the effect of a narrow beam is not a simple one of improved resolution. In the case of plane reflectors, it is the aperture of the horn that determine resolution. Narrow-beam horns are of larger aperture. Of course, narrow-beam horns concentrate more energy in the main lobe and improve sensitivity. Where the targets are small, or are not plane surfaces, narrow-beam horns are mandatory since sensitivity is crucial.

All the experiments just described involve the near-field of the horns. This complicates matters since the near-field patterns are not simple, and horns are generally designed for far-field performance. However, since most inspection applications will involve objects in the near-field, the present tests were also conducted at close range. A complete characterization of the instrument would require more elaborate tests, but those just described are adequate to show its capabilities and limitations for inspection applications, and they can be duplicated under inspection conditions.

D. DEFECT STANDARDS

The problem originally labeled defect standards actually includes two important matters. One is the preparation of some sort of standardized test block, much like those familiar in ultrasonic flaw detection. The other

is modeling techniques. In the case of defect standards, one must have a test block which has features resembling defects, but much simpler so that instrument performance can be evaluated with a minimum of complication and the assurance that results will be comparable to those obtained by other workers. Models, on the other hand, are often needed to help in the interpretation of data obtained in the inspection of parts. To be of use, a model must produce data very similar to that obtained from a real part, and must lend itself to the introduction of simulated defects. Essentially, one must have materials whose attentuation and dielectric constant can be controlled, and which can be conveniently shaped.

Since present inspection applications are chiefly concerned with cracks and separation of laminar structures, the most important defect standard is the one for air gaps. For convenience, Plexiglas has been chosen as the material for primary defect standards. It is likely to be available in any laboratory and is easily worked. The specimen manufactured for this purpose is shown in Figure 25. It is 12 x 12 x 4 in. and has stepped separations in two 2-in.-wide strips two in. apart. Individual steps are 2 x 1.5 in. and vary in thickness from 0.005 to 0.5 in. Their spacing and area have been chosen so that they intercept most of the effective beam of the Ku-band instrument. This specimen would also be usable at higher frequencies, although thinner separations would be desirable above K-band (18 - 26 GHz). The specimen is in two parts. One part has flat faces while the other has the steps milled into one face. The blocks are not bonded together, but are held by clamps. The thickness of the block allows the indication of the separations to be well removed from those of the front and back surfaces. By substituting a thin sheet for one of the blocks, the front or back surface reflection can be brought into close proximity with the steps to simulate a separation near the surface.

Figure 26 shows the results of scans across the assembled standard block. The arrangement was the same as that used for metallic reflectors. The settings of phase and manual depth scan were carefully optimized for the 0.005 in. separation and all separations were scanned. The smallest separation is easily seen. It will be noted that up to 0.050 in. the increase in the amplitude of the indication is uniform. With an infinitesimal

separation one would, on the basis of elementary theory, expect reflections from both the front and back surfaces of the gap. Suppose the instrument is adjusted so as to produce a positive peak for the front surface alone; theory predicts that there will be no phase shift at this Plexiglas-to-air interface, but that there will be one at the back surface, an air-to-Plexiglas interface. The reflection coefficient of a dielectric interface is:

$$R = \left[\frac{n - 1}{n + 1}\right]^2$$

and is, on the basis of our measured values of R, equal to 0.06 for a Plexiglas-air or air-Plexiglas interface. Various measured values average approximately 0.056. Using 0.06 it is seen that the back surface reflection will be 0.036 I_o, whereas, the front surface reflection is 0.06 I_o where I_o is the incident power. Since the two reflections are 180° out-of-phase, one should obtain an indication identical to that of a single reflector, and having an amplitude of 0.0036 I_o, or approximately 26 decibels below the signal reflected from a metallic plate. Since signals as much as 40 db below 100% reflection have been detected, this analysis would suggest that any finite separation is detectable, which is not to be believed. When the separation ceases to exist, it must also cease to reflect, and will undoubtedly do so continuously as discontinuous functions do not abound in nature although they are common enough in theory. It may be suspected from this that a plot of peak indication vs. separation thickness from the data of Figure 26 fails to pass through the point (0, 0) and thus requires an explanation. This is indeed the case. Figure 27 shows this plot, and the extrapolation of the curve does not pass through the origin. The explanation lies in the fact that reflection from a dielectric interface is by no means as simple as the elementary theory would suggest. J. A. Stratton's "Electromagnetic Theory," McGraw-Hill, 1941, Chapter IX, contains a discussion of the phenomena adequate for our purpose. For the case of an air gap surrounded by material of refractive index greater than 1.0, the reflection coefficient reduces to:

$$\bar{R} = \frac{2R\left(1 - \cos\frac{2wd}{c}\right)}{1 - 2R\cos\frac{2wd}{c} + R^2}$$

where $\bar{R}$ is the coefficient of the gap, R, is that of a single interface, w is

the angular frequency ($w = 2\pi f$), c the speed of light in air, and d is the gap width. For very small gaps this may be approximated by

$$R = \frac{8}{3} \quad \frac{R}{(1 - R)^2} \left[\frac{wd}{c}\right]^3 .$$

This tells us that the curve in Figure 27 should approach zero if extended to separations less than 5 mils, which is reasonable. It also shows that the reflection varies as the cube of the frequency, suggesting that a blurring due to the frequency sweep will be more severe. Indeed, it has been noted that on the primary display of reflection vs. depth trace, the indications of reflections from very thin gaps are blurred and the exact position is difficult to determine. Thus, while exact comparison with theory for very thin gaps is not possible, our results are at least reasonable. What can be said with certainty is that the minimum detectable air gap is less than 0.005 inches.

The remainder of the reflection vs. gap width curve of Figure 27 can be explained in a straightforward manner. At very small gap widths, the two reflections can be treated as a single reflector to a fair approximation. If the gap increases, the front and back reflections eventually move apart sufficiently to appear as two distinct peaks. Since the instrument has range resolution, it would be desirable to calculate the expected response to gaps of various widths in materials of various electrical properties, but the task is too formidable to undertake without a digital computer. This computation might be worthwhile if the FM interferometer finds extensive application. It is difficult to estimate the type of indication a given flaw would produce except under conditions similar to those of previous tests. The rough linearity of Figure 27 in the important 0 to 0.050 inches range of gap width does at least offer a means of making reasonable estimates.

When it is desired to make an estimate of the performance to be expected from the FM interferometer, it is recommended that single-frequency theory be used and the calculations include the mid-band frequency of the equipment. This will provide a good working approximation. If the quantities calculated are found to vary as the first power, or less of the frequency, fairly good results may be expected. Where the frequency dependence is of a higher power, results will deteriorate considerably. However, NDT engineers

are warned that very elementary theory is not adequate for this work. Although many approximations may be made, one should start with reasonably exact equations and proceed with caution, making certain that any simplifying assumptions are justified. Stratton's book mentioned earlier in this section is recommended.

E. MODELING TECHNIQUES

Because of the complexity to be expected in production parts, it is very probable that the user of an FM interferometer will occasionally get into difficulties in the interpretation of data, or in estimating sensitivity to various defects. It is often difficult to get full-scale hardware with built-in typical defects for study. When it is not possible to make reliable calculations, a reliable model is required. Fortunately, models are fairly successful. By consulting tables such as those given by Von Hippel, one can see that most plastics have refractive indices between 1.3 and 2, although some materials have much higher indices. Plaster-of-Paris is very convenient for model making, and has a refractive index of 1.78 to 1.80. This may be raised by adding aluminum powder. Casting resins are useful, and their refractive indices may be controlled by adding aluminum powder, magnesium oxide powder, or some other material of high dielectric constant. Of course, commercial sheet stock of Plexiglas or polystyrene is useful. Cement furnishes a good material if moderately high loss is desired. Absorbed water greatly increases both loss and dielectric constant in any material, but the water in hydrated crystals does not increase either dramatically. Both cement and Plaster-of-Paris incorporate considerable water into their crystalline structure upon curing, but when drying removes all additional water, they become fairly transparent to microwave energy. It might also be noted that the use of aluminum powder to raise the refractive index does not greatly increase the absorption, as the fine particles do not raise conductivity over dimensions comparable to the wavelength.

One of the more useful devices for such experiments is a sandbox. A small Plexiglas tank was filled with 30-mesh masonry sand. A sand-to-Plexiglas interface has a reflection coefficient of approximately 0.003, and hence the reflection from it is approximately 25 db below that from a perfect conductor (reflection coefficient = 1.0). This is not detectable under inspection

conditions. It is thus possible to use Plexiglas freely to support other objects in the tank since they are invisible when the tank is filled with sand. Styrofoam is a solid which very closely resembled empty space. With a supply of plastic sheet, plaster, and powders of various dielectric constant and absorption, it would be possible to build models which would accurately represent articles to be inspected.

V. THE FREQUENCY DOMAIN INTERFEROMETER AS AN INSPECTION DEVICE

To test the FM interferometer as an inspection device, a selection of actual production parts was obtained for the purpose of realistic testing. Experience with the defect standards had shown that the scanning and specimen handling procedures were not separable from instrumentation problems, and a great deal of knowledge was gained from this work. The results of the other studies are undoubtedly of more practical use because of the experiments under realistic inspection conditions. The parts examined were the TITAN III ablative skirt, aircraft tires, and the POLARIS A3 first stage nozzle receptacles (the cavity in the motor into which are fitted the rotatable nozzles of which only the exit cone protrudes beyond the aft head of the motor case). As a result of the tests about to be described, it is believed that the applicability of the FM interferometer to nondestructive testing has been successfully demonstrated.

A. THE TITAN III ABLATIVE NOZZLE SKIRT

Figures 28 and 29 show the skirt and inspection fixture. The skirt has an ablative liner, an inner shell of glass cloth and honeycomb, and an outer shell of additional glass cloth layers. At the aft end, there is a segmented flange of aluminum which is imbedded in the structure of the skirt and contains bolt holes for attaching an aft closure. The closure is removed by explosive charges prior to ignition of the motor. Examination of the entire skirt for defects is performed, but initially, the major effort was concentrated on the region of the segmented ring. There is a possibility of damage to this region in handling and in the explosive removal of the closure. For this reason, skirts have been examined before and after tests during which the closures were explosively ejected.

For inspection, the skirt was placed on a motor-driven turntable

with the aft end up. The turntable drive was geared to a precision potentiometer to produce a voltage for the X-axis of an X-Y plotter to obtain a defect map of the flange area. The signal analyzer was used with the Ka-band (26 - 40 GHz) microwave system in the waveguide configuration shown in Figure 1A. The horn was connected to the slotted line by a length of flexible waveguide. Positioning of the horn is by means of a spring-loaded A-arm which presses a two-wheeled horn mount against the inside of the ablative liner. The horn was adjusted to send a beam perpendicularly against the inside surface of the flange segments buried in the rim of the skirt. The return signal was then viewed on the basic display and the reflection from the flange segments identified. The turntable was rotated until a gap between flange segments was under the horn. This produced a marked decrease in the reflected signal. Visual examination of the flange revealed the presence of voids between flange segments so that the logical starting point of a flange-to-liner separation is at the gap between segments. When the signal analyzer is put on manual depth scan and set to the depth corresponding to the flange-to-liner interface the basic display can be switched from the oscilloscope to the X-Y plotter and a plot made of reflected signal vs. angular position on the skirt. Figure 30 shows the results obtained. The dips are the gaps between flange segments where the reflection should diminish. This scan covers a region where there is no separation at the inner surface of the flange. The marked sections in Figure 30 show regions where there are indications of some structural anomalies. The signal strength reflected from the inner surface of the flange segments does not return to the baseline as rapidly as that from a normal section. One possible explanation is that a crack has started between the segments and has extended for a short distance along the bond between flange segment and liner. On this basis, suspected defects were reported. Subsequent visual examination showed that the ends of the suspect segments were out of line at the surface , and radiographs, two of which were reproduced in Figures 31 and 32, confirm that the concealed portion of segments in question were separated from the liner. Figures 31 and 32 are contact prints, so that an air gap is lighter than the surrounding area in Figure 31, whereas in Figure 32, there is no light line at the interface indicating the absence of a gap.

Before regions other than the flange were inspected on complete

skirts, sections were made up with built-in defects in the form of saw cuts in the ablative liner, and separations between the various layers. Figure 33 shows such a defect specimen. It was inspected in much the same manner as the entire skirt except that the specimen was mounted on a compound carriage for linear motion rather than on a turntable. Figure 34 shows the results with the specimen above for comparison. The correspondence between horizontal scale on the chart and the actual specimen width is almost one-to-one. The distances from the edge of the specimen shown in the photograph are indicated on the chart at the right of each trace. The resultant map of the defects is quite accurate. On the basis of these experiments, the entire ablative liner and its bond to the honeycomb as well as the segmented flange are being inspected. The TITAN NDT program included the construction of an FM interferometer and the necessary inspection equipment and labor required for the above investigation was provided by the USAF Space and Missile Systems Organization through the TITAN Program.

B. AIRCRAFT TIRES

Another potential application is the inspection of military and commercial jet-aircraft tires. Figures 35 and 36 show two types of tire in cross section. The section shown in Figure 35 is a 46 x 16 jet aircraft tire. A full scale tire with delaminations built-in at various depths in the tread and sidewall was prepared by Thompson Aircraft Tire Company. Bonded and unbonded balance pads and patches were also applied to the inner surface. All laminar-type defects were detected by slow scanning and observing the full-depth trace on the CRT of the signal analyzer. Efforts to pursuade interested agencies to extend microwave development to the inspection of large tires are strongly recommended. The one in Figure 36 is an experimental type being developed by Aerojet/Von Karman Center. It is a tubeless type with a built-in glass-epoxy filament-wound rim section. Figure 37 shows the tire on the turntable during an exploratory experiment. Only two of the glass-epoxy tires were available and both appeared free of defects.

C. POLARIS A3 FIRST STAGE NOZZLE RECEPTACLE

The POLARIS A3 first stage motors have four nozzles, recessed into the case of the motor except for the exit cones. The receptacle is protected by thick insulation to prevent the flame front from reaching any part of the

nozzle other than the entrance cone. Separations between any part of the chamber insulation and the propellant grain are considered critical. Separations are ordinarily detected by tangential betatron (radiographic) inspection, but in the nozzle receptacle area, the thick complex structure precludes a reliable inspection. POLARIS has supplied models and live motors. A special microwave probe was constructed which fits into the nozzle receptacle. K-band (18 - 26 GHz) was used for the POLARIS inspection. Figure 38 shows the microwave head and Figure 39 shows it in place on an A3 motor. Figure 40 shows typical traces which were obtained from a defect model. This model was made by casting propellant into a full-scale section of an aft head insulator. The traces are of additional interest as they show the difference between monophase and omniphase scans. The continuous curve is a monophase scan in each trace, while the vertical bars were produced by manual rotation of the phase control. The microwave probe was rotated around the nozzle in increments, and at each increment the phase control was rotated through 360°. The horn can be set to the desired depth in the nozzle receptacle. The charts were produced by an X-Y plotter whose X-axis drive is obtained from the battery and helipot visible in Figure 38. The sections of the traces in Figure 40 where the vertical bars are closely spaced resulted from reducing the increment of angular position in order to see how an automatic omniphase plot would appear. Such a trace resembles the envelope of the vertical bars. The only genuine indications are at 0° and 90°, and thus it can be seen that the omniphase plot is far easier to interpret. The monophase component results from the phase control always being returned to the same position while the microwave probe was rotated to the next position. The omniphase plot obviously eliminates two spurious peaks. The loss of signal between 90° and 270° results from the shape of the receptacle.

Although the inspection was challenging, the detection of a 0.003 in. simulated separation has been demonstrated and the results were encouraging.

D. TESTING WAVEGUIDE COMPONENTS

This program has shown a great tendency to go off in unexpected directions on its own momentum. One of the more unlikely directions is the testing of waveguide components. This was not expected, although it is logical enough. Since the original intent was to utilize existing microwave technology,

rather than to advance it, and because an elaborate and very careful experimental program would be required, the matter has not been exhaustively pursued to date. There is, however, reason to believe that the FM interferometer will be extremely useful in testing waveguide components.

The traditional method involves standing wave ratio (SWR) measurements. If a microwave source is connected to the component under test through a slotted line fitted with a movable probe, it is possible to observe the standing wave pattern produced when the reflections from the test component interfere with the signal going to the test piece. A great deal of information can be obtained in this way, but all that is obtained from a single measurement is the amplitude and phase of the reflected signal. Any number of sine waves at a single frequency can be added and the result is a sine wave at that same frequency. Only the phase and amplitude change. Furthermore, when one observes that a wave has a certain frequency and phase at a given point, there is an infinite number of combinations of sources which could have produced it. In the case of SWR measurements, an observed standing wave pattern could result from one reflecting discontinuity or an infinite number of combinations, several of which are quite likely to be found. The only way to resolve this ambiguity is to repeat the measurement at different frequencies until enough simultaneous equations are generated to obtain a unique solution, or at least one with a high probability of being the correct one. The measurements are tedious and the data reduction is complex. The SWR technique lacks range resolution, and this is the cause of much of the difficulty. In the case of coaxial lines, a type of waveguide with great bandwidth and capable of carrying DC signals, time-domain reflectometry solves the problem. With recently introduced sampling oscilloscopes, the effect of a response to several GHz is obtained with repetitive signals. A voltage step with exceedingly fast rise is sent down the line and any reflection is displayed on a sampling oscilloscope. The position of the reflector can be accurately determined and the nature of the impedance change it represents can be deduced from the amplitude and phase change of the reflection. This method is extensively used, but cannot be applied to rectangular, and other single conductor waveguide, since such guides do not have the bandwidth required.

The FM interferometer has range resolution and can show phase

shift upon reflection, and it works with rectangular waveguide as well as with coaxial. Furthermore, the equipment may well prove less troublesome than the fast-rise pulsers, precision triggers and sampling oscilloscopes needed for time-domain reflectometry.

Experience with waveguide testing using the FM interferometer was confined to examining extensions on the end of the system frequently added to meet the needs of various inspections. It is quite easy to recognize a defective horn and to tell whether the mouth is damaged, or whether the flange is loose. Some mitered elbows were constructed rather crudely as an emergency measure and differences in their quality were obvious. The problem of correcting for waveguide dispersion has already been mentioned. In general, this problem becomes more severe as the length of waveguide increases. Further work is required to provide the necessary adjustments in such generators to compensate for dispersion. Should this succeed, waveguide testing might well be one of the most important applications of the FM interferometer and should be very carefully investigated.

VI. CONCLUSIONS

As a result of the work described in this report, FM microwave interferometers have been tested in the frequency bands 1 - 2 GHz, 12.4 - 18.6 GHz, 18 - 26 GHz, and 26 - 40 GHz. Although not tested, it can be assumed that the bands from 2 - 12.5 GHz are equally usable, and it is probable that the technique is applicable below 1 GHz and above 40 GHz, at least for some purposes.

As a nondestructive test instrument, the FM interferometer has been studied in laboratory tests well enough to allow estimates of performance in selected inspection applications. Generally, it appears that the most promising applications are the detection of laminar defects in non-metallic structures, and the determination of such properties of materials as refractive index and perhaps eventually absorption. The testing of waveguide components is also a very promising application. The inspection of solid propellant grains for very small voids and porosity would not provide much sensitivity. On the other hand, the detection of cracks, and especially separations of grain from case insulation would be a very good application for the FM interferometer.

Even in cases where high energy radiography is already in use and giving satisfaction for such an inspection, the microwave inspection could be extremely useful. Since the radiographic detection of a separation requires that the X-ray beam be directed at the edge of the separation, a cylindrical object such as a rocket motor requires tangential inspection. A conical object such as the ablative nozzle skirt discussed in this report requires the same treatment. Each exposure shows the condition along a line only, so that area coverage with a finite number of exposures is impossible. And, if the beam does not pass through the defective area at the tangent, the exposure is wasted. With a finite number of exposures, this becomes a hit-or-miss proposition for concealed flaws. The inspection of Polaris A3 motors is a good example of this, and any other motor with a non-metallic case would fall into the same category. The ideal method would be to screen all motors by microwave inspection prior to radiographic inspection; no tangential exposures need to be made except where microwave inspection indicated unusual conditions. There the radiographs would be utilized to their full potential for showing-up the details of the flaw. The area information, which radiography does not supply in tangential inspection would be obtained from the microwave inspection. For subsequent inspection of the same motor after storage and handling, microwave inspection alone could indicate whether there had been any increase in the area of separation. This would result in considerable improvement in accuracy, speed and economy.

The measurement of refractive index shows surprising accuracy and convenience. This is an application which should be investigated further and an effort should be made to determine plane wave attentuation similarly. These measurements might well be useful both in general laboratory work and as process controls in polymer chemistry. The latter operation could probably be made largely automatic and might be done on the processing line rather than in the laboratory.

The testing of waveguide components is a promising but essentially unexplored field of application. It is definitely worth further study.

Moisture detection is also a good prospect as water has an anomalously high dielectric constant and very high absorption. There also appears to be a great difference between absorbed water and that actually included in crystalline structure.

In summary then, it can be said that a second generation instrument has been produced which has, in laboratory tests, successfully inspected production parts. One third generation instrument is now in use for production inspections and others are contemplated. In addition to flaw detection, there is a good prospect of producing versions suitable for measuring refractive index and microwave absorption. Finally, a version for testing waveguide components can probably be developed. The following list contains what are now considered the most promising applications not yet investigated:

a. Testing of waveguide components.

b. Process control in polymer chemistry (measurement of refractive index and absorption).

c. Moisture detection.

d. Radar altimeters.

e. Soil studies and detection of water-filled fissures in hard rock tunneling operations.

The frequency domain microwave interferometer has now been developed to a sufficient degree that it is quite reasonable to consider it available to the nondestructive test engineer. As might be expected, there are many variations in technique to be investigated and since there have been continuous improvements, no definite set of performance limits is yet available. Nevertheless, there are quite a number of inspection tasks which the instrument can perform and the reports of this contract should suffice to identify those to which it is certainly applicable.

The most promising applications are those involving laminar dielectric structures in which separations and delaminations are the common defects. Epoxies, phenolics and similar resins are quite transparent to microwaves, and if they are reinforced with filaments, cloths or tapes of glass, asbestos, or some similar materials, they remain so. (Metallic or carbon fibers, being conductive will render the composite opaque to microwave energy.) Voids and regions in which the resin does not fully impregnate the filler or reinforcement can be detected as flaws. Some bulk properties can also be measured. The microwave refractive index can be measured as a nondestructive test and may correlate with other properties.

Large volumes of material, such as a solid propellant grain can in some cases be inspected. Present formulations usually involve an organic binder such

as polybutadiene or polyurethane with a large quantity of solids such as aluminum powder and oxidizer such as ammonium perchlorate. These propellants vary in their transparency to microwaves, depending upon many factors. Aluminum, even at rather high concentrations increases refractive index more than absorption if it is in the form of powder. Propellants with fine wires or staples are generally opaque. Cracks and voids are detectable as flaws and porosity is sometimes detectable as a variation in refractive index and absorption. Many propellants do not change refractive index to any great extent upon curing. The change in absorption is slight, and the FDI does not yet furnish a really precise absorption measurement. This means that uncured grains may be inspected, but also means that the FDI is not very useful for monitoring that cure.

In connection with solid-propellant rocket motors, one of the best applications deserves special mention. Motors with non-metallic cases are readily examined with the FDI for separations between the grain and the case insulation. This defect, in certain regions of the motor can provide a disastrous increase in burning area when the flame front reaches the separation. Case-grain separations have caused a great deal of trouble in many solid-propellant rocket programs, and inspecting motors for this defect can involve substantial effort both in the manufacturing plant and the field. High energy radiography is the technique employed. No radiographic technique now in use can give 100% area coverage since the inspection is tangential and only shows the band in cross section. Strictly speaking the area covered is zero, the line data being converted to area by assuming the line representative of finite area. This is of course a valid assumption but one must then assume a shape and size for the separated region, and this is pure conjecture unless an exceedingly large number of exposures are made.

A much better and more economical method would be to inspect the entire motor with the microwave FDI and record a defect map immediately after cure. This would identify all suspect areas. Radiographic inspection could then show details in those suspect areas. Subsequent inspections could be confined to the identified separations in most cases, and it would be possible to detect growth of separations far more easily than with radiography.

Such an inspection, combining microwave and radiographic methods would be better by far than either one separately, and both faster and more economical than radiography alone, since radiographic exposures would be made only where defects are present. In fact, motors well within the accept limits on separations would probably require no tangential radiography. One of the tests described for the hand-held probes involved the detection of such separations in an A-3 Polaris motor specimen.

The design and operation of the microwave frequency domain interferometer has now progressed sufficiently that nondestructive test engineers should be able to apply it where it is capable of making a contribution to their testing program. The body of knowledge derived from these microwave studies has been incorporated into an Applications Guide and published under separate cover. This Guide is designed to assist the NDT engineer in determining the applicability of microwave testing to his inspection and development problems.

DISPLAYED FUNCTION

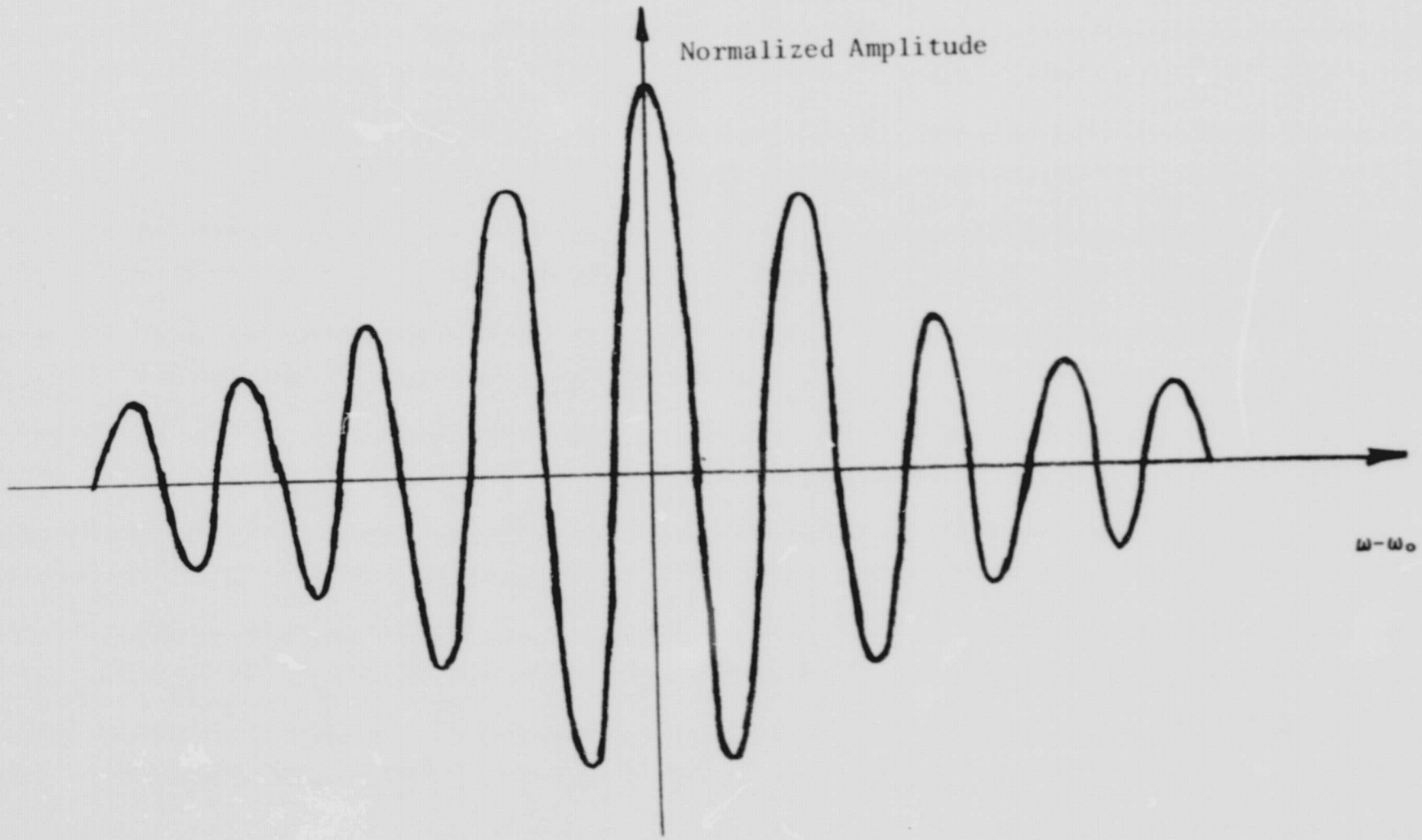

Figure 1

MULTIPLEX ANALYZER

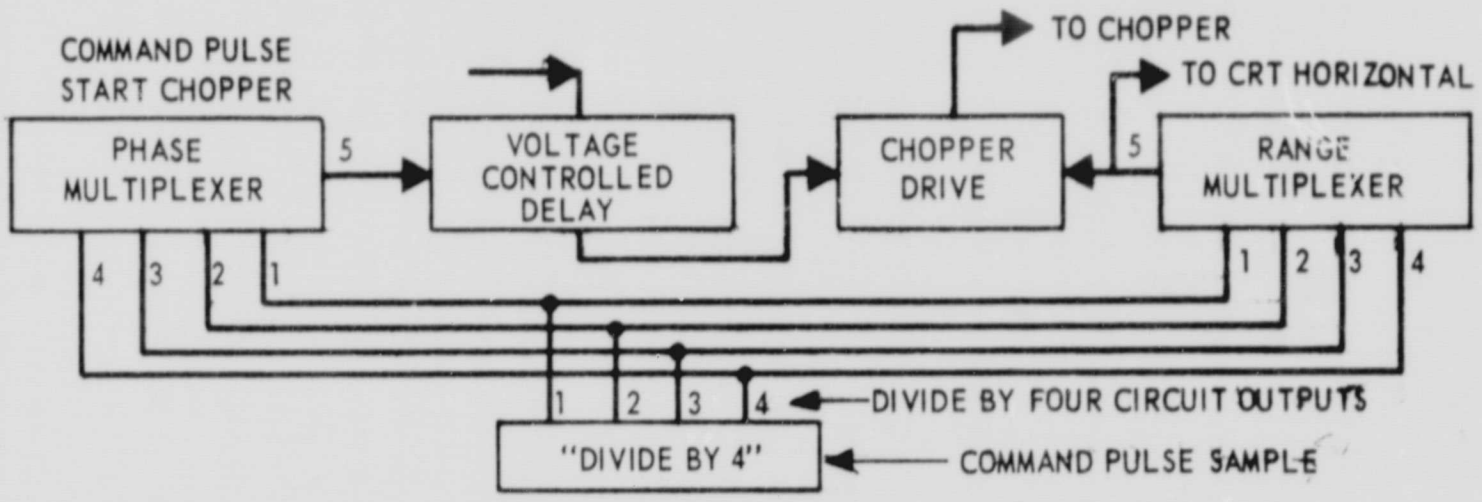

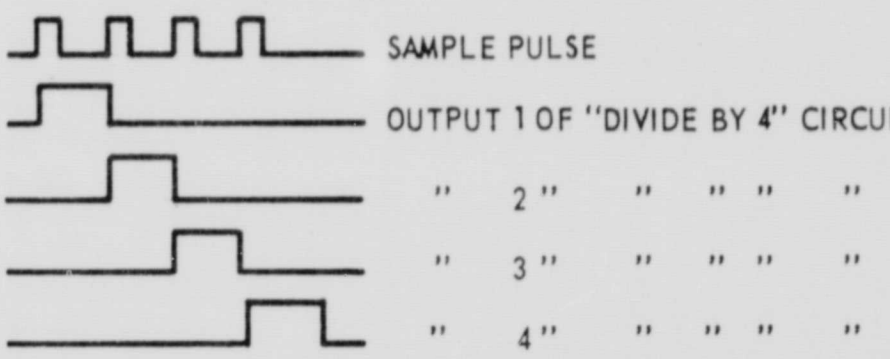

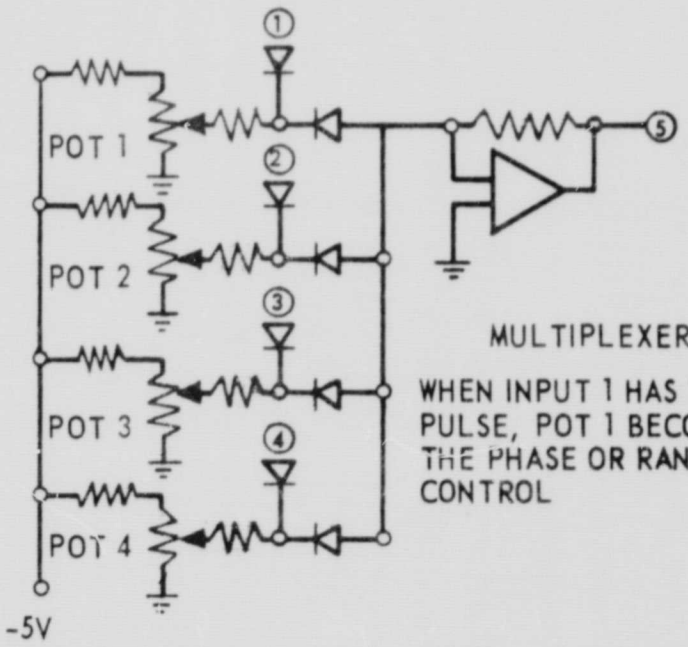

MULTIPLEXER

WHEN INPUT 1 HAS THE PULSE, POT 1 BECOMES THE PHASE OR RANGE CONTROL

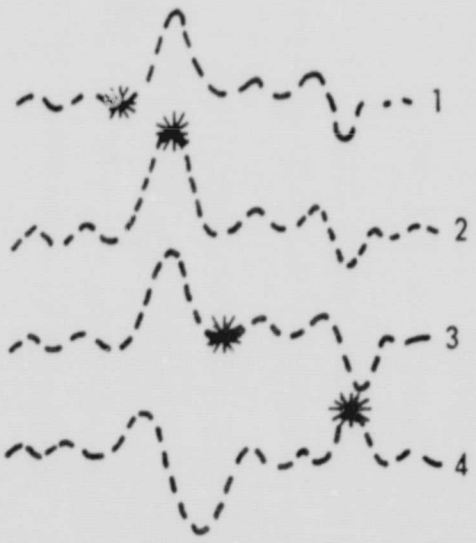

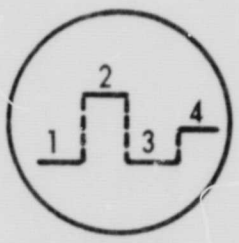

DISPLAY

Figure 2

SIMPLEST WAVEGUIDE SYSTEM

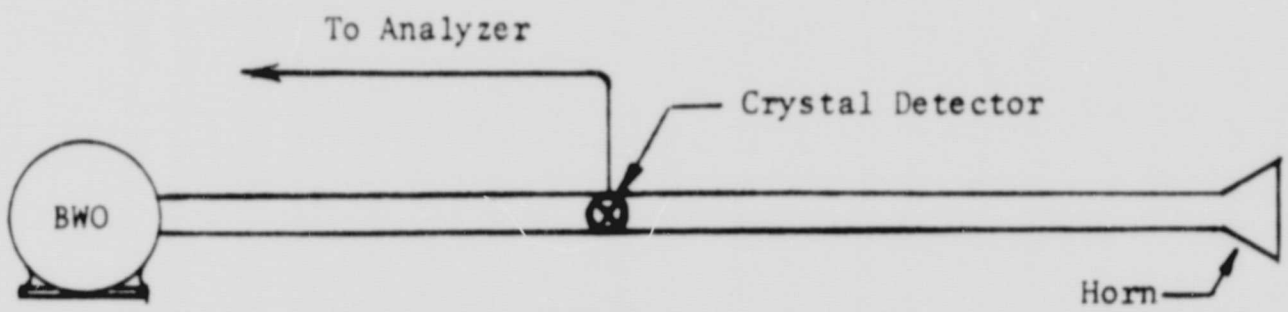

Slotted Line

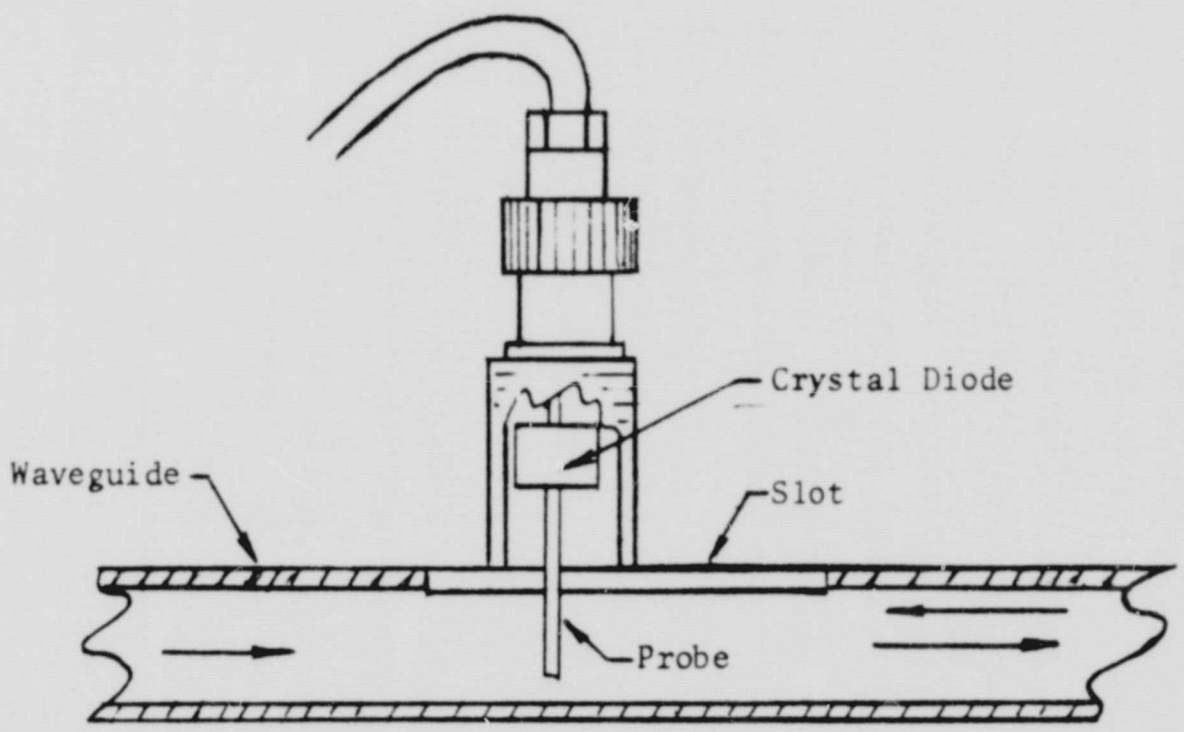

Isolator cannot be used on this side; Signals go both ways

Coaxial Mount

Deep probe penetration required for a strong signal gives rise to large reflections

Figure 3

FORMS OF WAVEGUIDE SYSTEM

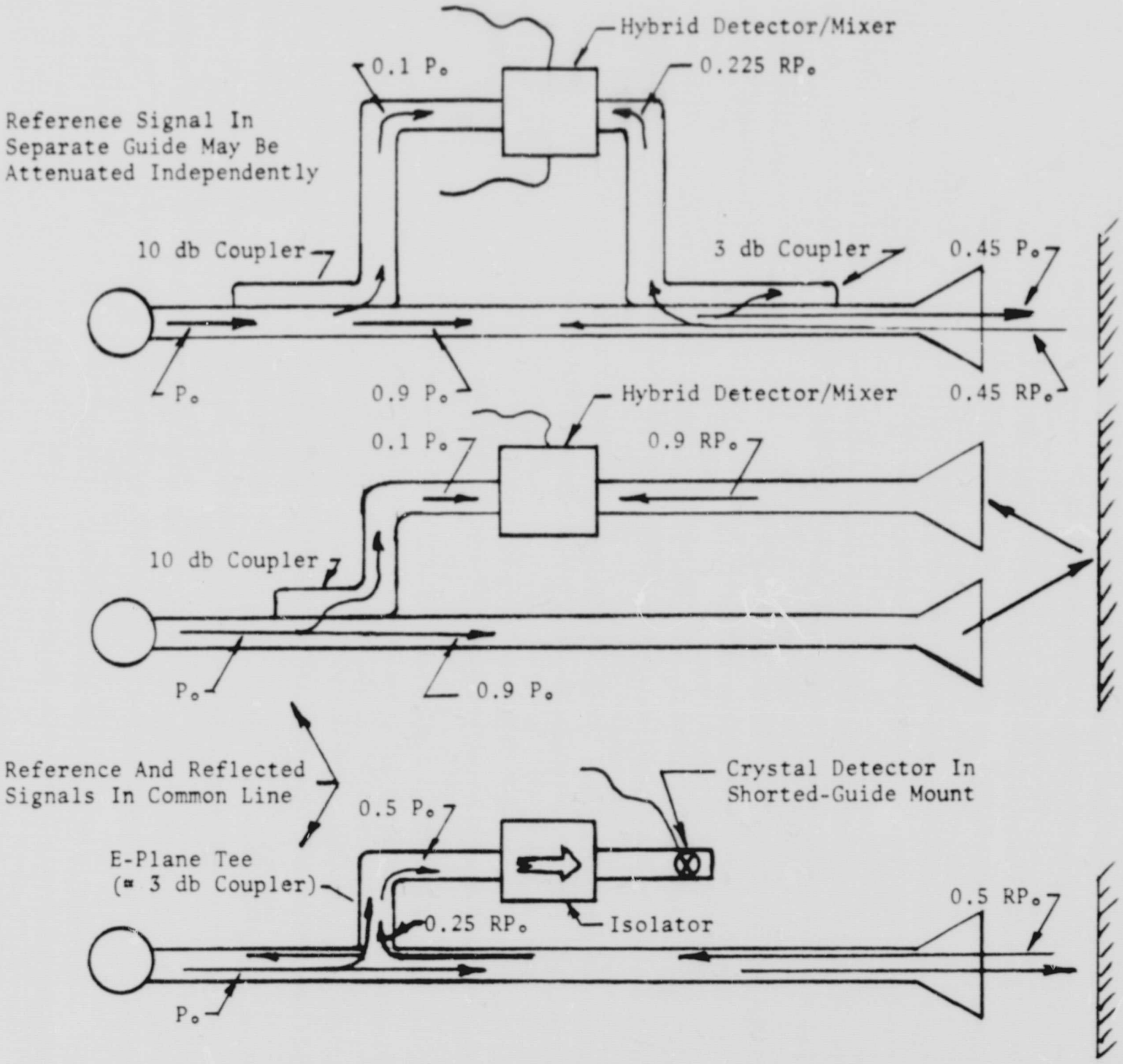

P_o is the power output of the microwave oscillator.

R is the fraction of radiated power returned to the horn.

Figure 4 Sheet 1 of 2

FORMS OF WAVEGUIDE SYSTEM

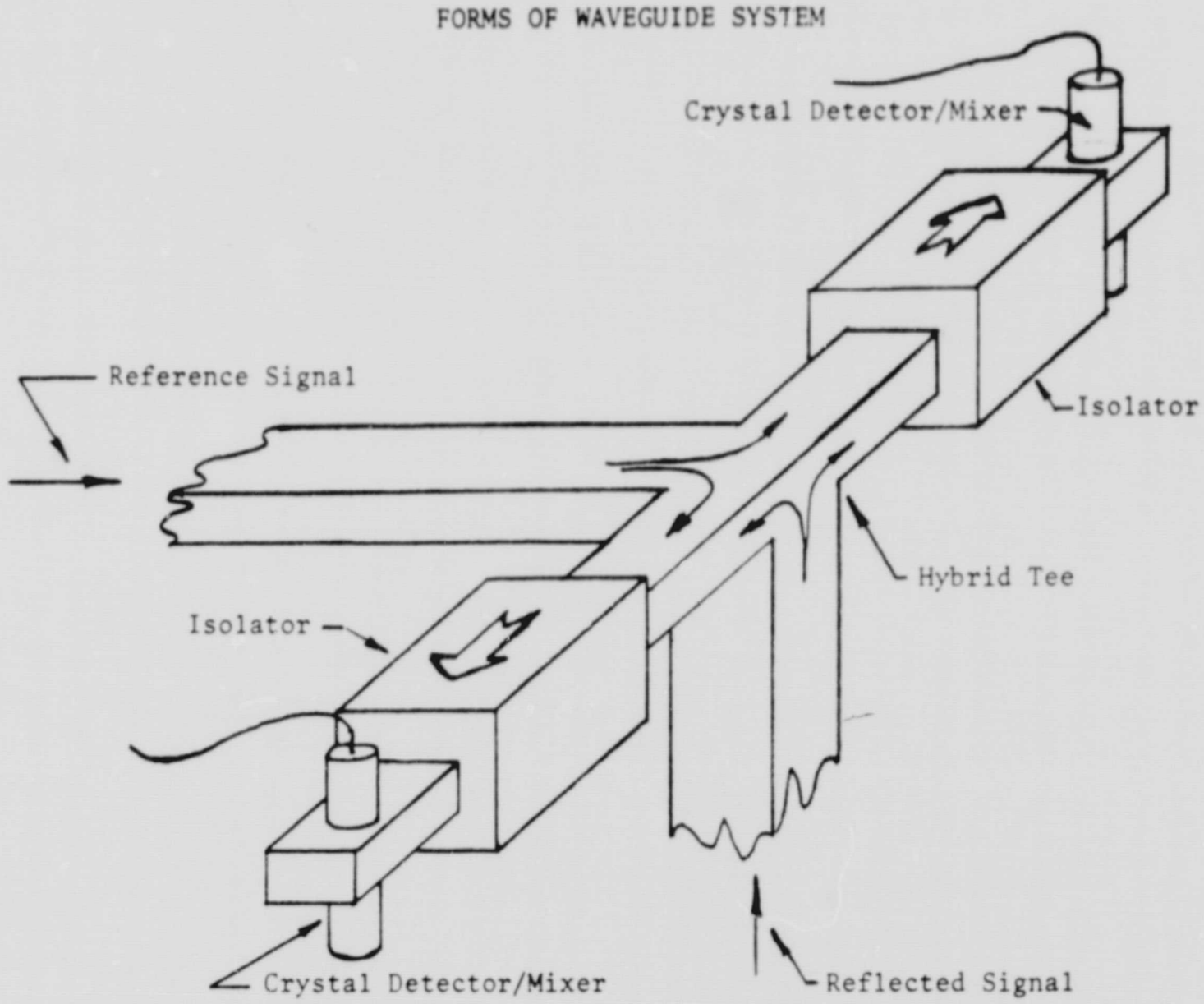

Detail Of Hybrid Detector/Mixer

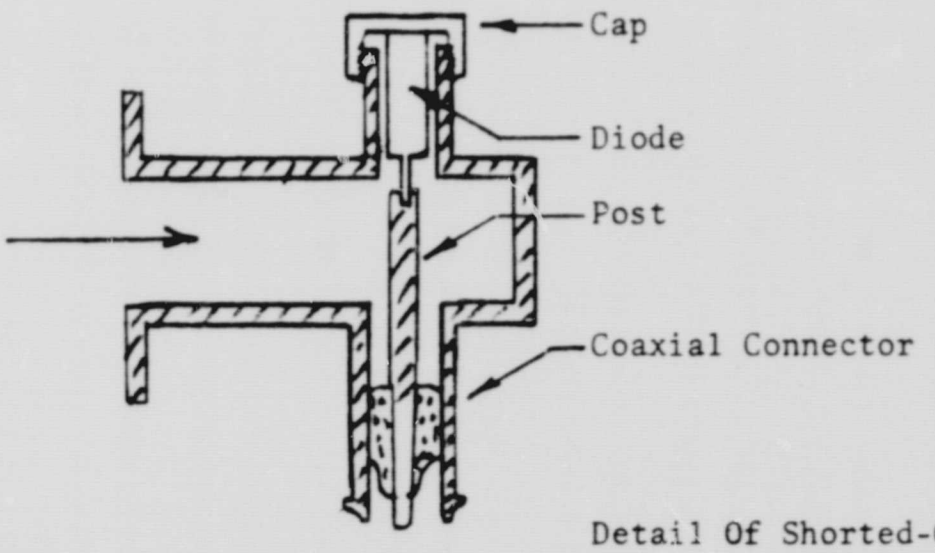

Detail Of Shorted-Guide Detector Mount

Figure 4 Sheet 2 of 2

HAND PROBE

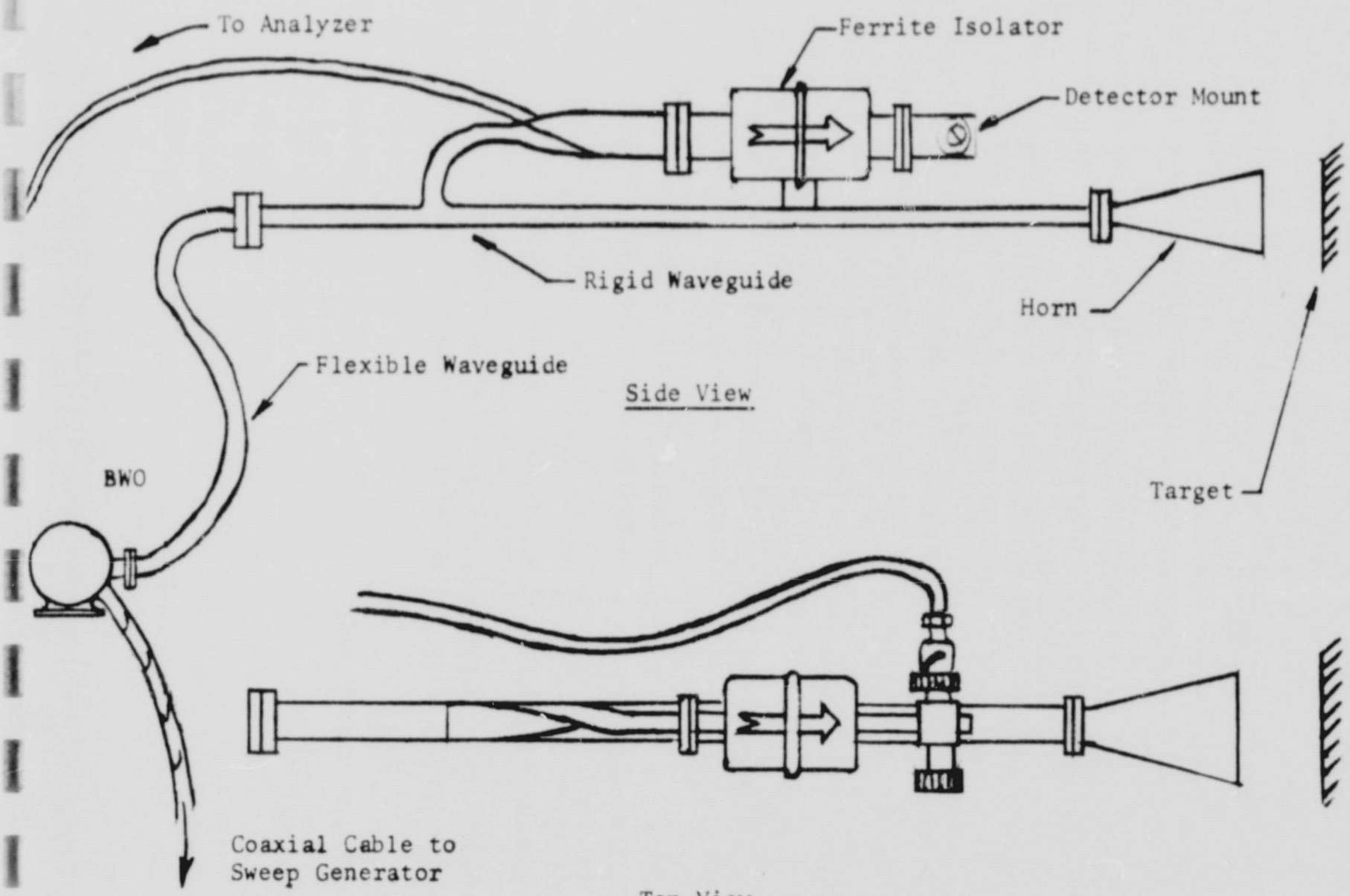

Figure 5

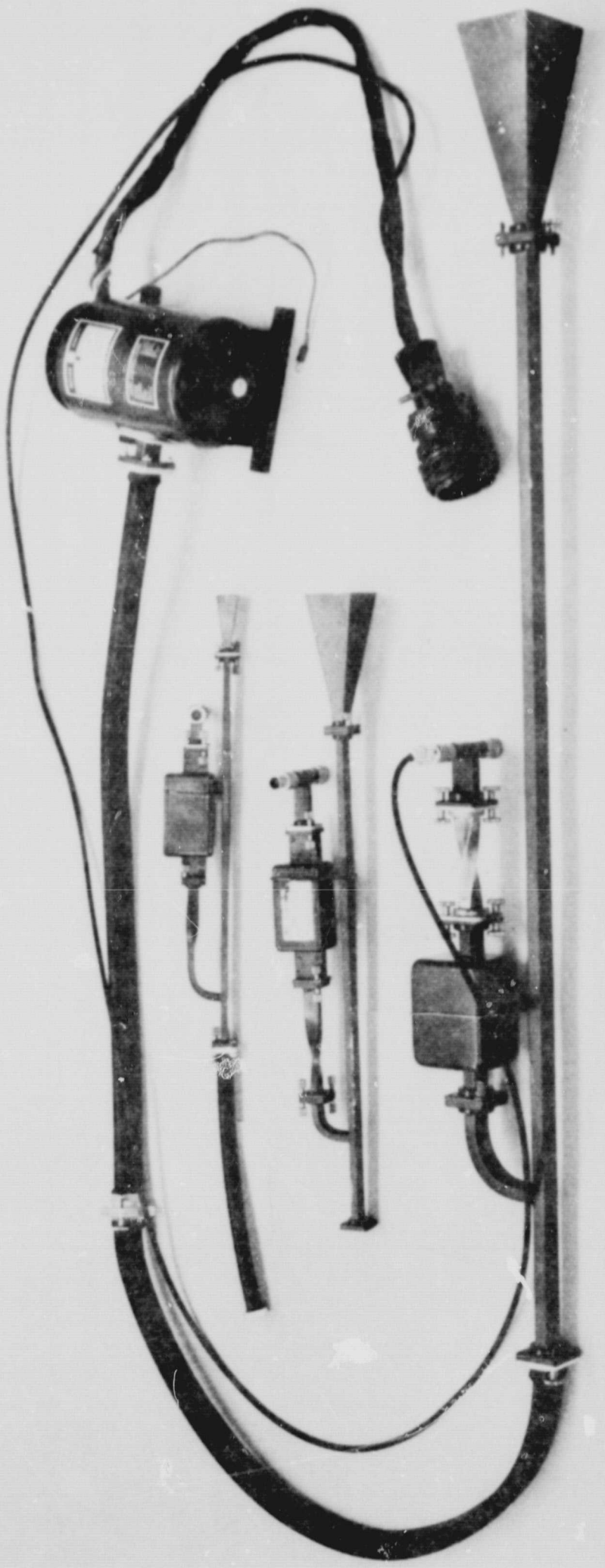

Figure 6

FREQUENCY GENERATION ALTERNATIVES

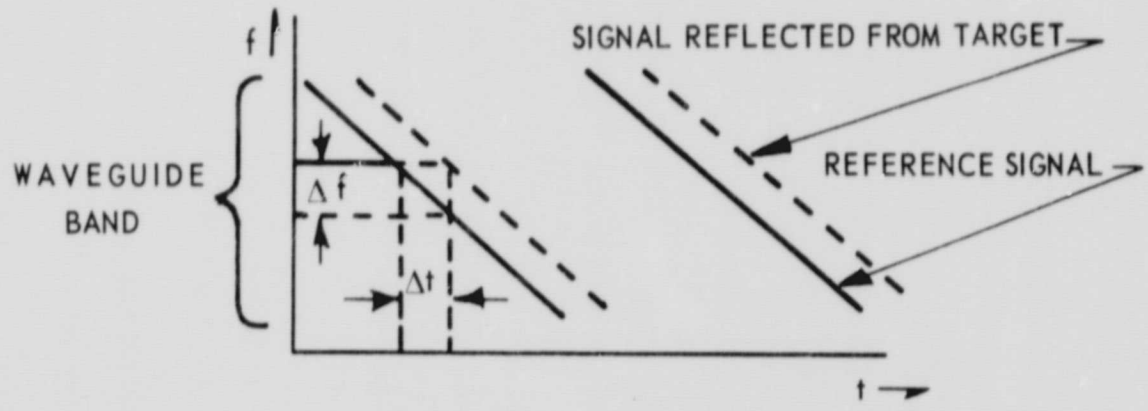

A. ORIGINAL METHOD

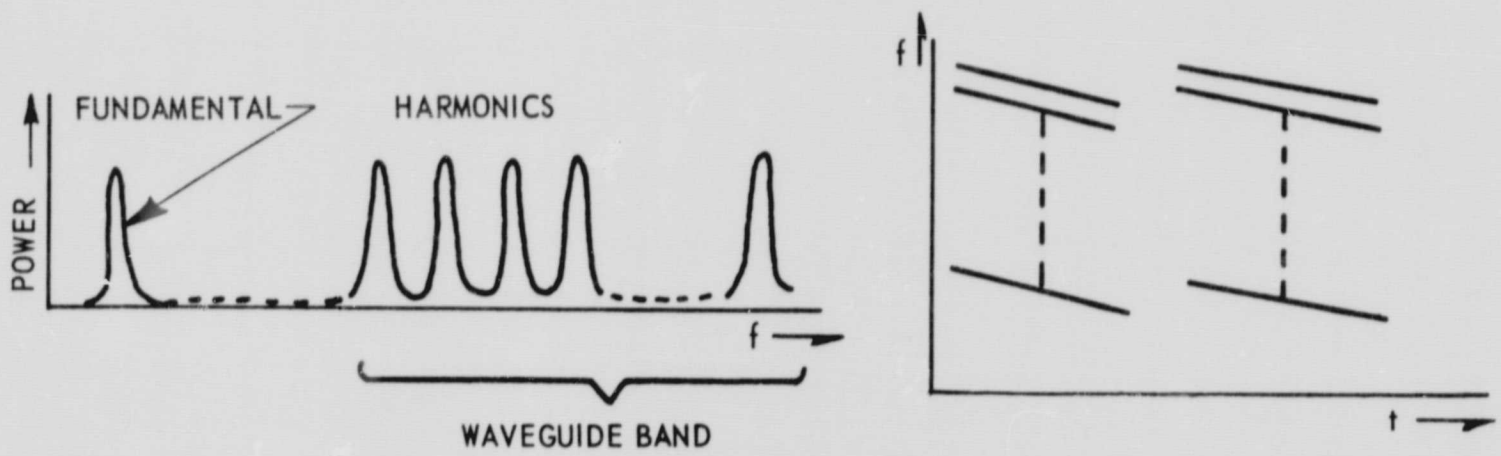

B. HARMONIC COMB METHOD

Figure 7

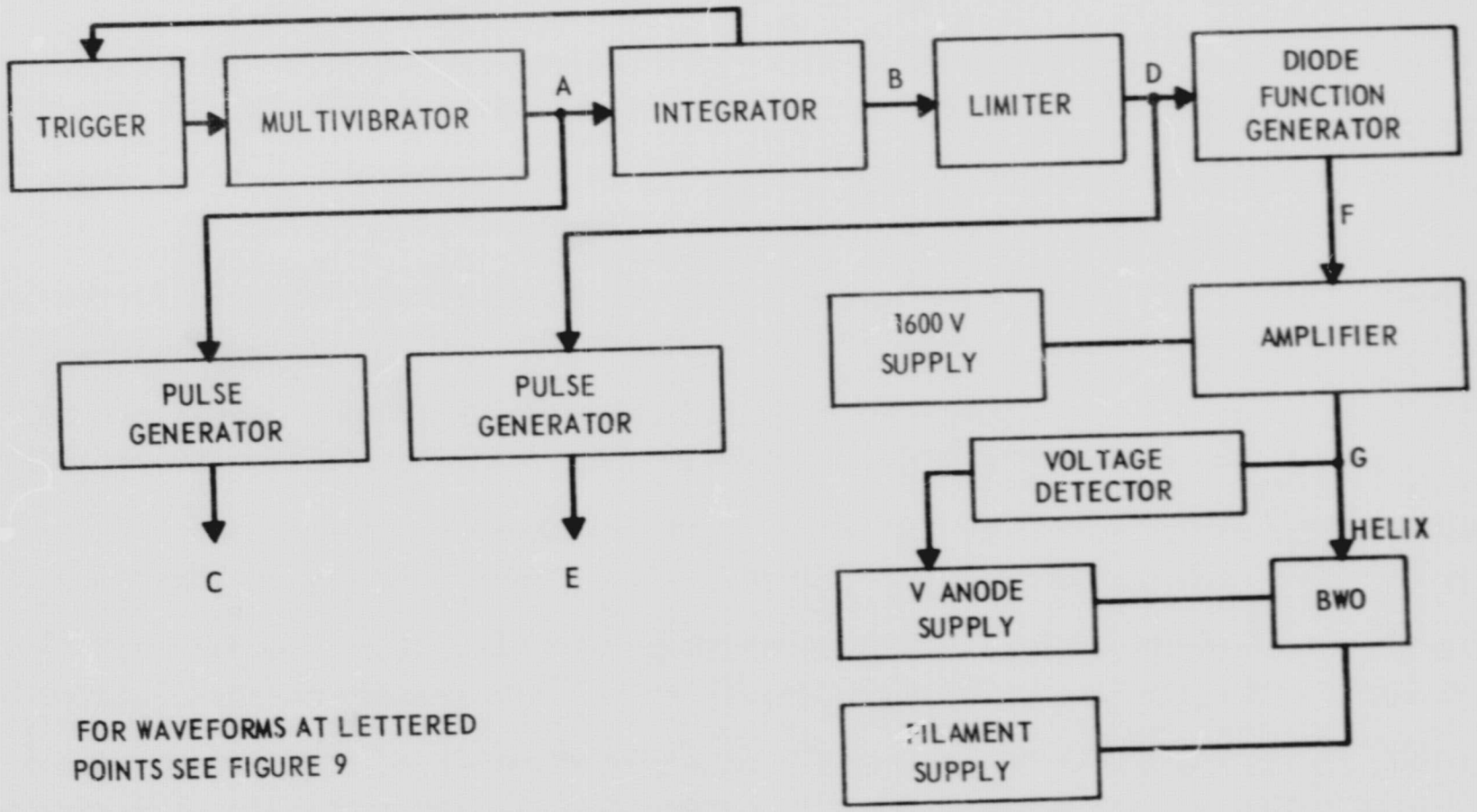

Figure 8

BLOCK DIAGRAM OF SWEEP GENERATOR

WAVEFORMS IN SWEEP GENERATOR

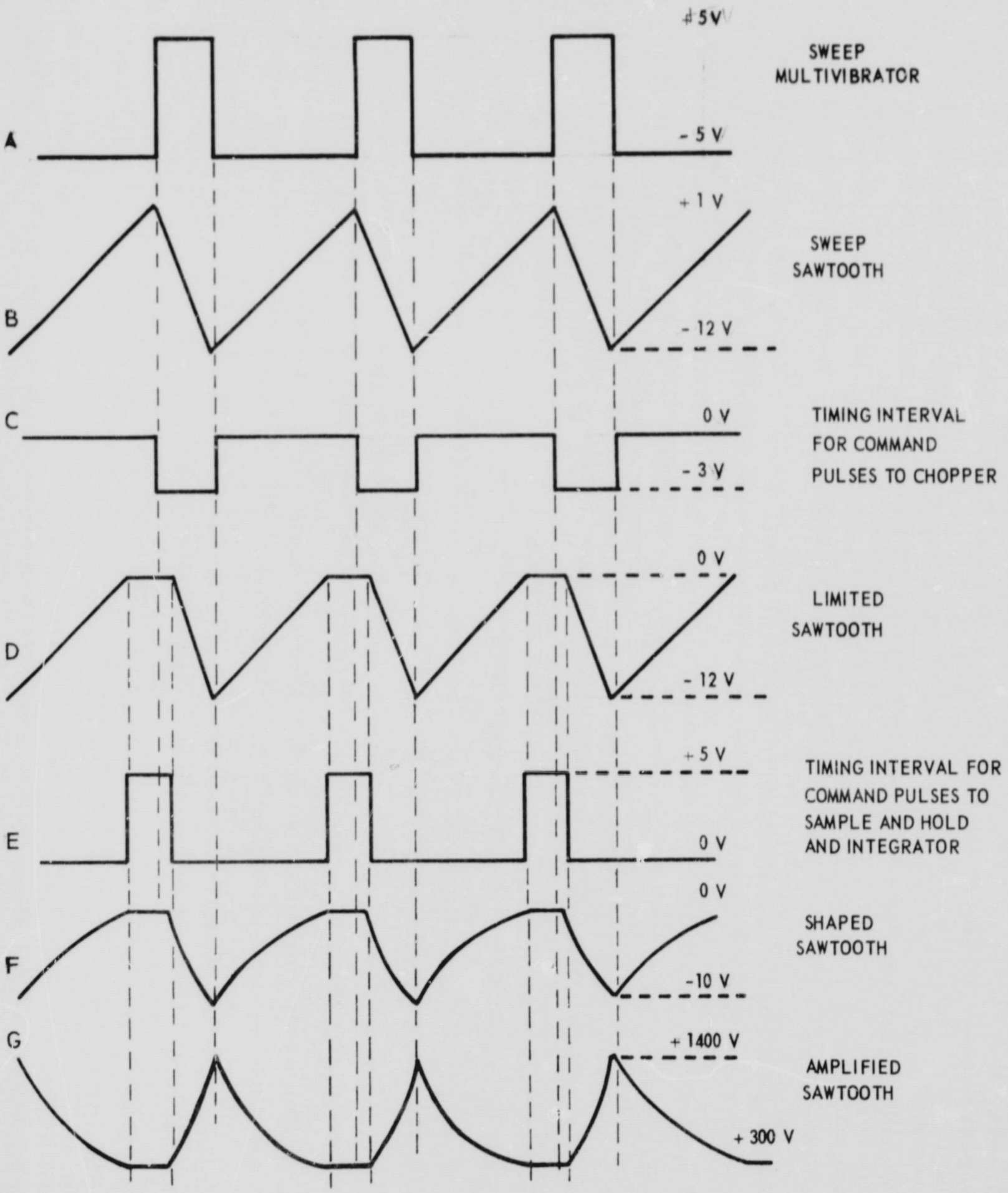

Figure 9

OSCILLOSCOPE PRESENTATION OF A SINGLE REFLECTOR

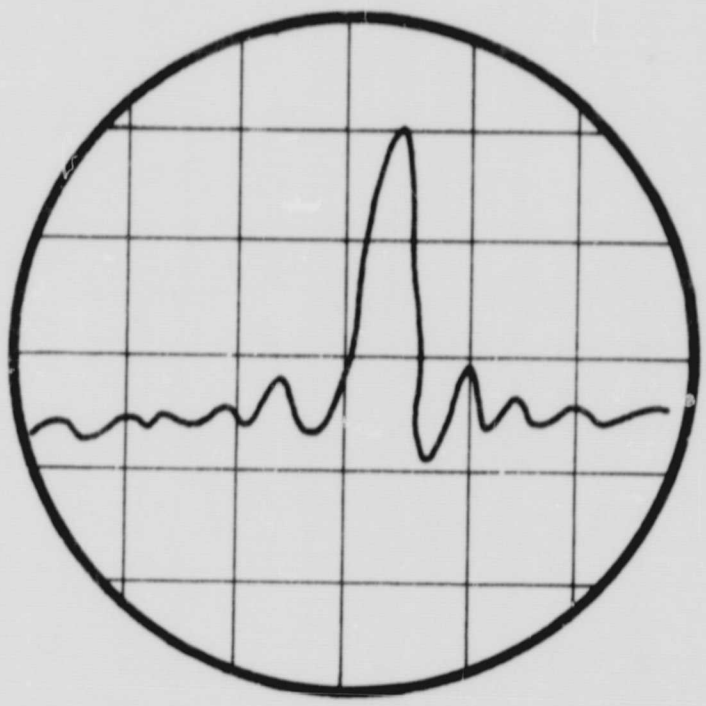

Figure 10

WAVEGUIDE SYSTEMS

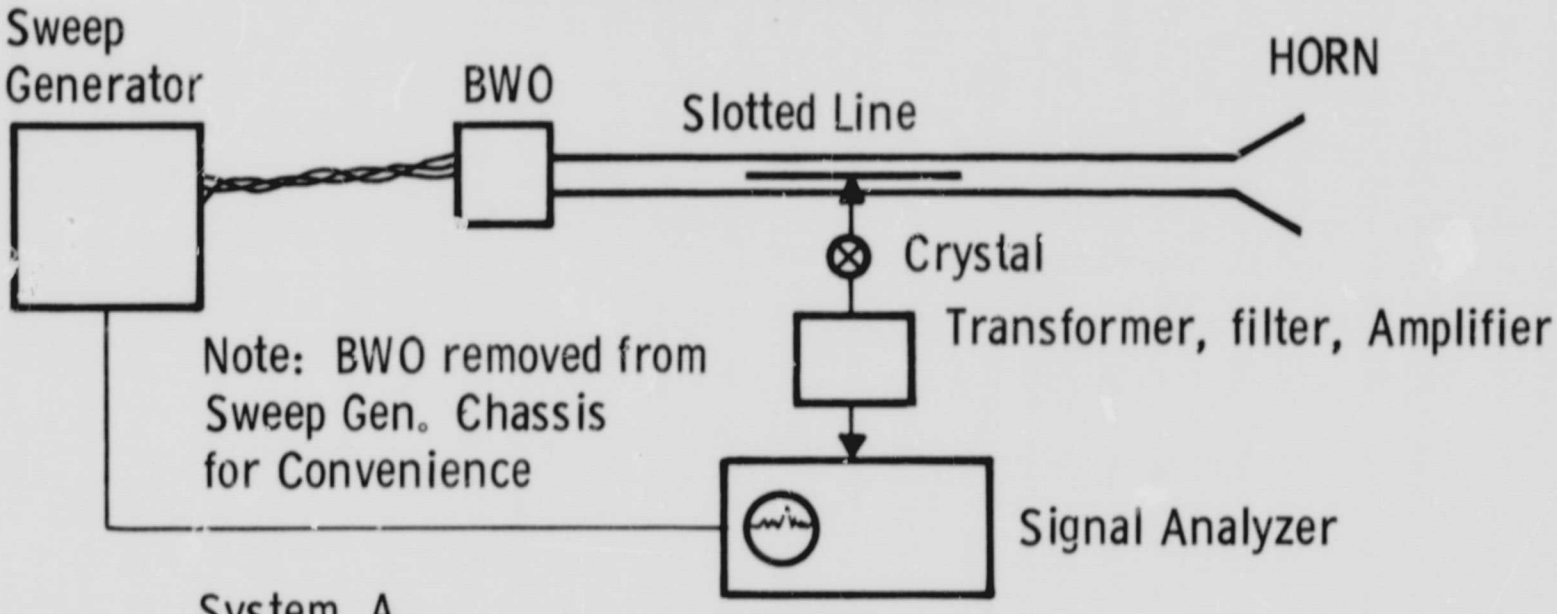

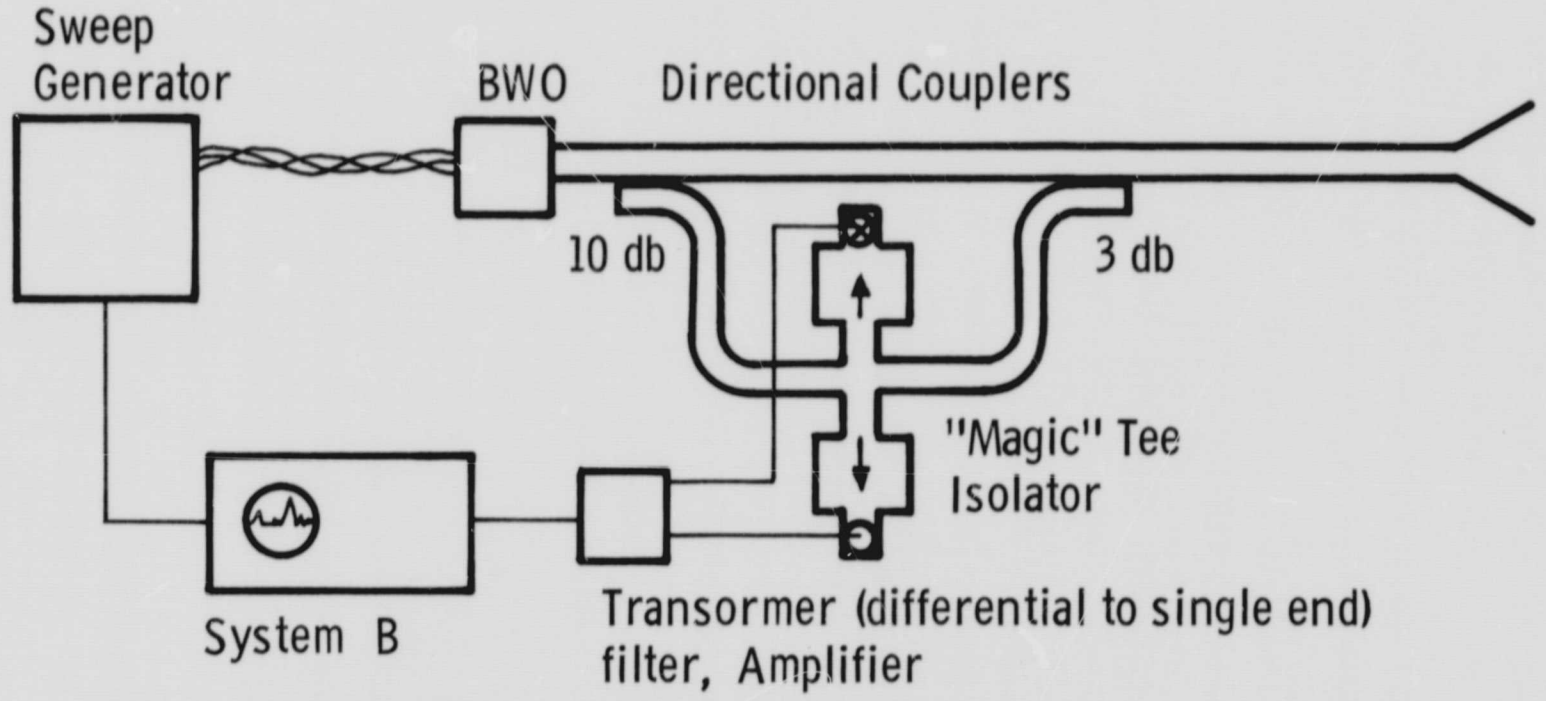

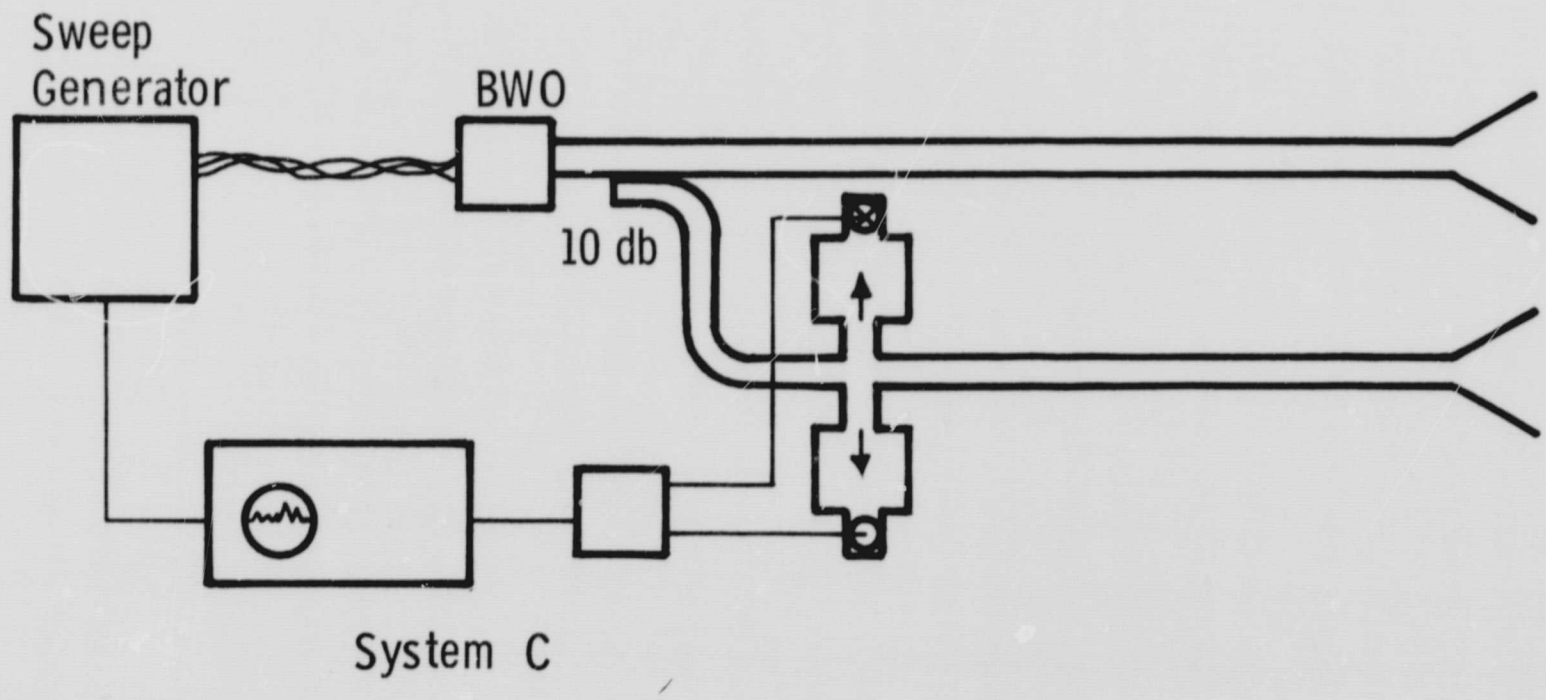

Figure 11

PRIMARY DISPLAY PATTERNS USED IN ESTABLISHING A FIXED-DEPTH C-SCAN

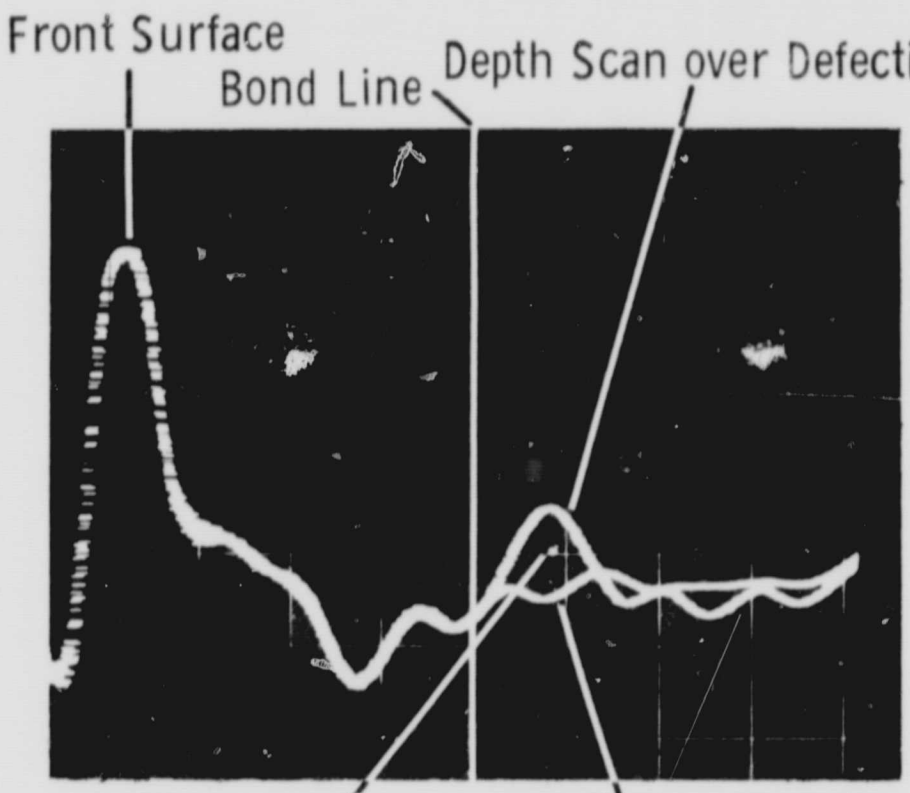

The Defect map is made by scanning across specimen with the signal analyzer set as shown above the DC level (vertical position of Spot) is recorded

Figure 12

RANGE INDICATION BY MONOPHASE DEPTH SCANS

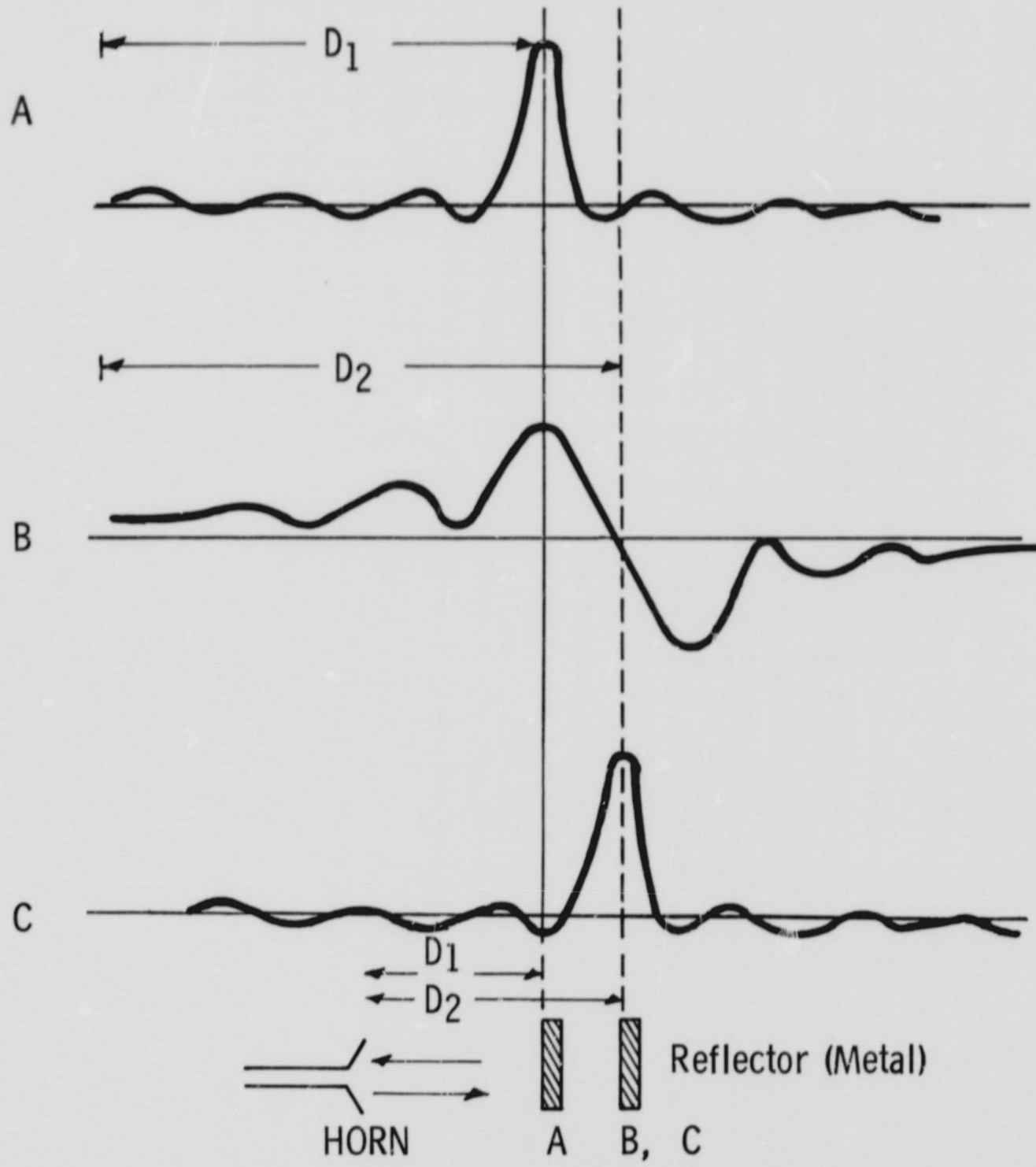

B & C Show the indications obtained when the target range is increased (in this case by 1/4 the wave length of the initial frequency of the microwave sweep. Trace B results if the Phase control is left unchanged as range increases, C is result of restoring the display to positive peak form. Note that range indication is preserved when phase adjustment is made.

Figure 13

OMNIPHASE DEPTH SCANS

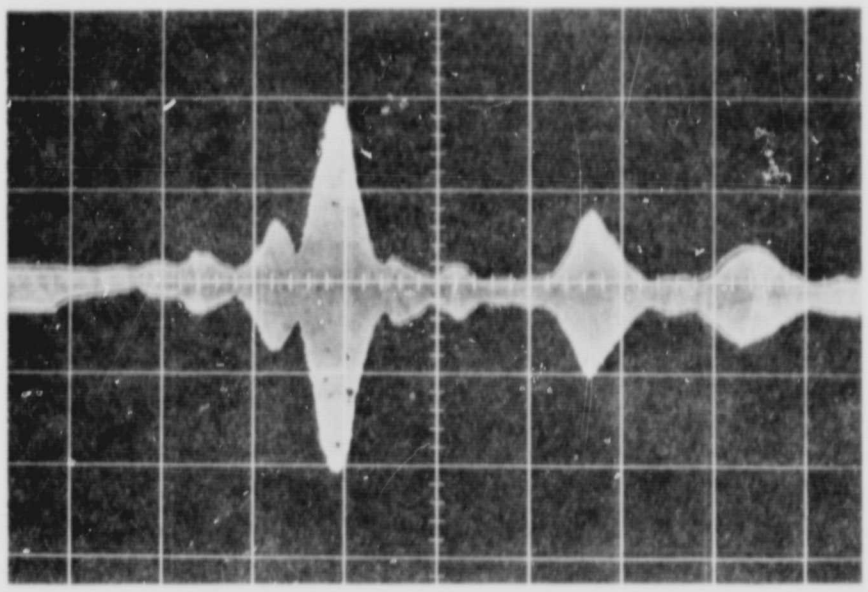

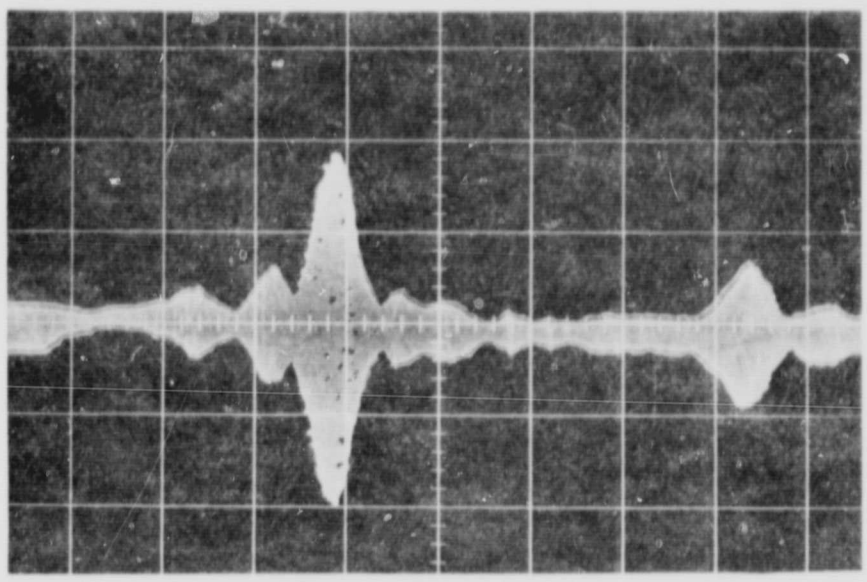

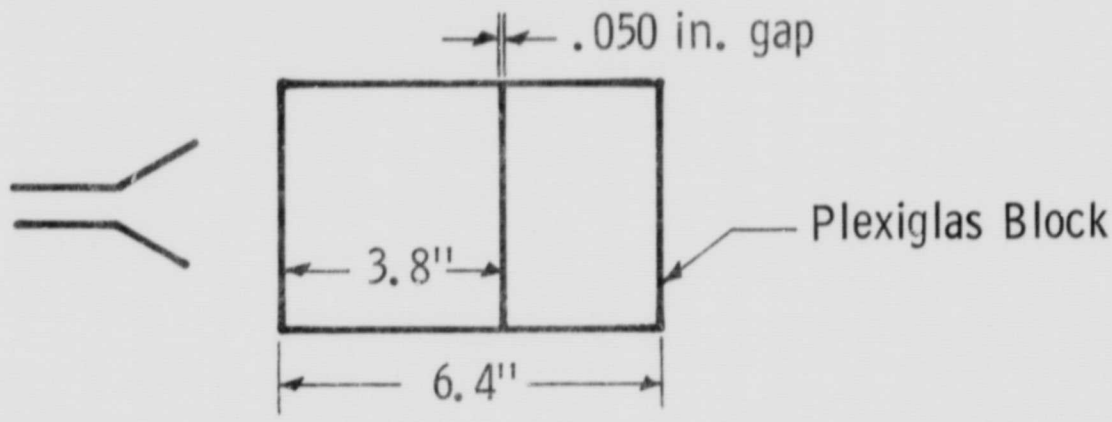

All omniphase traces have the same general form regardless of horizontal position. Compare with the monophase scans shown in Figure 3.

Figure 14

RANGE CALIBRATION Ku BAND TWO-HORN SYSTEM

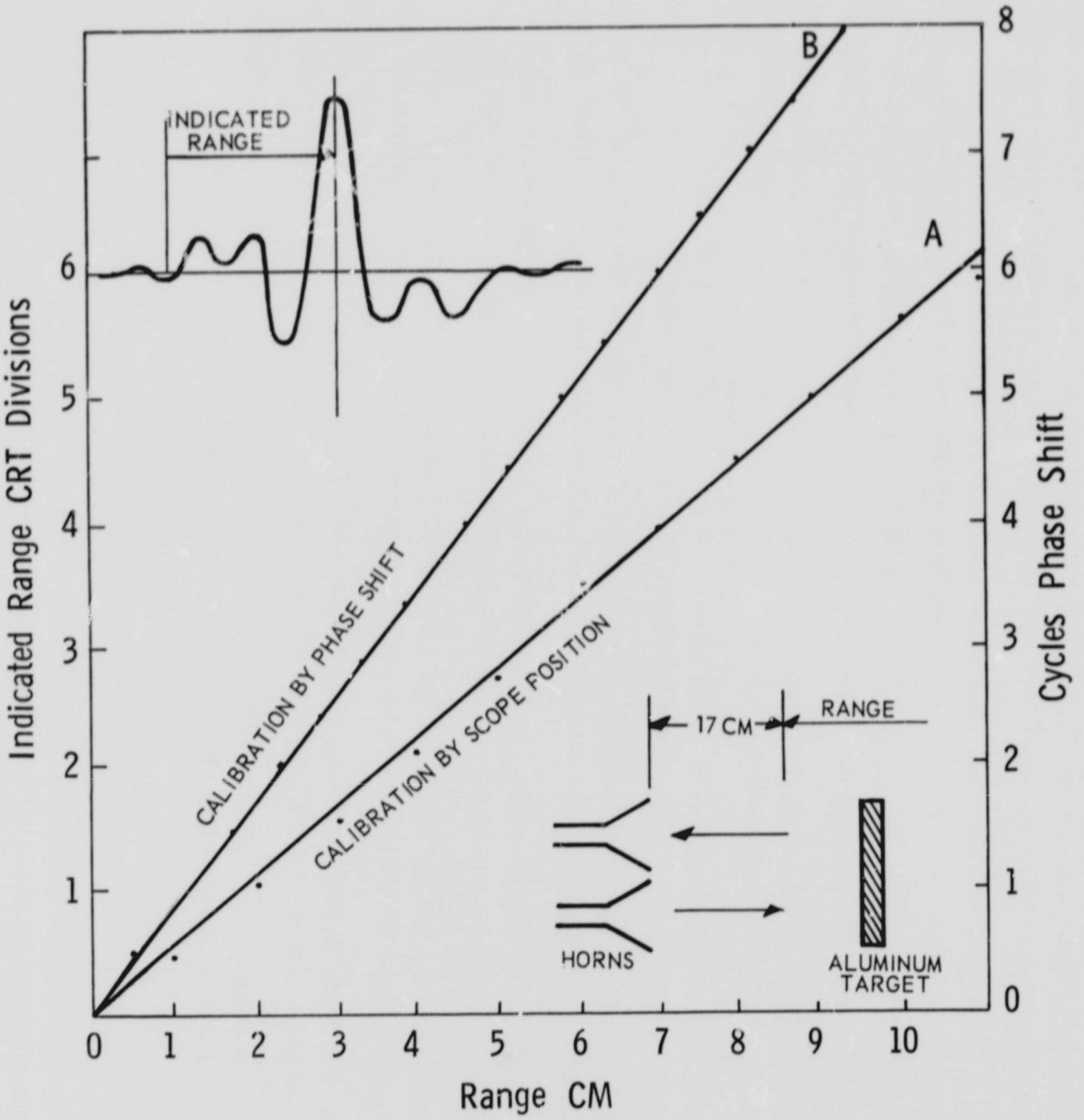

Figure 15

EFFECT OF MULTIPLE REFLECTIONS ON RANGE RESOLUTION

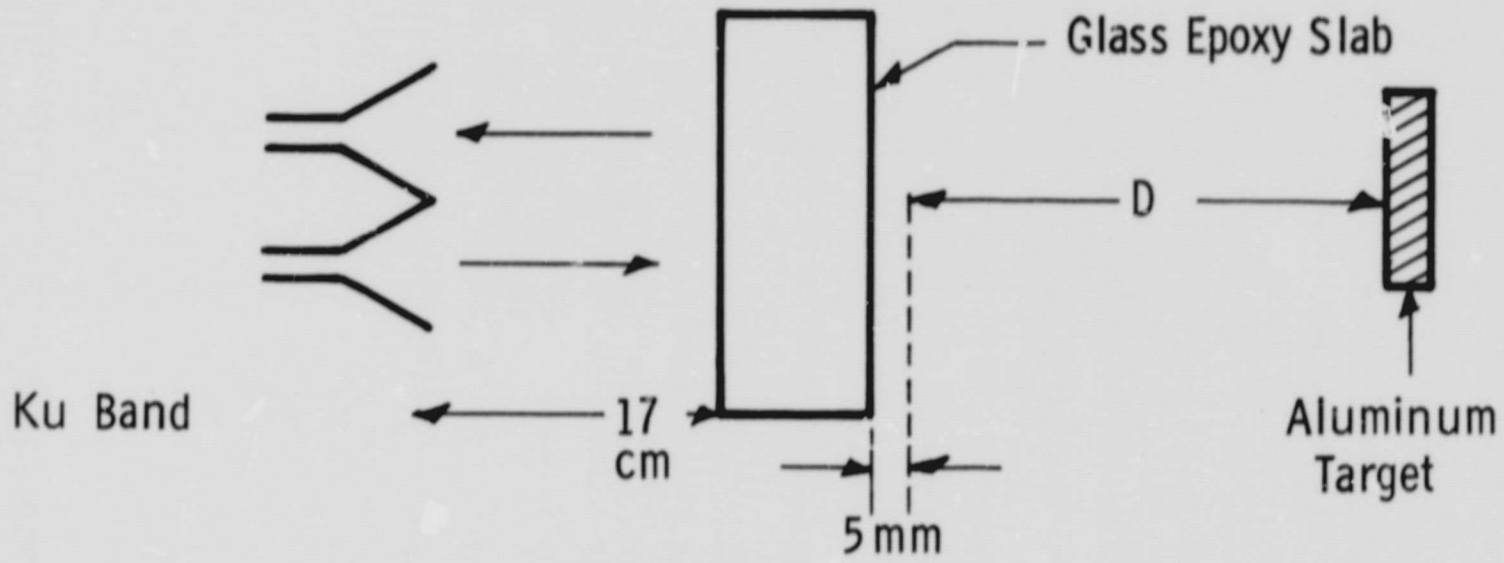

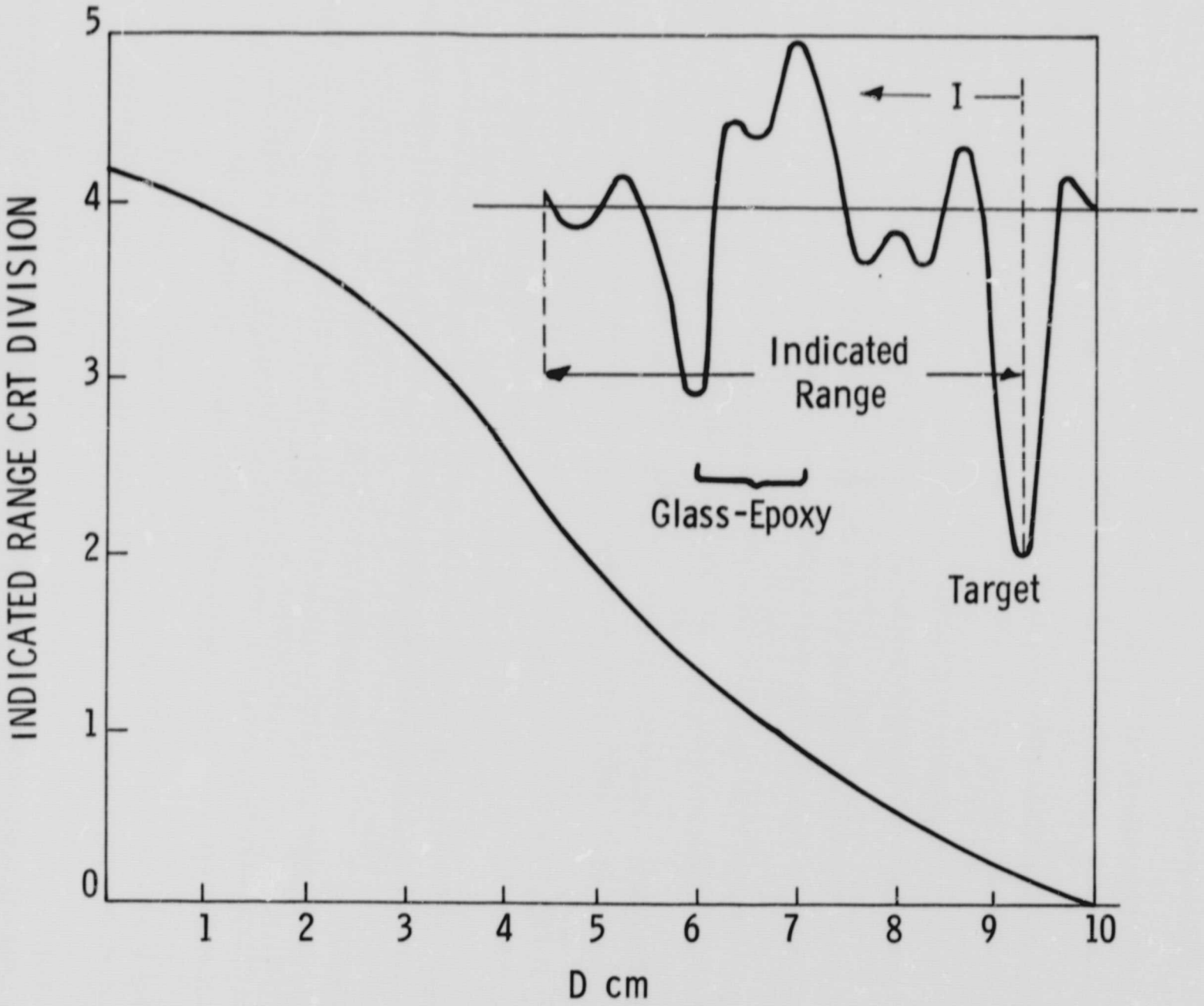

Figure 16

HORN SPECIMEN REFLECTOR ARRANGEMENT

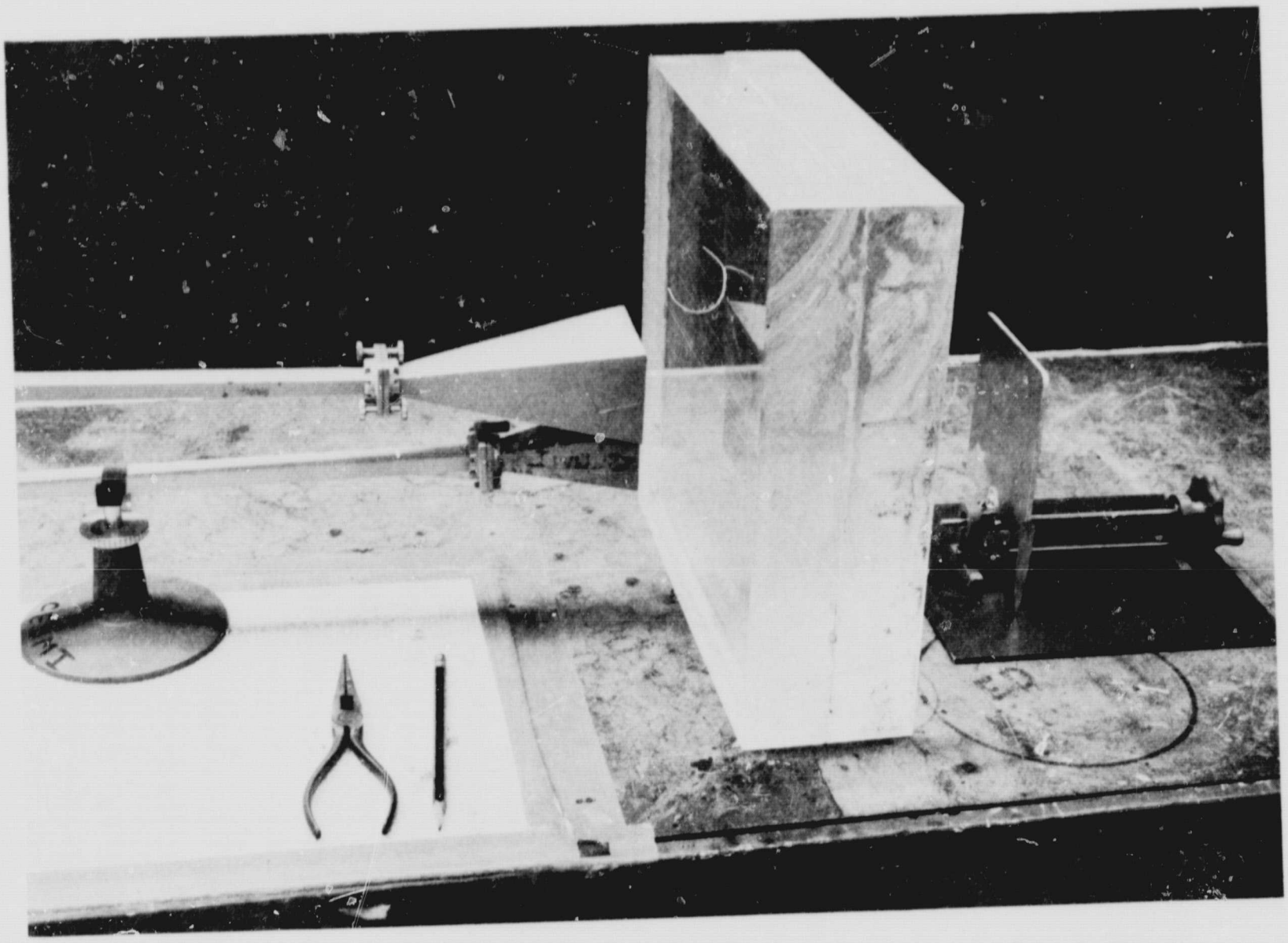

Figure 17

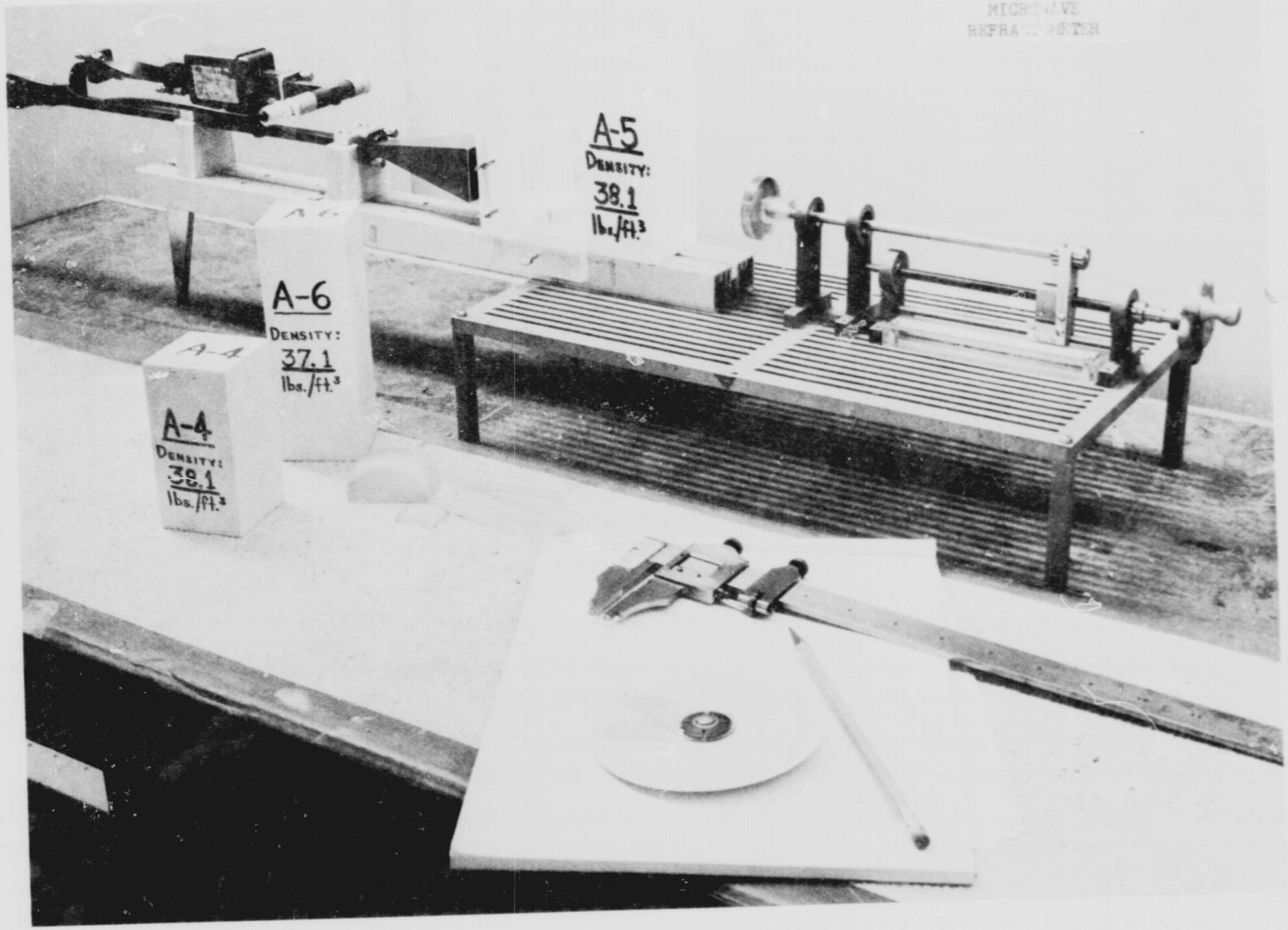
MICROWAVE
REFRACTOMETER
A-5
DENSITY:
38.1
lbs./ft.³
A-6
DENSITY:
37.1
lbs./ft.³
A-4
DENSITY:
38.1
lbs./ft.³

Figure 18

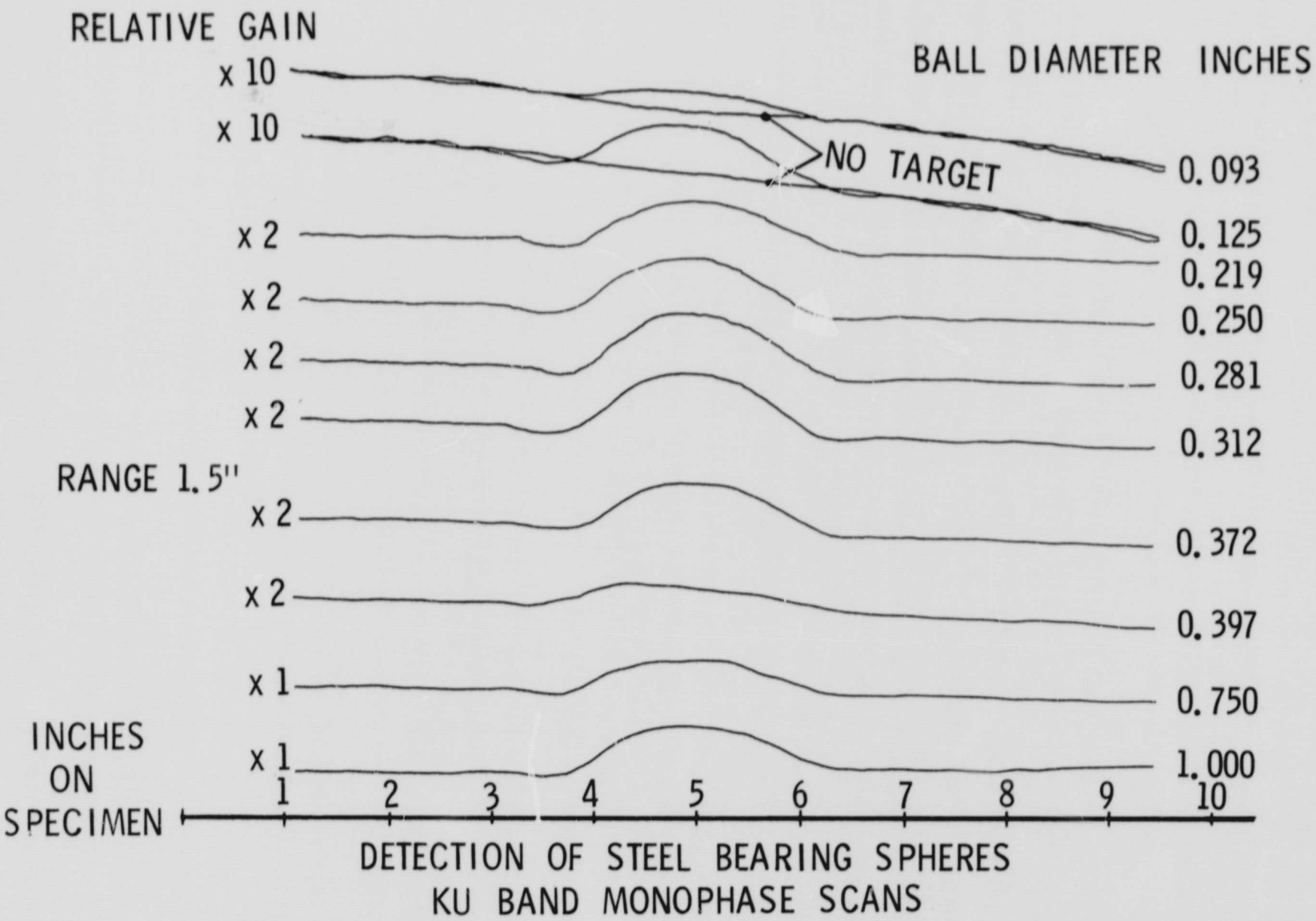

DETECTION OF STEEL BEARING SPHERES
KU BAND MONOPHASE SCANS

Figure 19

THEORETICAL RADAR CROSS SECTION OF A SPHERE

a = Radius; λ = Wavelength

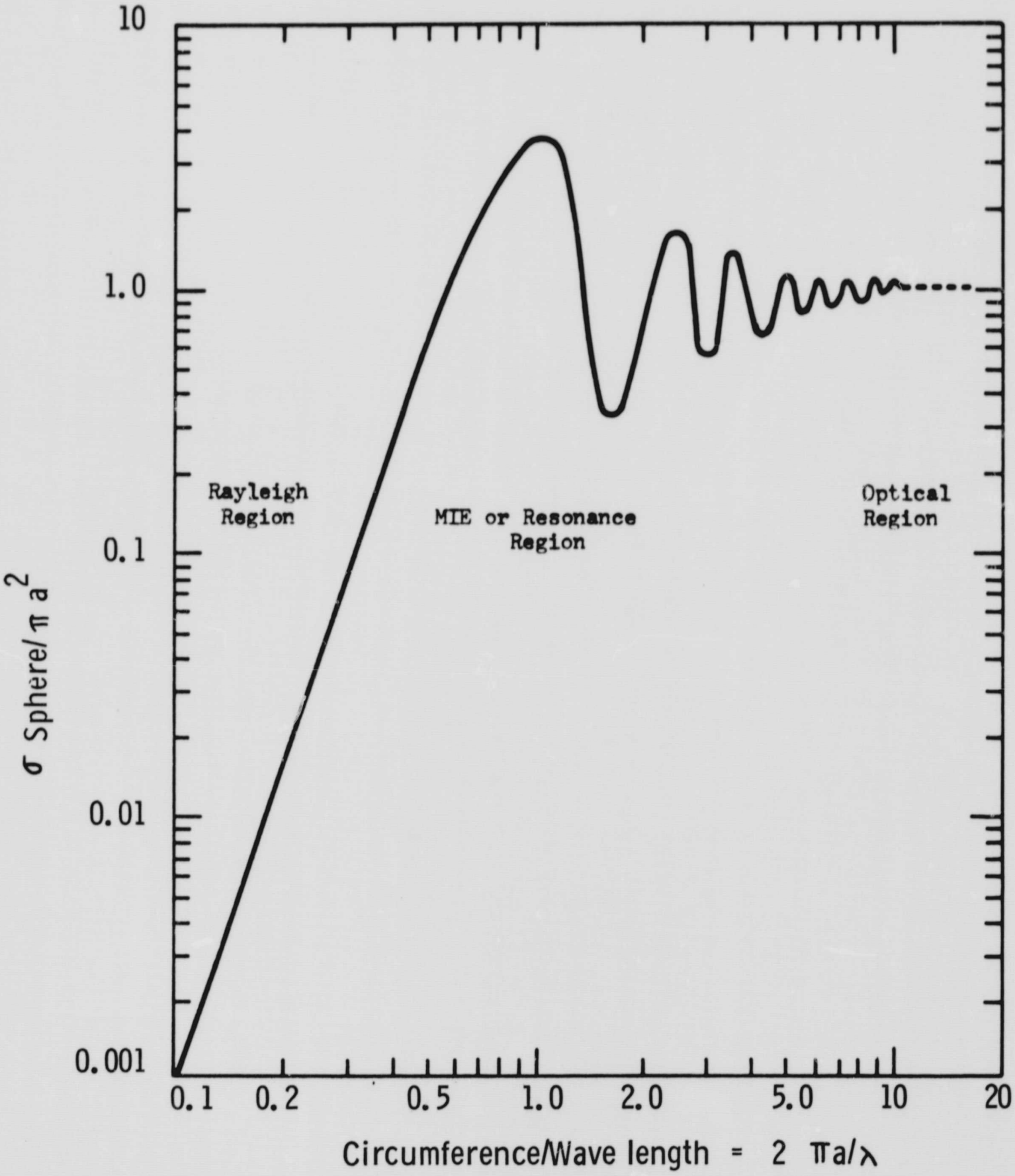

Figure 20

REFLECTION FROM A SPHERE

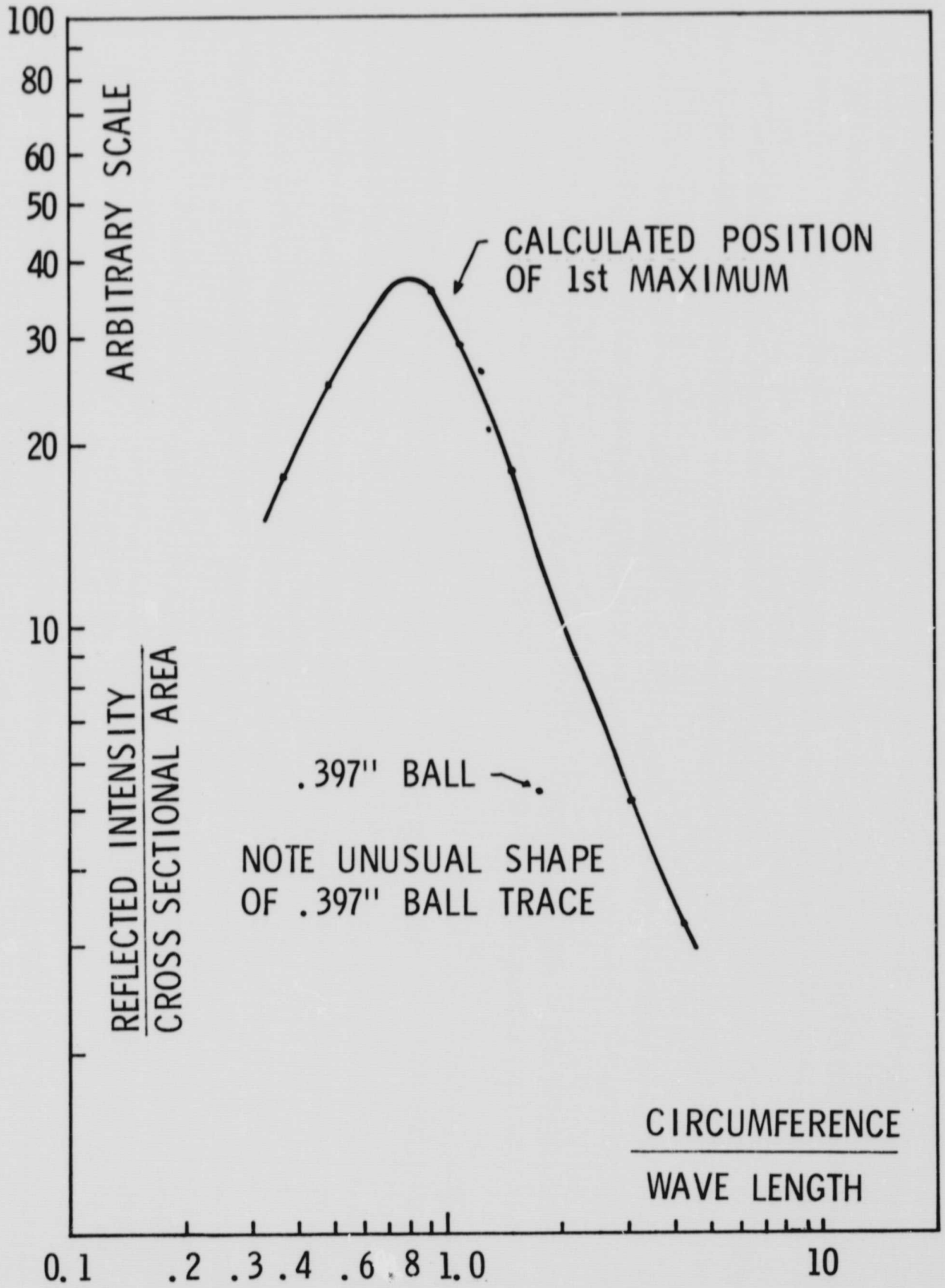

Figure 21

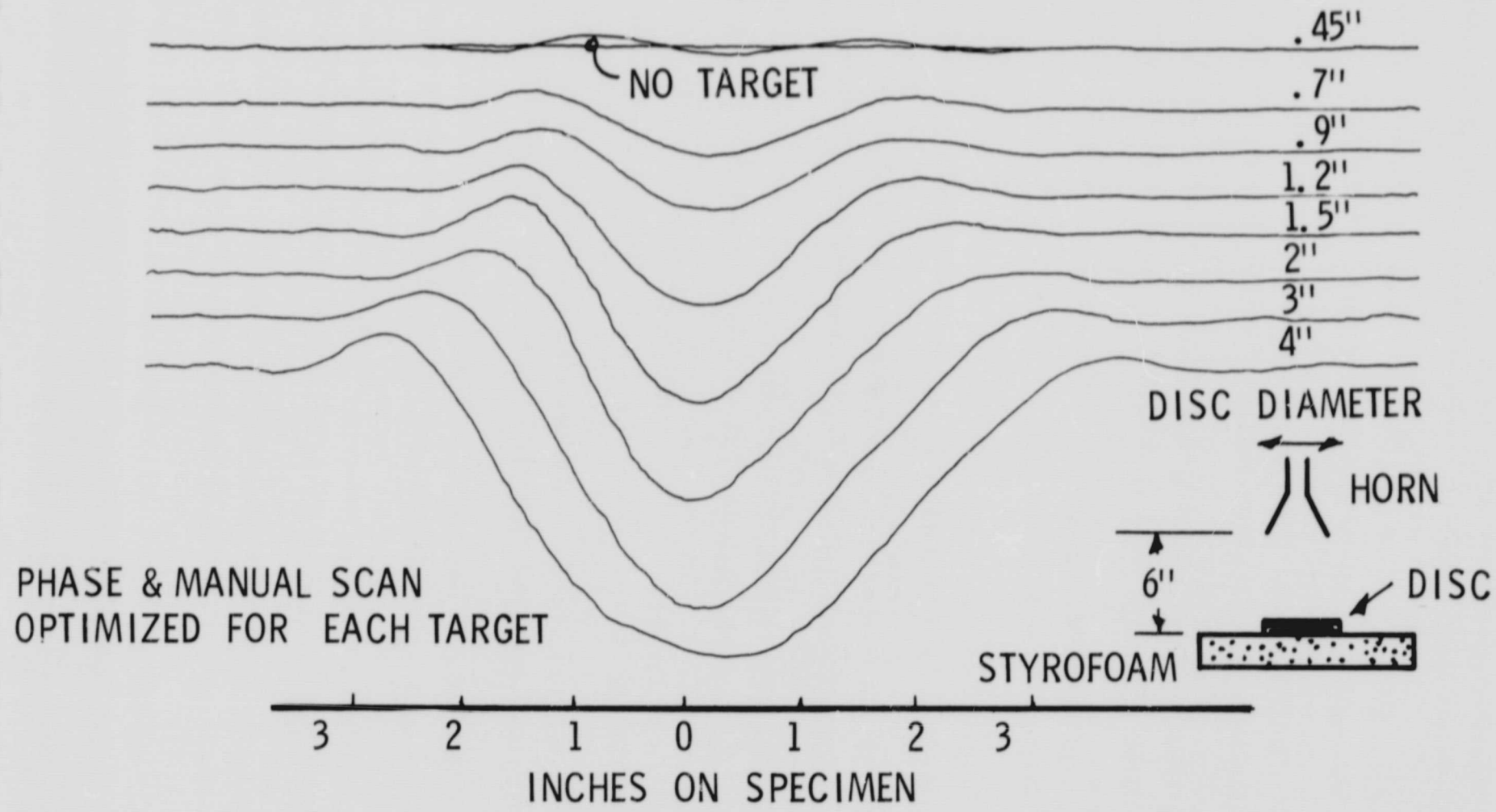

DETECTION OF PLANE METAL DISCS IN AIR

KU BAND MONOPHASE SCANS RANGE 6 INCHES

Figure 22

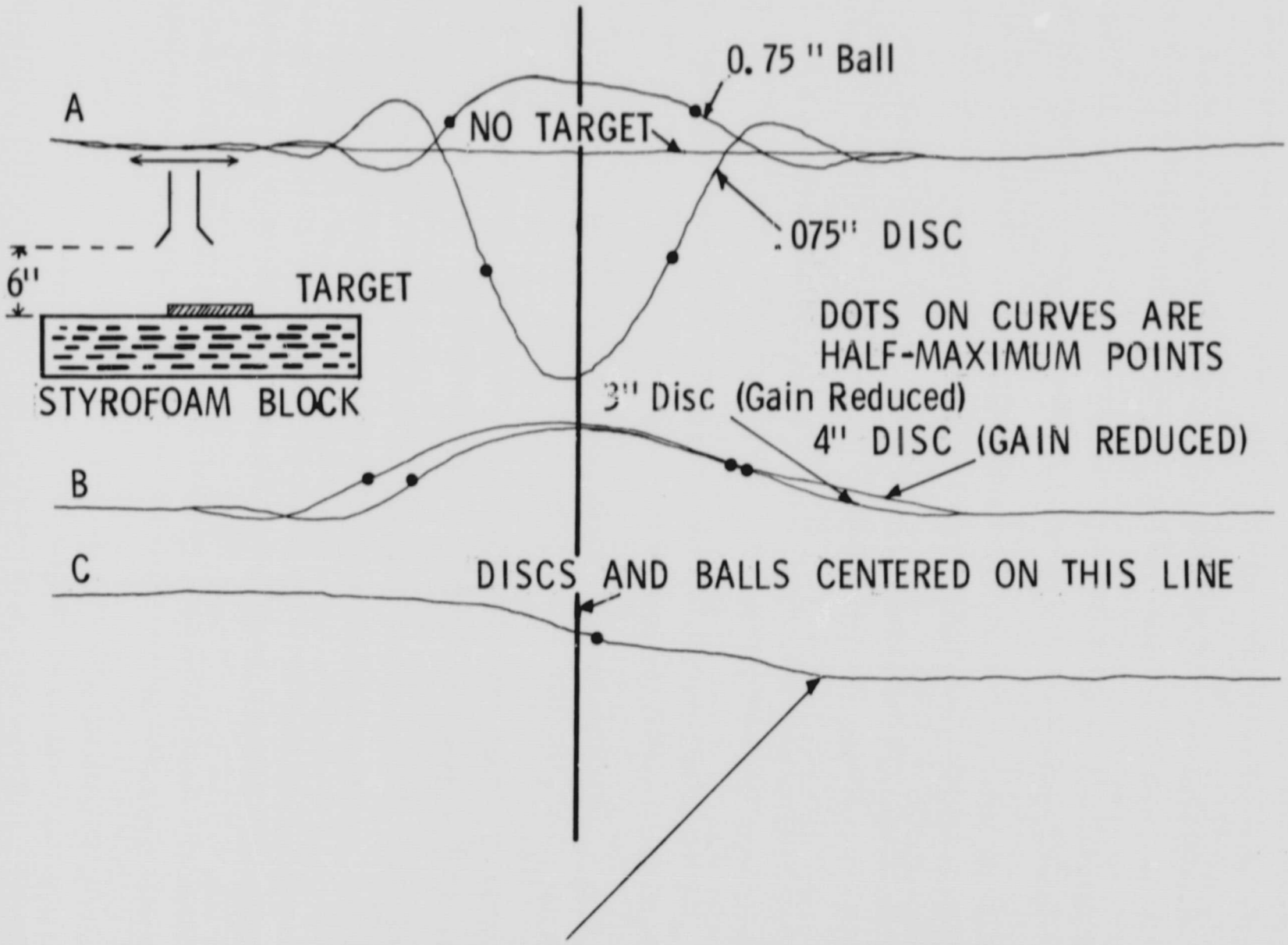

"SEMI-INFINITE" PLANE (GAIN REDUCED)
(METAL PLATE TO LEFT OF CENTERLINE)

COMPARISON OF INDICATIONS OF SPHERE, DISC,
SEMI-INFINITE PLATE KU BAND MONOPHASE SCANS

1" ON SPECIMEN

Figure 23

GEOMETRIC BEAM DEFINITION

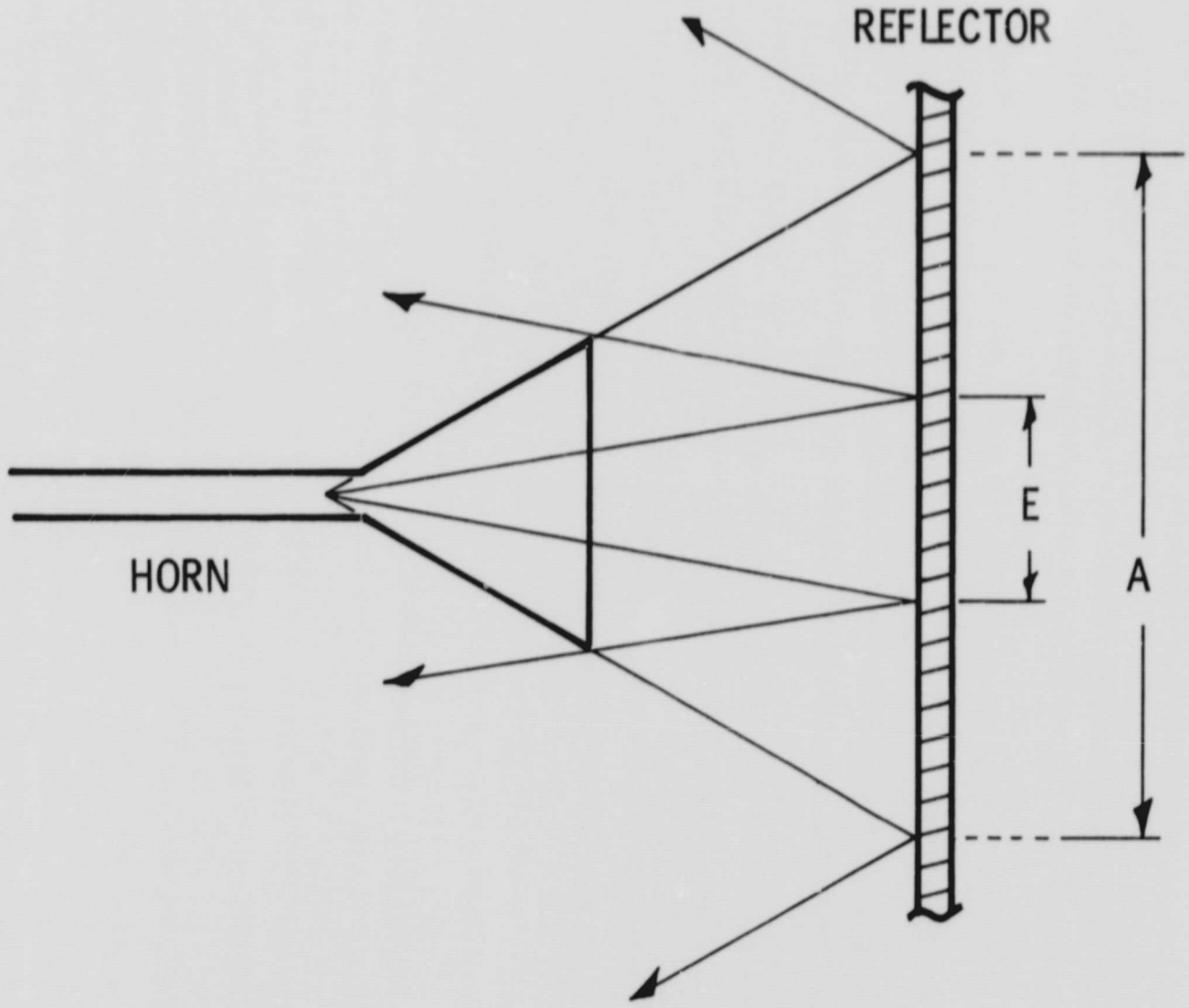

A ACTUAL BEAM

E EFFECTIVE BEAM

Figure 24

DEFECT STANDARD FOR SEPARATION

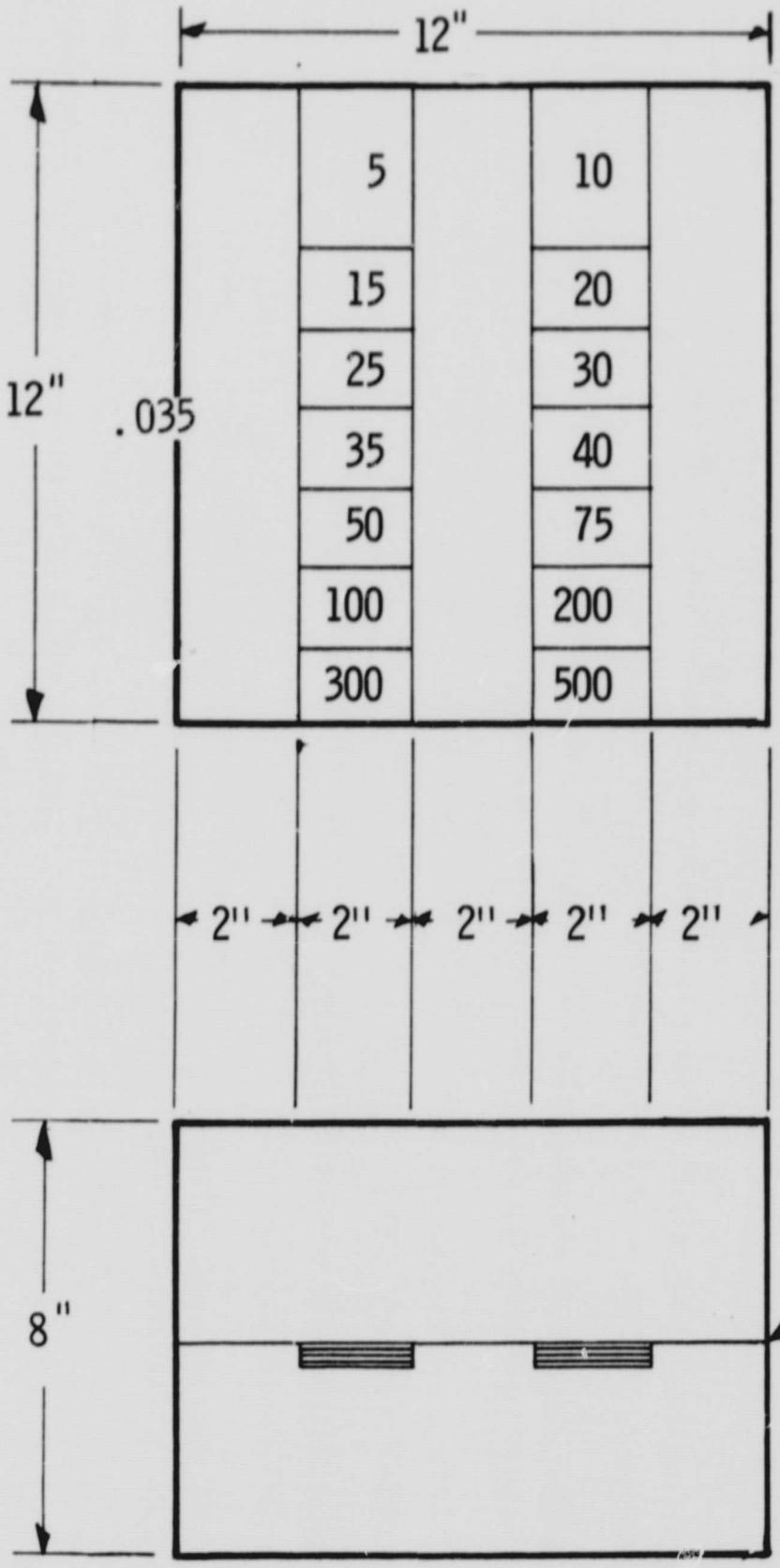

Numbers on steps
Indicate depth in mils

Material: Plexiglas
(Methyl Methocrylate,)
Rohm & Haas

Figure 25

KU BAND MONOPHASE SCANS OF
PLEXIGLAS SEPARATION STANDARD

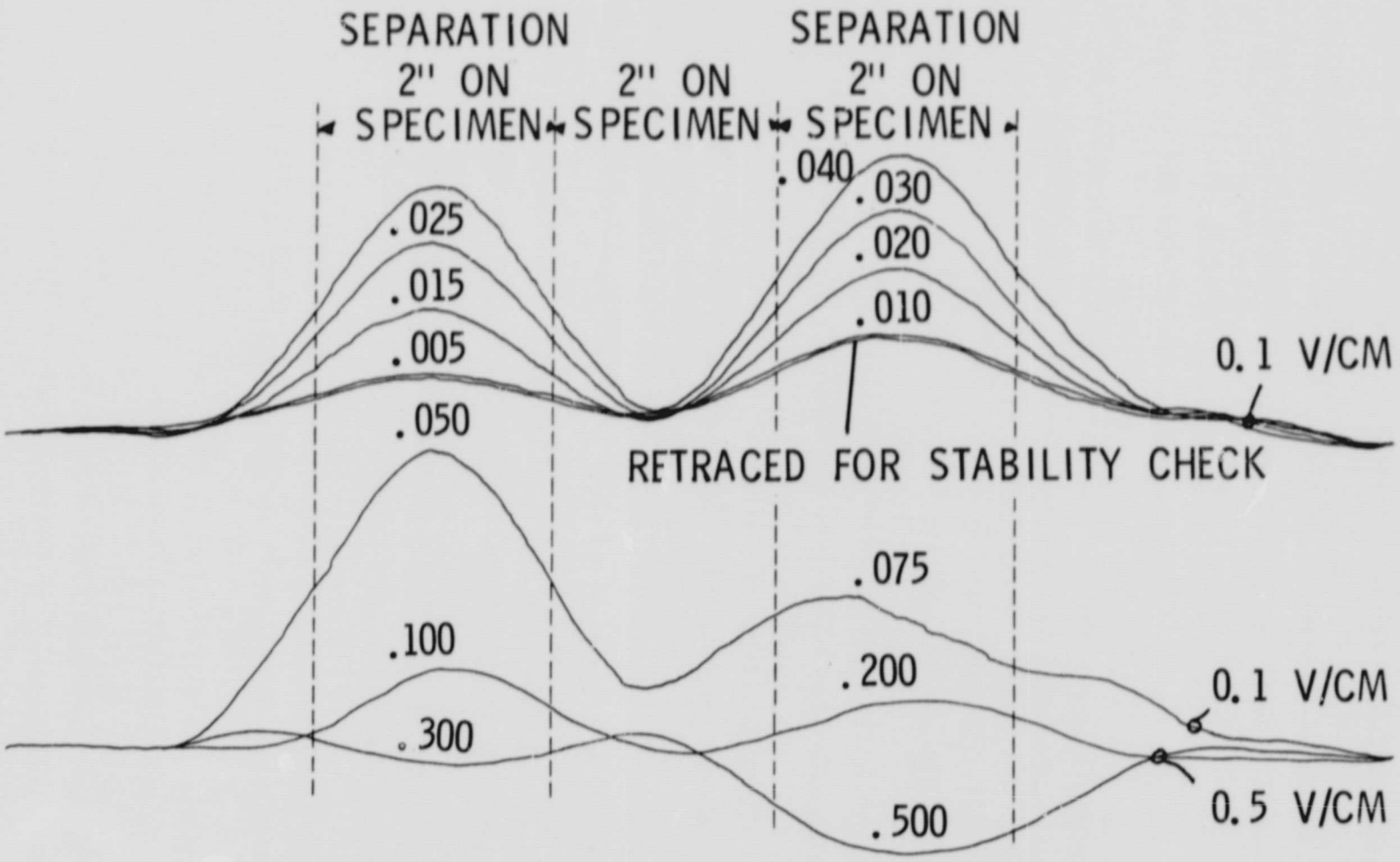

MANUAL RANGE SCAN AND PHASE SETTINGS
OPTIMUM FOR 5 MIL SEPARATION

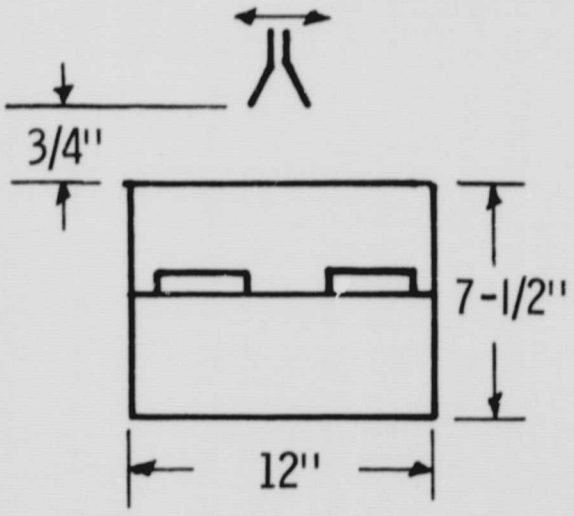

Figure 26

MAXIMUM INDICATION VS SEPARATION THICKNESS DATA

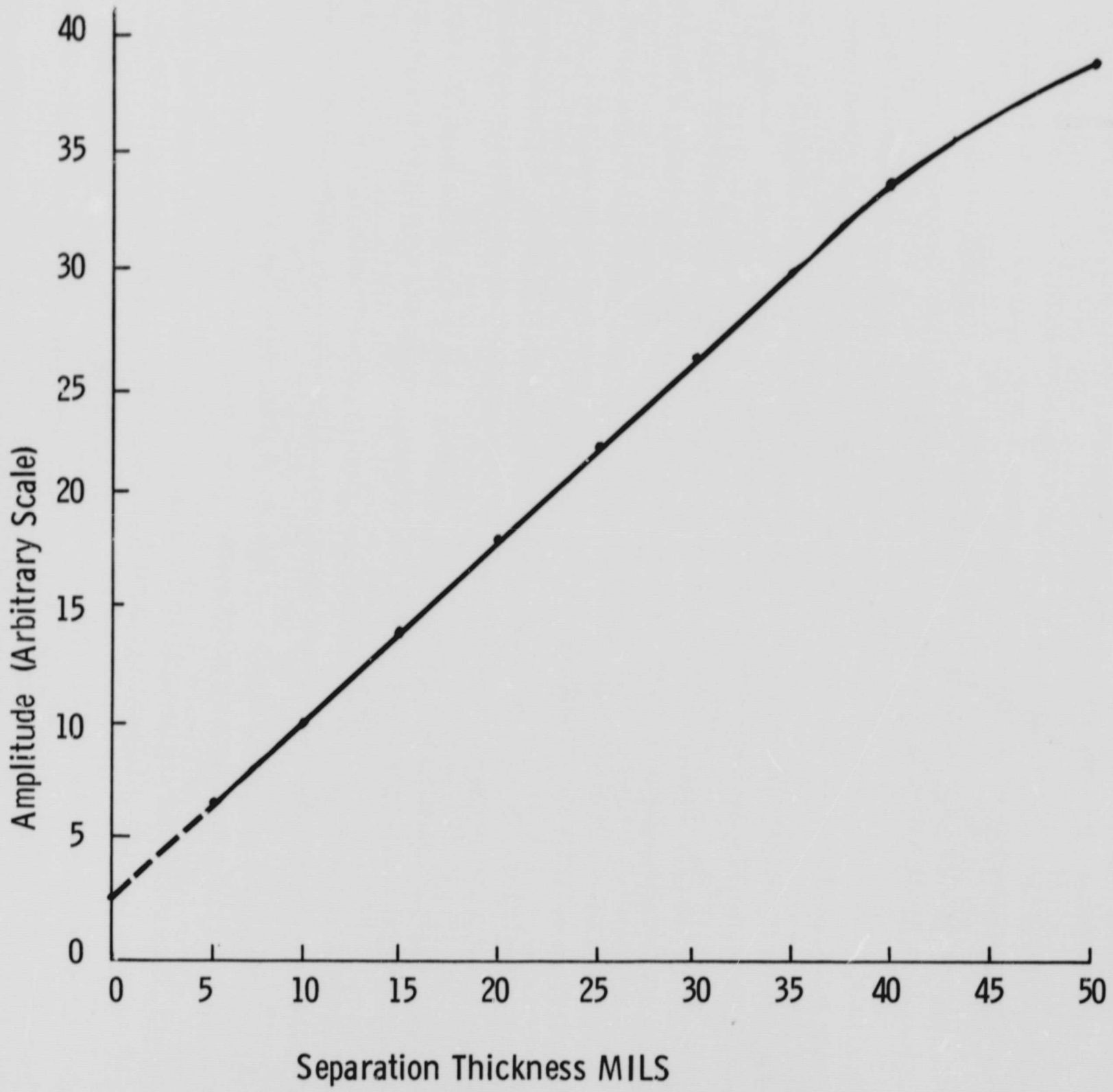

Figure 27

FLANGE DETAIL OF TITAN III ABLATIVE NOZZLE SKIRT

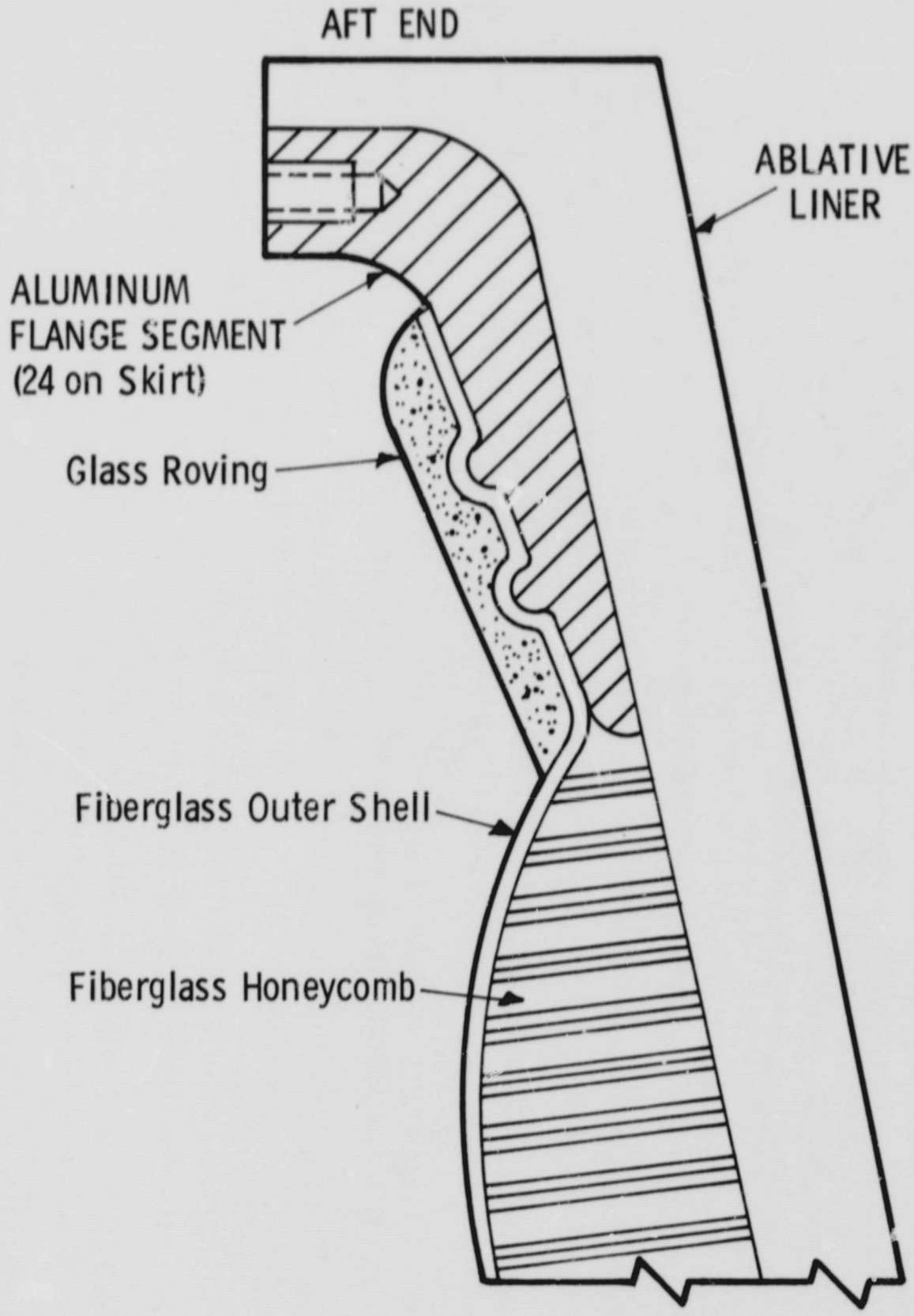

Figure 28

INSPECTION OF TITAN III ABLATIVE NOZZLE SKIRT

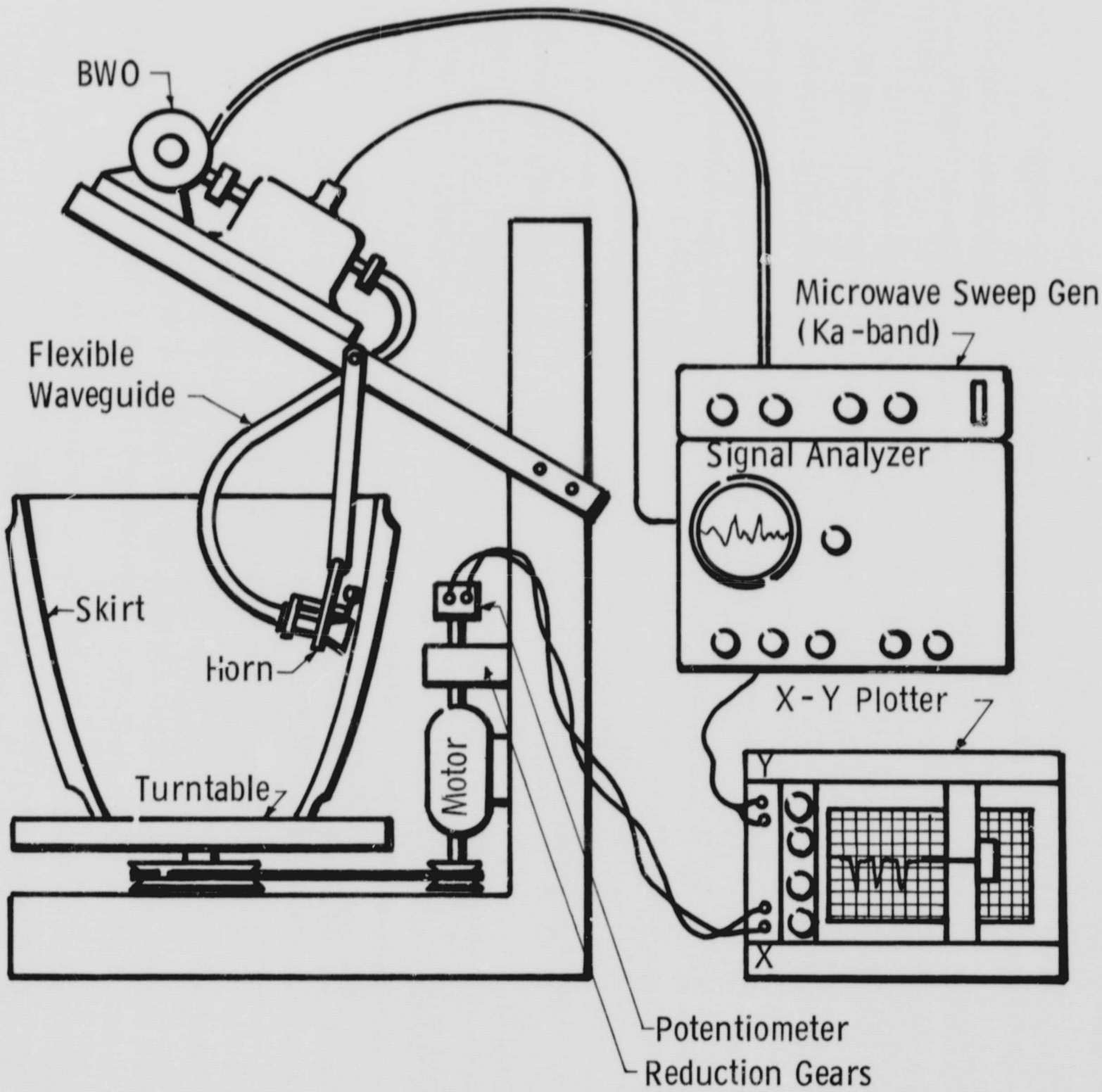

Figure 29

INSPECTION RECORD OF TITAN ABLATIVE SKIRT, FLANGE AREA

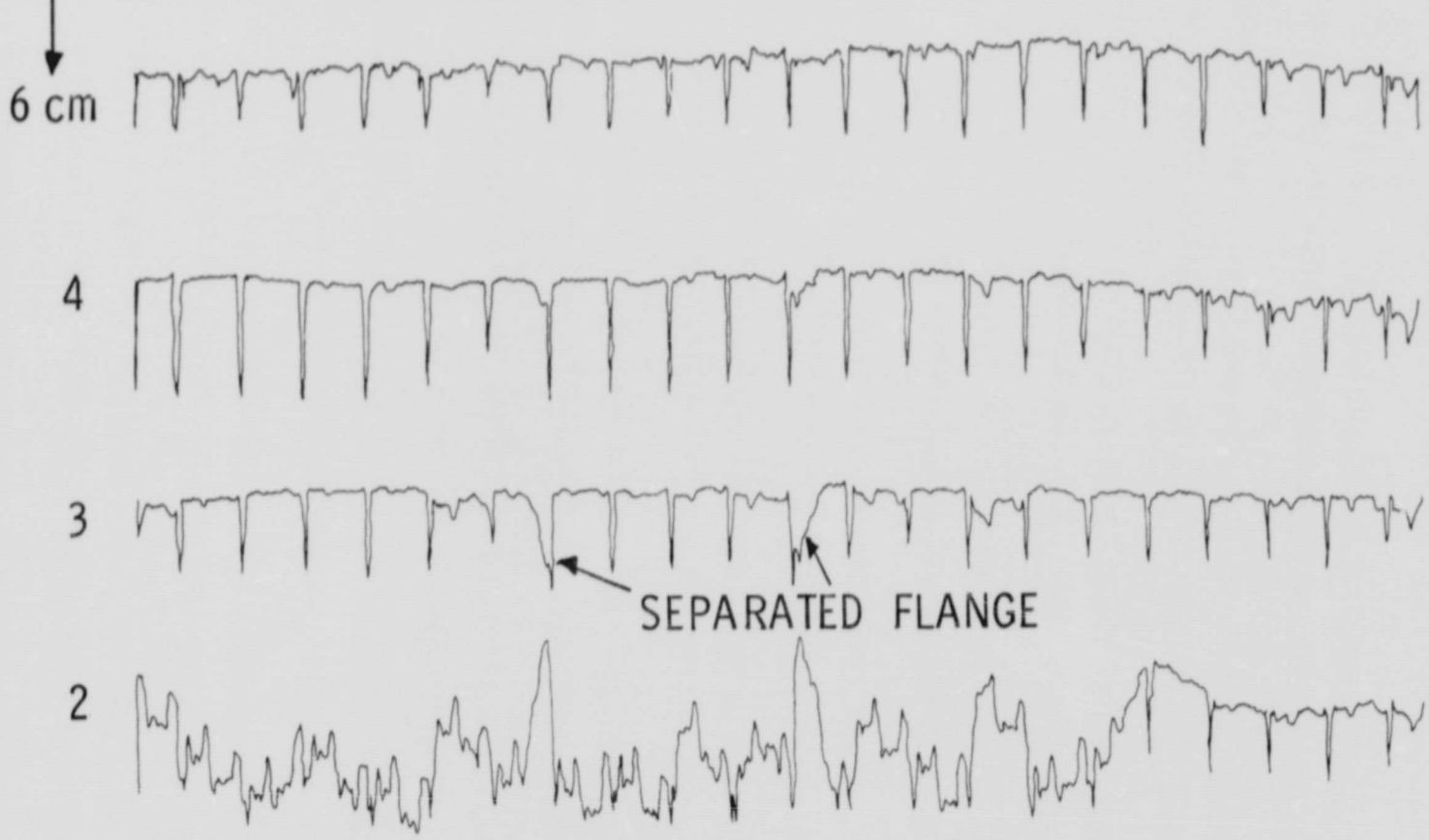

Figure 30

RADIOGRAPH CONTACT PRINT OF TITAN III ABLATIVE SKIRT
SHOWING BONDED FLANGE SEGMENT

Figure 31

RADIOGRAPH CONTACT PRINT OF TITAN III ABLATIVE SKIRT SHOWING SEPARATED FLANGE SEGMENT

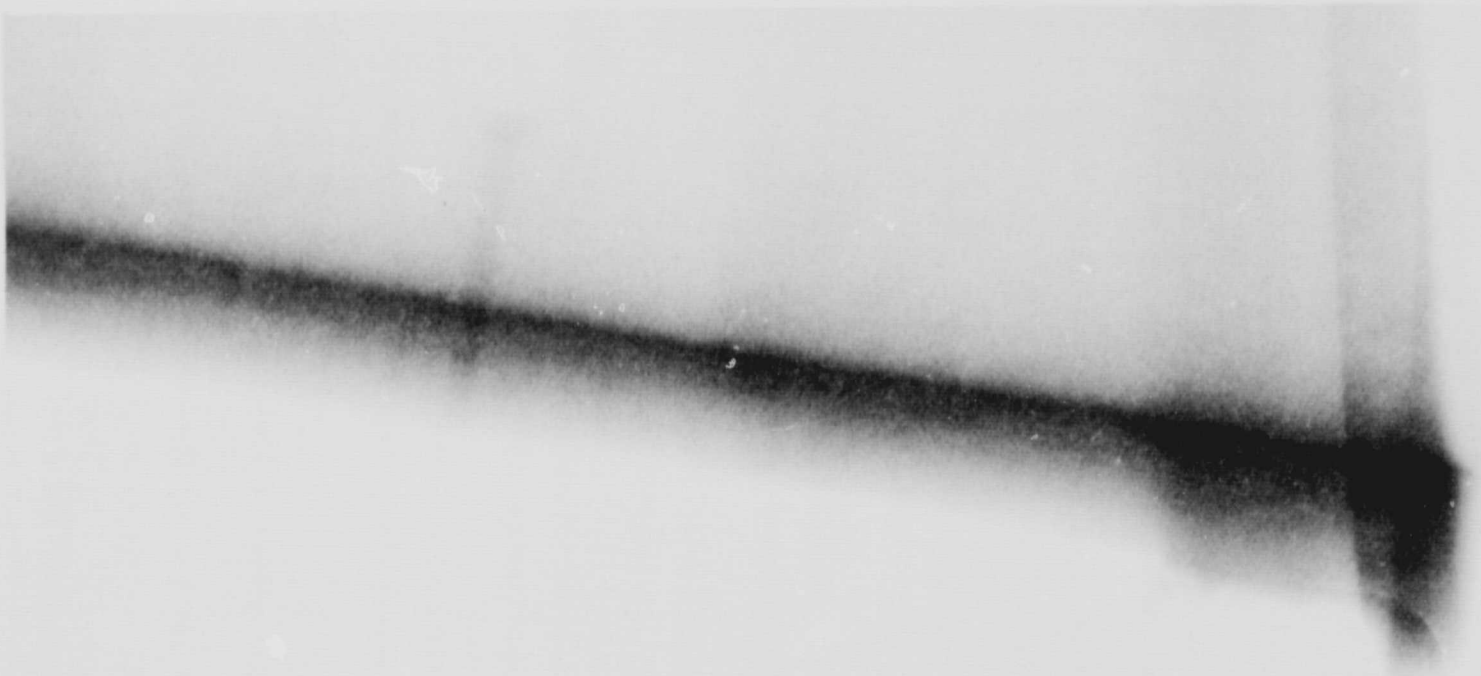

10.5.65

Figure 32

TITAN III ABLATIVE NOZZLE SKIRT DEFECT SPECIMEN

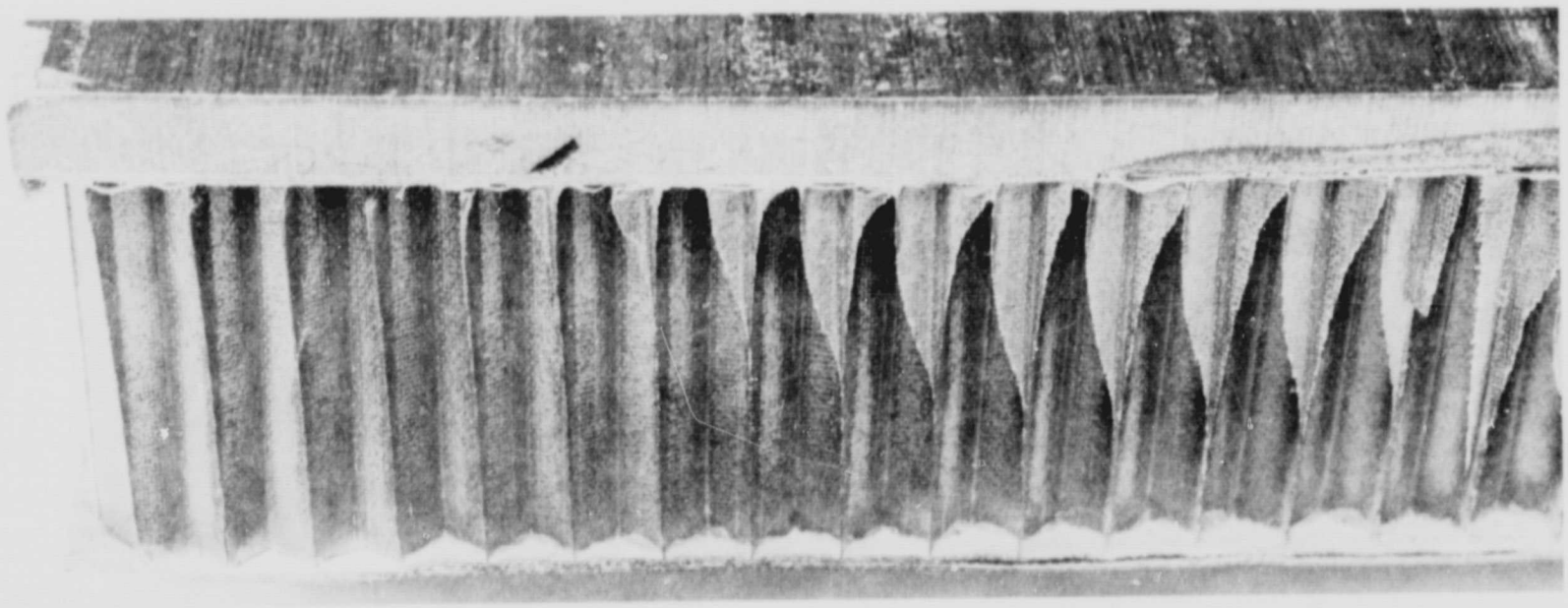

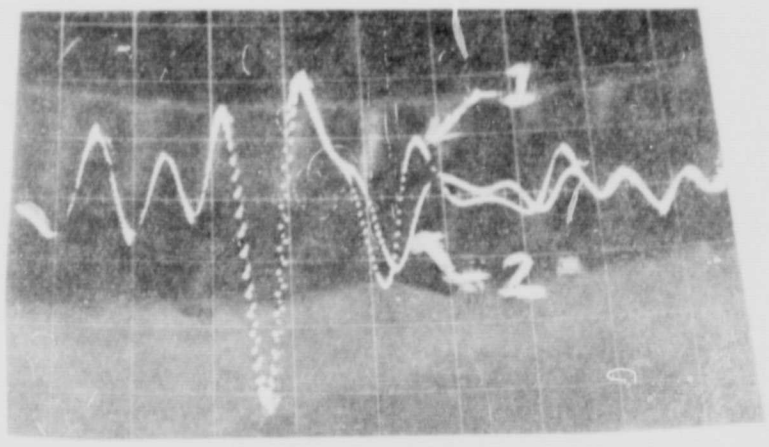

THE UPPER PHOTO SHOWS THE SAW-CUT IN THE ABLATIVE LINER. THE CUT IS ORIENTED PARALLEL TO THE TAPE WRAP. CURVE 1 IS OBTAINED BY DEPTH-RANGE SCANNING OVER A NORMAL AREA. CURVE 2 IS OBTAINED OVER THE SAW-CUT AREA. DISTORTION IS SHOWN OVER A WIDE RANGE SINCE THE CUT IS NOT PARALLEL TO THE FRONT SURFACE.

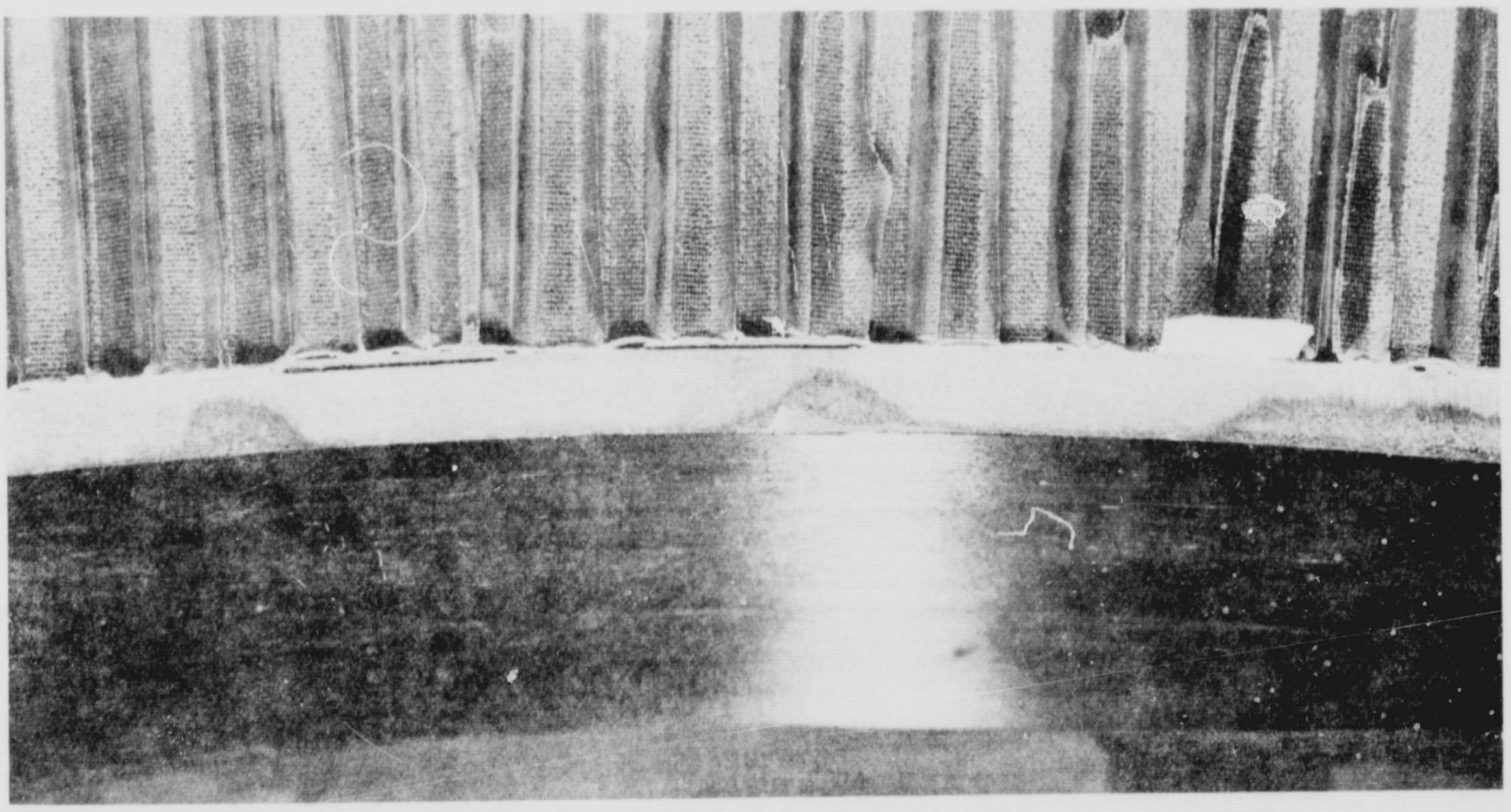

TITAN III ABLATIVE NOZZLE SKIRT DEFECT SPECIMEN WITH INSPECTION RECORD

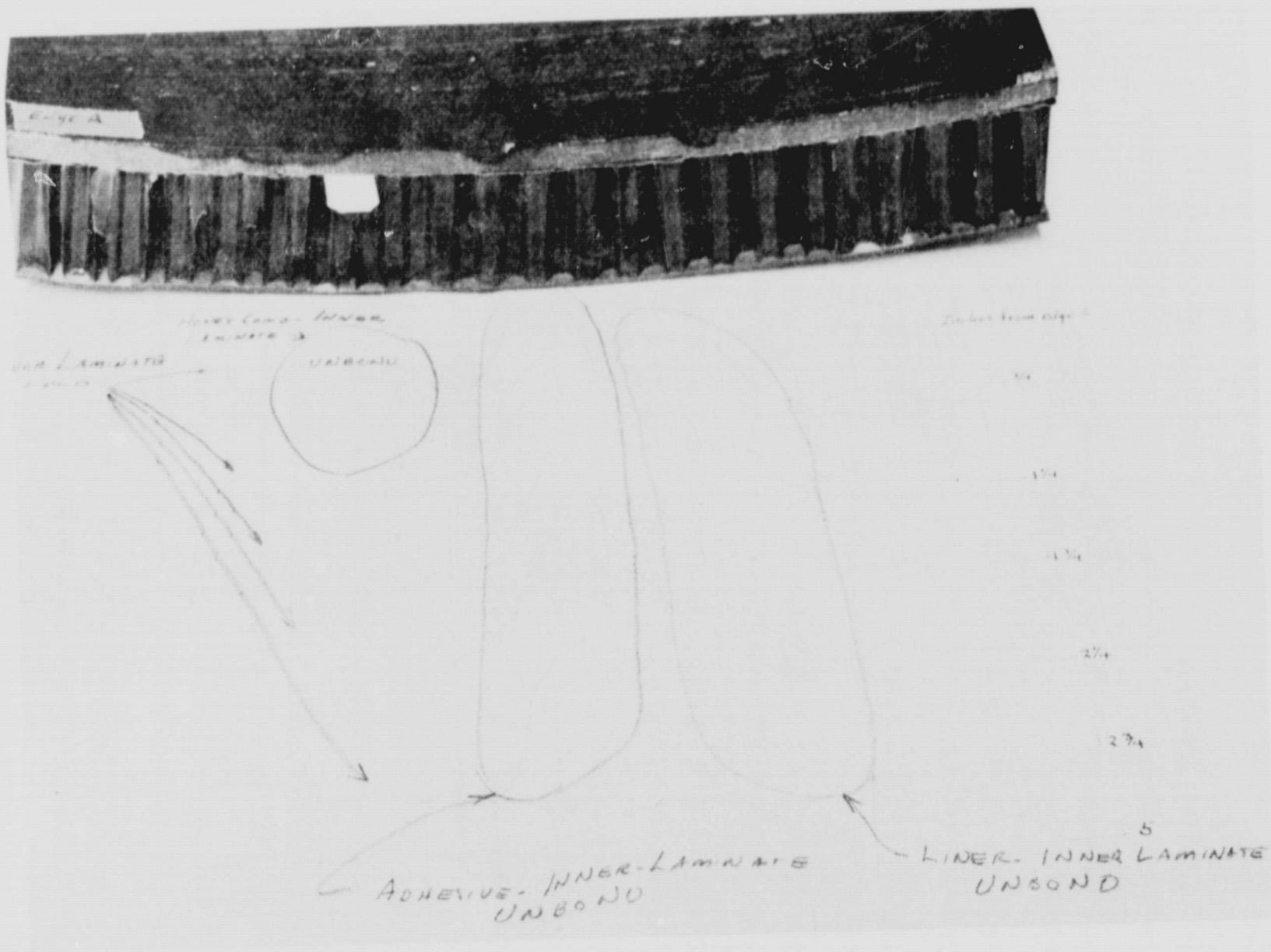

Figure 34

PRODUCTION TYPE JET AIRCRAFT TIRE SECTION

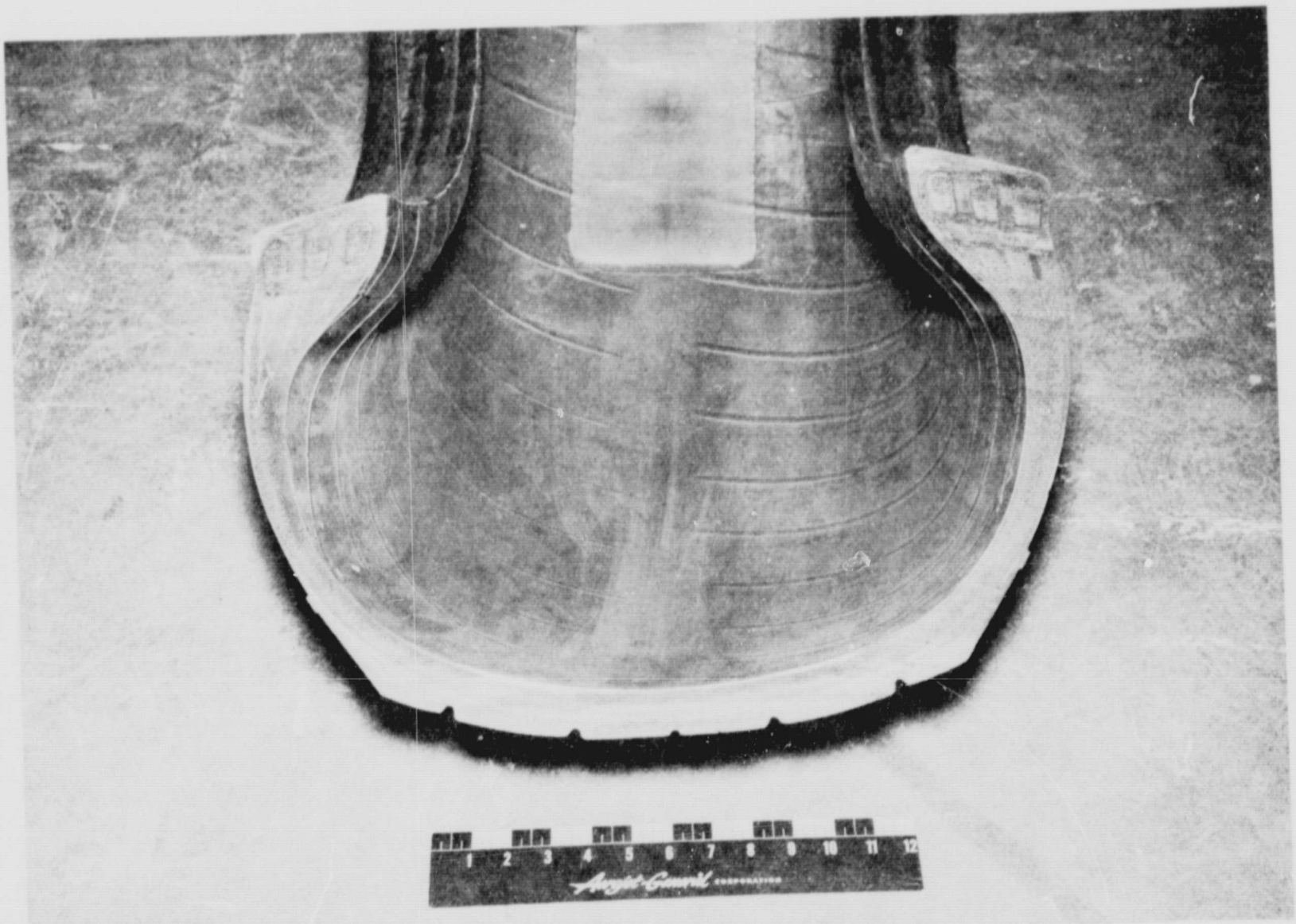

Figure 35

EXPERIMENTAL TYPE JET AIRCRAFT TIRE SECTION

Figure 36

FILAMENT-WOUND AIRCRAFT TIRE UNDER INSPECTION

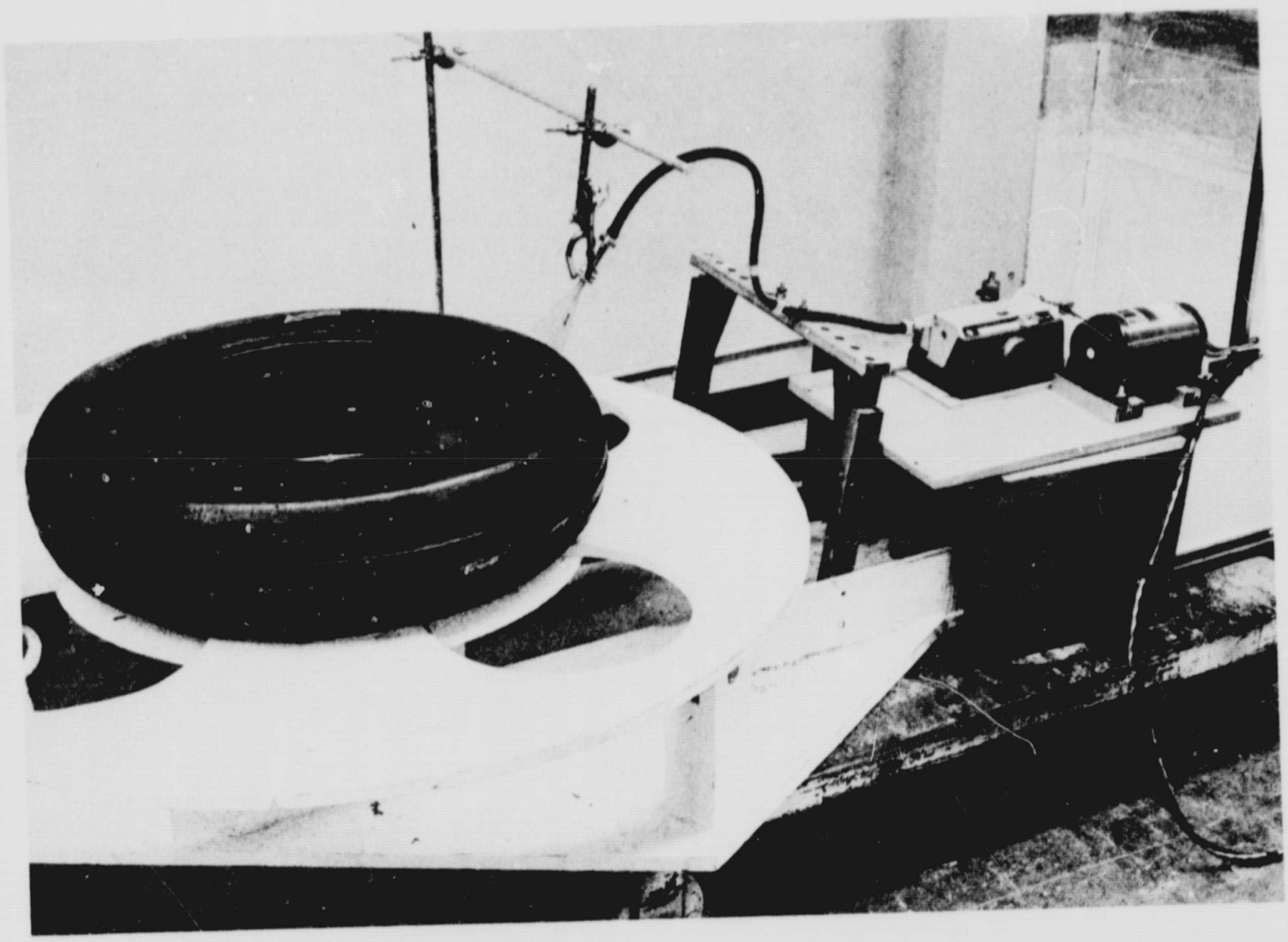

Figure 37

K-BAND MICROWAVE PROBE FOR INSPECTING POLARIS A3
1ST STAGE NOZZLE RECEPTACLES

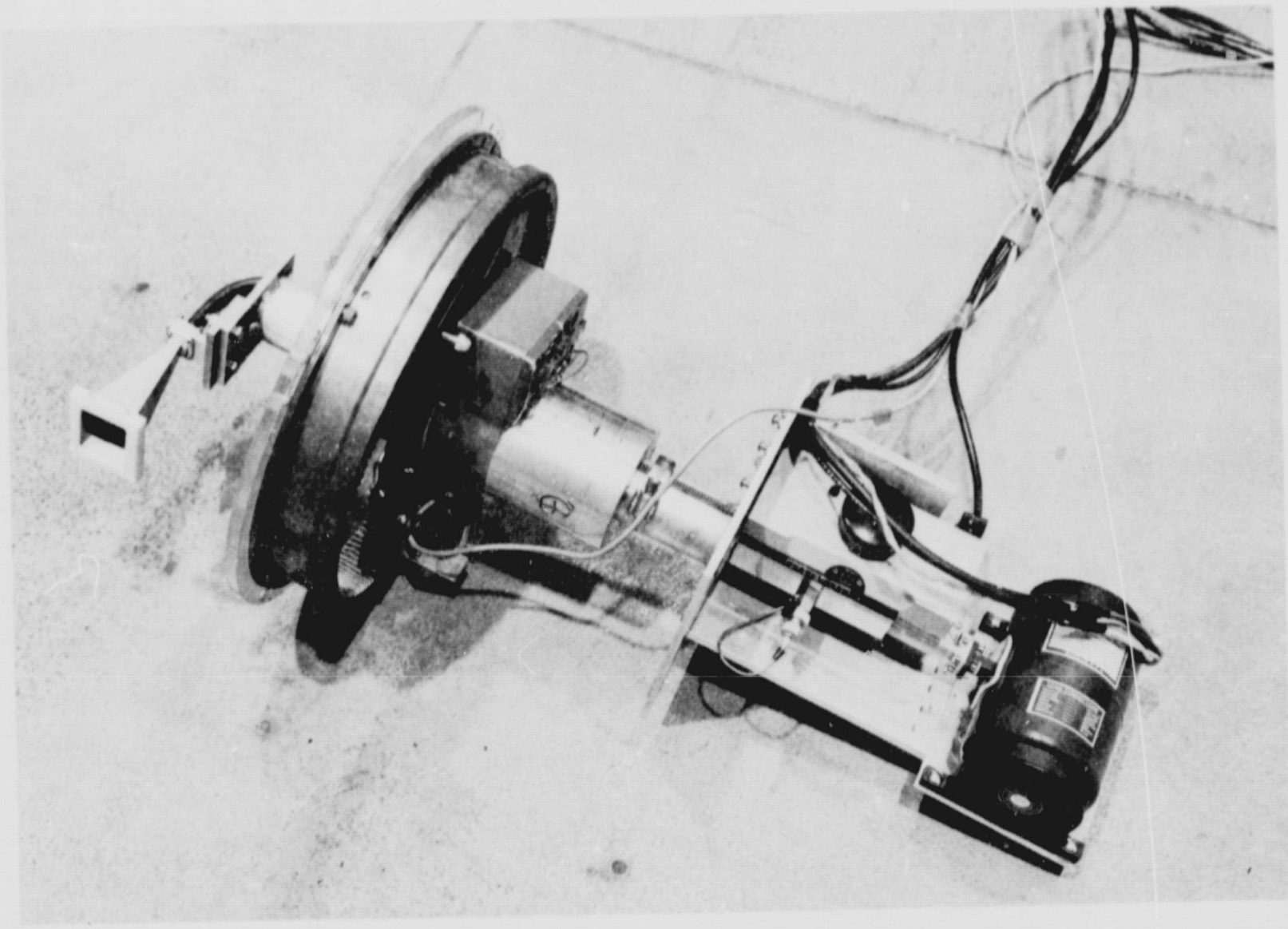

Figure 38

K-BAND MICROWAVE PROBE IN PLACE IN POLARIS NOZZLE RECEPTACLE

Figure 39

INSPECTION RECORD OF POLARIS A3 NOZZLE RECEPTACLE DEFECT SPECIMEN

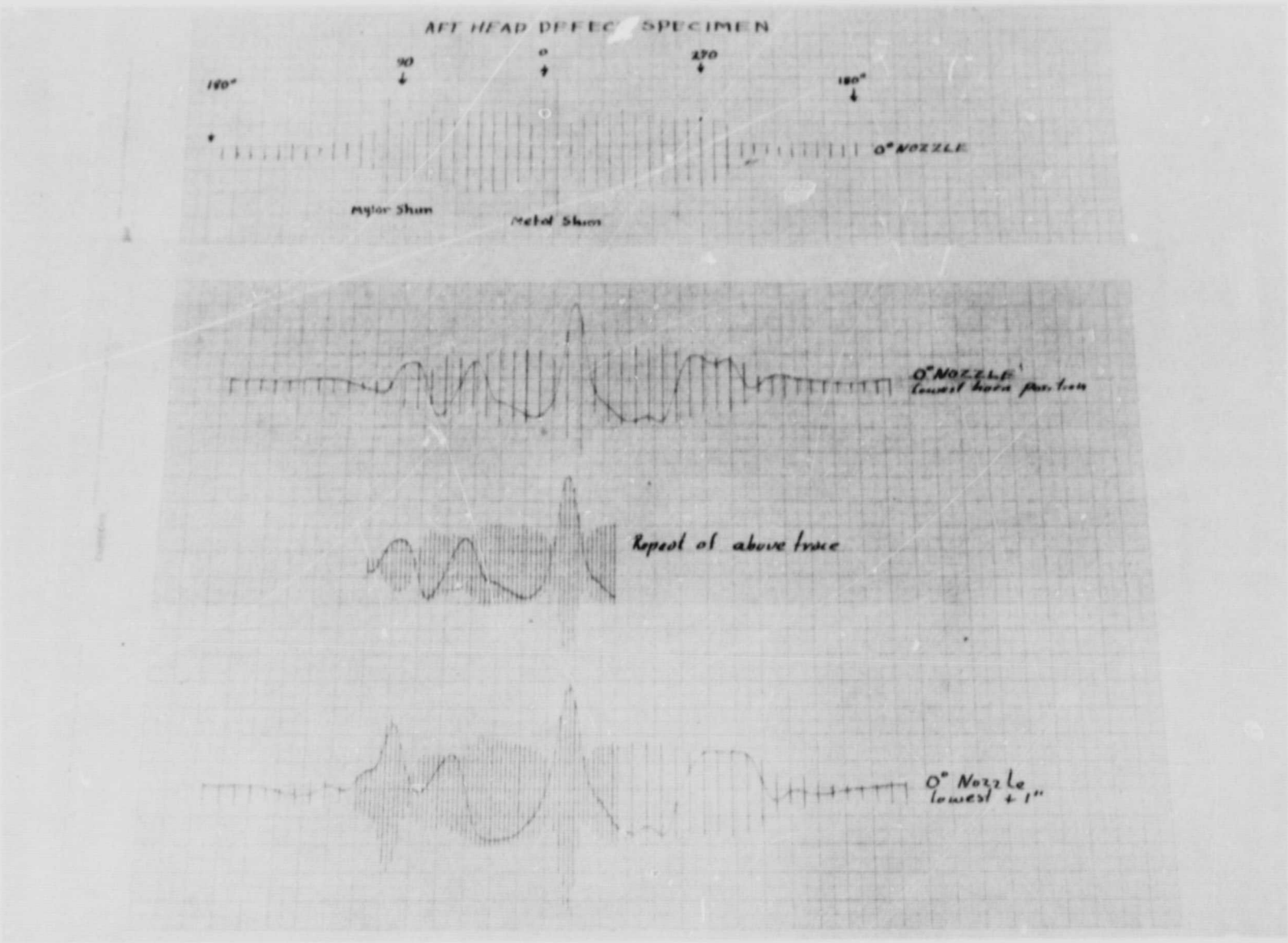

Figure 40

APPENDIX A

AN ANALYSIS OF THE FM MICROWAVE INTERFEROMETER SIGNAL ANALYZER

I General Discussion

The FM Microwave Interferometer is used for locating and resolving discontinuities in dielectrics. In its application to nondestructive testing (NDT) it is used much the same way as pulse-echo ultrasonics is used. The purpose of this paper is to describe its principle of operation.

It is natural for NDT practitioners whose attention is drawn to microwaves to consider the possibility of ranging defects with a pulse-echo device. What is needed, it would appear, is an ultra-high resolution radar. The radar beam would be directed into the dielectric being inspected. Any discontinuities would reflect back a portion of the pulse, and the time of arrival of the reflected pulse could be used to locate the defect. To get high resolution, it would be necessary to produce a pulse as short in duration as possible.

There are both practical and theoretical difficulties in building such a system. A more general analysis of the problem shows that a large microwave bandwidth is all that is required for high resolution. A convenient way to get this is to linearly sweep the microwave transmitter frequency shown in Figure 1. The microwave signal travels down the waveguide and is reflected from discontinuities in front of the horn. The crystal detector then sees two signals, the transmitted signal and the reflected signal.

The detector output contains the sum and difference frequencies. Since the sweep is linear, the difference frequency is a constant as shown in Figure 2. A mathematical analysis in Section II shows the detected signal for a single reflector to be:

APPENDIX A

$$S_d(t) = \frac{A}{2} \cos (w_o - w't)\tau \qquad o \leq t \leq T$$

$$S_d(t) = o \qquad T < t \leq T_r$$

A = the amplitude

$w_o = 2\pi f_o$ = the starting microwave angular frequency

$w' = \frac{w_o - w_1}{T}$ = the microwave sweep rate

τ = the time of travel of the microwave signal from the detector to reflector and back to the detector

t = time

T = sweep duration

T_r = sweep repetition period

As can be seen the frequency ($w'\tau$) is proportional to τ, hence distance. Furthermore, the phase ($w_o \tau$) is proportional to distance.

It would appear that several reflectors in the beam could be resolved by frequency analyzing the signal. A natural device for doing this is a spectrum analyzer. The power spectrum of the signal from one reflector is derived in Section II:

$$P_s(m) = \frac{1}{2T_r^2} \frac{\sin^2 \left(\frac{\pi m}{T_r} - \frac{w'\tau}{2} \right) T}{\left(\frac{\pi m}{T_r} - \frac{w'\tau}{2} \right)^2}$$

where $P_s(m)$ = power at frequency $\frac{2\pi m}{T_r}$

m = an integer

Note that the phase information in the received signal is lost, i.e., there is no $w_o \tau$ term. Furthermore, the spectrum is a line spectrum. For example, if T_r were 0.001 sec, there would be power only at harmonics of one Kilohertz. Finally note that the power spectrum is always positive.

APPENDIX A

The FM Microwave Interferometer does not take the power spectrum. A cross-correlation detector is used. Its output derived in Section II:

$$C(w) = \frac{\sin\left[(w - w'\tau)\,T + w_o\tau\right] - \sin w_o\tau}{w - w'}$$

where $C(w)$ = cross-correlation detector output

$w = 2\pi f$ = angular frequency

Note that the phase information ($w_o\tau$) is retained. The signal may be either positive or negative. Further note that the frequency term occurs as $w_o\tau$ in this transform, not $\frac{w_o\tau}{2}$ as in the power spectrum. Hence, the transform method yields twice the resolution.

The significance of these observations is shown in Figure 3. Suppose the microwave transmitter is operating in K band, i.e., sweeping from 26.5 GHz to 18 GHz. Suppose that the duty cycle is 50%, i.e., $T = 0.5T_r$. Suppose further that a reflector is placed in the beam at such a point that it produces a beat frequency ($w'\tau$) which is an exact multiple of the repetition frequency ($w'\tau = \frac{2\pi m}{T_r} = 2\pi\ mf_r$ where m is an integer). Then the display of this signal on a high resolution spectrum analyzer is shown in Figure 3a. For convenience the horizontal axis is shown in distance rather than frequency or delay time. The spectral envelope is dotted in and goes to zero at 18 mm.

A display of the correlation detector output for the same signal is shown in 3b. In this case the phase is zero ($w_o\tau$ is a multiple of 2π). Note this display is a smooth curve and goes to zero in 9 mm.

Now suppose the reflector moves a distance that causes the phase to shift $\frac{\pi}{2}$ radians.

$$w_o\delta\tau = 2\pi f_o \frac{2\delta D}{C} = \frac{\pi}{2}$$

APPENDIX A

This corresponds to a distance of

$$\delta D = \frac{C}{8f_o} = \frac{3 \times 10^{10}}{8(26.5 \times 10^9)} = 0.14 \text{ cm} = 1.4 \text{ mm}$$

where $\delta\tau$ = the change in delay time

δD = the distance moved

C = velocity of light

$f_o = \frac{w_o}{2\pi}$ = microwave starting frequency

The display of the spectrum analyzer and correlation detector are shown in Figures 3c and 3d, respectively. Note that the position of the lines in the spectrum do not move - only the position of the envelope. The only indication of the change in position of the reflector is the slightly unsymmetrical sideband structure.

In sharp contrast the change in the correlation detector output is most conspicuous. Initially the curve had a shape like:

$$y = \frac{\sin x}{x}$$

The new curve has a

$$y = \frac{\cos x - 1}{x}$$

shape. This curve crosses zero at the 1.4 mm mark. A further 1.4 mm movement of the reflector has a relatively minor effect on the spectrum analyzer output but changes the correlation detector output to a curve like:

$$y = -\frac{\sin x}{x}$$ shown in Figures 3e and 3f.

APPENDIX A

The negative peak on this curve occurs at 2.8 mm. Further increments of 1.4 mm changes the correlation detector output to a curve like:

$$y = -\frac{\cos x - 1}{x}$$

then back to

$$y = \frac{\sin x}{x}$$

This distance (5.6 mm) corresponds to 2π radians.

Some experimental results in Ku band (12.4 to 18 GHz) are shown in Figure 4. Figure 4a shows the front (at 2.7 cm) and back (7.0 cm) reflection from a 2-in.-thick block of plexiglas. Note that the front reflector is in phase and the back approximately 180° out of phase. Figure 4b shows a single stationary reflector with the phase control rotated by 90° increments. Figure 4c shows the reflection from a reflector moved in 2.7 mm increments. Note the final position is displaced 0.5 cm on the display. This represents a distance of 1.08 cm displacement.

In practice an operator can easily see a 30° shift corresponding to a 0.46 mm distance in air. In a dielectric the resolution is better because the velocity of light (or microwaves) is c/n where n is the index of refraction. For most dielectrics n is about 1.5 to 2.

If the microwave horn were scanning a laminar structure for delaminations, the position of the delamination could be determined to better than 0.5 mm in K band. Higher microwave frequencies would result in still higher resolution.

APPENDIX A

II Deviation of Equations

Suppose the transmitted microwave signal is

$$S_t(t) = \sin [(w_o - w't)t] \qquad o \leq t \leq T$$

$$S_t(t) = 0 \qquad T < t \leq T_r$$

The received signal is then

$$S_r(t) = \sin [(w_o - w'(t + \tau))\ (t + \tau)] \qquad o < t < T$$

Where: w_o = starting microwave frequency

$w' = \frac{w_o - w_1}{T}$ = sweep rate

w_1 = final microwave frequency

T = sweep period

T_r = sweep repetition period

t = time

τ = delay time

The component of the detected signal containing the difference frequency is then

$$S_d = A \sin [(w_o - w't)t] \sin \left\{[w_o - w'\ (t + \tau)]\ (t + \tau)\right\}$$

Assume $\tau << t$. Then

$$S_d = A \sin [(w_o - w't)t] \sin (w_o - w't)t + (w_o - w't)\tau$$

$$= A \sin [(w_o - w't)t] \sin (w_o - w't)t \cos(w_o - w't)\tau$$

$$+ \cos(w_o - w't)t \sin (w_o - w't)\tau]$$

$$= \frac{A}{2} \left\{[1 - \cos[2(w_o - w't)\ t] \cos[(w_o - w't)\tau]\right.$$

$$\left. + \sin [2(w_o - w't)t] \sin (w_o - w't)\tau]\right\}$$

$$= \frac{A}{2} \left\{\cos[(w_o - w't)\tau] - \cos[(w_o - w't)(2t + \tau)]\right\}$$

APPENDIX A

The second term contains microwave frequencies only and is filtered.

Thus

$$S_d = \frac{A}{2} \cos[(w_o - w't)\tau]$$

The power spectra is determined by first expanding S_d in a Fourier series: (set A/2 = 1 for convenience)

$$S_d = \cos[(w_o - w't)\tau] = \sum_{m=o}^{\infty} a_m \cos 2\pi\, m\, f_r t + b_m \sin 2\pi\, m\, f_r t$$

Where:

$$a_m = \frac{1}{T_r} \int_o^{T_r} S_d(t) \cos \frac{2\pi mt}{T_r}\, dt$$

$$= \frac{1}{T_r} \int_o^{T} \cos(w_o - w't)\tau \cos \frac{2\pi mt}{T_r}\, dt$$

$$= \frac{1}{2T_r} \int_o^{T} \cos(w_o - w't)\tau + \frac{2\pi mt}{T_r}] + \cos[(w_o - w't)\tau - \frac{2\pi mt}{T_r}]dt$$

$$= \frac{1}{2T_r} \left[\frac{\sin \left[(\frac{2\pi m}{T_r} - w'\tau)t + w_o\tau\right]}{\frac{2\pi m}{T_r} - w'\tau} + \frac{\sin \left[(\frac{2\pi m}{T_r} + w'\tau)t + w_o\tau\right]}{\frac{2\pi m}{T_r} + w'\tau} \right]_o^T$$

In the region of interest, that is where $2\pi m/T_r \approx w'\tau$, the second term will be much smaller than the first and can be ignored. Hence

$$a_m = \frac{1}{2T_r} \left[\frac{\sin \left[(\frac{2\pi m}{T_r} - w'\tau)T + w_o\tau\right] - \sin w_o\tau}{\frac{2\pi m}{T_r} - w'\tau} \right]$$

Similarly b_m can be computed:

$$b_m = \frac{1}{2T_r} \left[\frac{\cos \left[(\frac{2\pi m}{T_r} - w'\tau)t + w_o\tau\right] - \cos w_o\tau}{\frac{2\pi m}{T_r} - w'\tau} \right]$$

APPENDIX A

The expansion for the power spectrum then becomes

$$C_m^2 = a_m^2 + b_m^2$$

$$= \frac{1}{4T_r^2\left(\frac{2\pi m}{T_r} - w'\tau\right)^2}\left\{ 2 - 2 \sin w_o\tau \sin \left[\left(\frac{2Tm}{T_r} - w'\tau\right)T + w_o\tau\right]\right.$$

$$\left. - 2 \cos w_o\tau \cos \left[\left(\frac{2\pi m}{T_r} - w'\tau\right)T + w_o\tau\right] \right\}$$

$$= \frac{1}{4T_r^2\left(\frac{2\pi m}{T_r} - w'\tau\right)^2}\left\{2 - 2 \cos \left(\frac{2\pi m}{T_r} - w'\tau\right)T \right\}$$

$$= \frac{1}{2T_r^2} \frac{\sin^2\left(\frac{\pi m}{T_r} - \frac{w'\tau}{2}\right)T}{\left(\frac{\pi m}{T_r} - \frac{w'\tau}{2}\right)^2}$$

The signal processing computer produces an output defined by

$$C(w) = \int_o^T S_d(t)\ e\ (t,w)dt$$

Where:

$e(t,w) = 1$ when $\frac{n}{f} \leq t \leq \frac{2n+1}{2f_r}$ and $o \leq t \leq T$

$e(t,w) = o$ otherwise

Where: $n=1,2,\ldots, [1 + fT]$

$w = 2\pi f =$ local generator frequency

$$C(w) = \int_o^T S_d(t)\ e(t,w)dt$$

$$= \sum_{n=o}^{[1 + fT]} \int_{\frac{n}{f}}^{\frac{2n+1}{2f}} \sin (w_o - w't)\tau\ dt$$

APPENDIX A

$$= \sum_{n=o}^{[1 + fT]} \left[\frac{\cos(w_o - w't)\tau}{w'\tau} \right]^{\frac{2n+1}{2f}}_{\frac{n}{f}}$$

$$= \frac{1}{w'\tau} \sum_{n=o}^{[1 + fT]} \left\{ \cos\left[w_o\tau - \frac{w'(2n+1)\tau}{2f} \right] - \cos\left[w_o\tau - \frac{w'n\tau}{f_r} \right] \right\}$$

Use the following four identities:

(1) $\frac{w'\tau}{w} (2n+1)\pi \equiv (2n+1)\pi + \left(\frac{w'\tau}{w} - 1 \right) (2n+1)\pi$

(2) $\cos[X + (2n+1)\pi] \equiv - \cos X$

(3) $\frac{w'\tau}{w} 2n\pi \equiv 2n\pi + \left(\frac{w'\tau}{w} - 1 \right) 2n\pi$

(4) $\cos(X + 2n\pi) \equiv \cos X$

to get

$$C(w) = \frac{1}{w'\tau} \sum_{n=o}^{[1 + fT]} \left\{ - \cos \left[w_o\tau - \left(\frac{w'\tau}{w} - 1 \right) (2n+1)\pi \right] \right.$$

$$\left. - \cos \left[w_o\tau - \left(\frac{w'\tau}{w} \right) 1 \quad 2n\pi \right] \right\}$$

Now consider the region where $w \approx w'\tau$ that is the computer generated frequency is approximately the signal frequency. Then the term

$$\left(\frac{w'\tau}{w} - 1 \right) << 1$$

and the summation can be approximated by an integral

$$C(w) = \frac{1}{w'\tau} \int_o^{fT} \left\{ - \cos \left[w_o\tau - \left(\frac{w'\tau}{w} - 1 \right) (2n+1)\pi \right] \right.$$

$$\left. - \cos \left[w_o\tau - \left(\frac{w'\tau}{w} - 1 \right) 2n\pi \right] \right\} dn$$

APPENDIX A

$$= \frac{-1}{w'\tau}\left\{ \frac{\sin\left[-\left(\frac{w'\tau}{w} - 1\right)(2fT + 1)\pi + w_o\tau\right] - \sin\left[-\left(\frac{w'\tau}{w} - 1\right)\pi + w_o\tau\right]}{-2\pi\,\frac{w'\tau}{w} - 1} \right.$$

$$\left. + \frac{\sin\left[-\left(\frac{w'\tau}{w} - 1\right)2\pi fT + w_o\tau\right] - \sin w_o\tau}{-2\pi\left(\frac{w'\tau}{w} - 1\right)} \right\}$$

Further consider the case where $fT \gg 1$. That is where the time interval [o, T] contains many cycles. Then the first and third terms are approximately equal as are the second and fourth. Thus

$$C(w) = \frac{1}{2w'\,w}\;\frac{\sin\left[(w - w'\tau)T + w_o\tau\right] - \sin w_o\tau}{w - w'\tau}$$

APPENDIX A

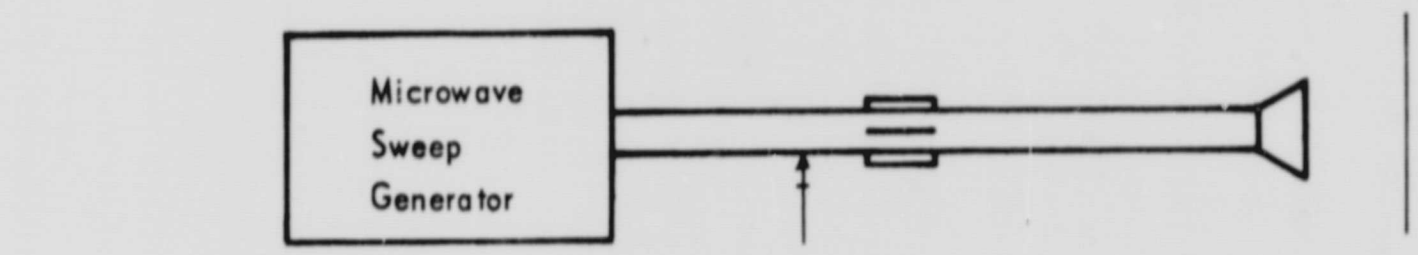

TRANSMITTED SIGNAL:

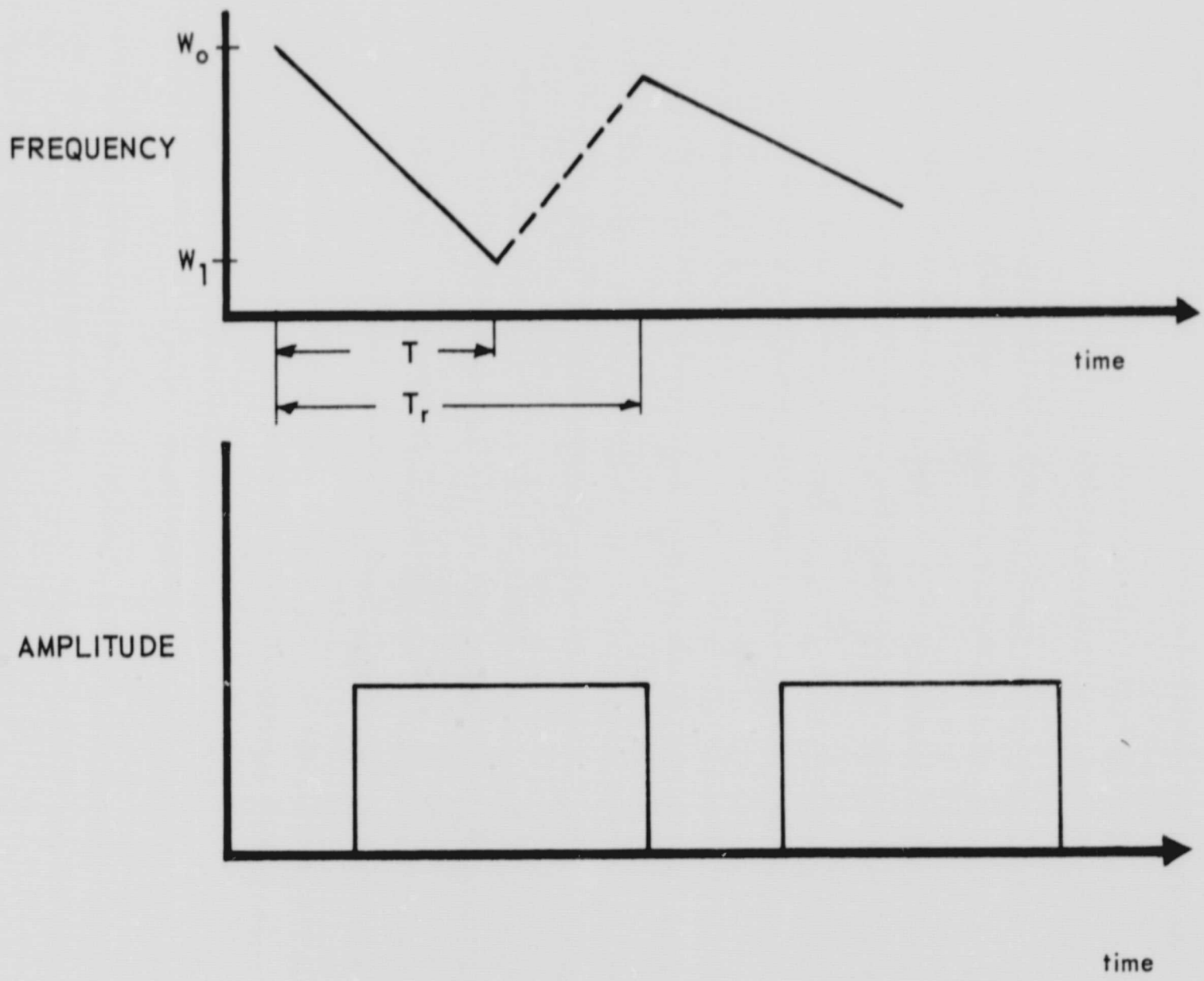

Basic FM Technique

Figure 1

APPENDIX A

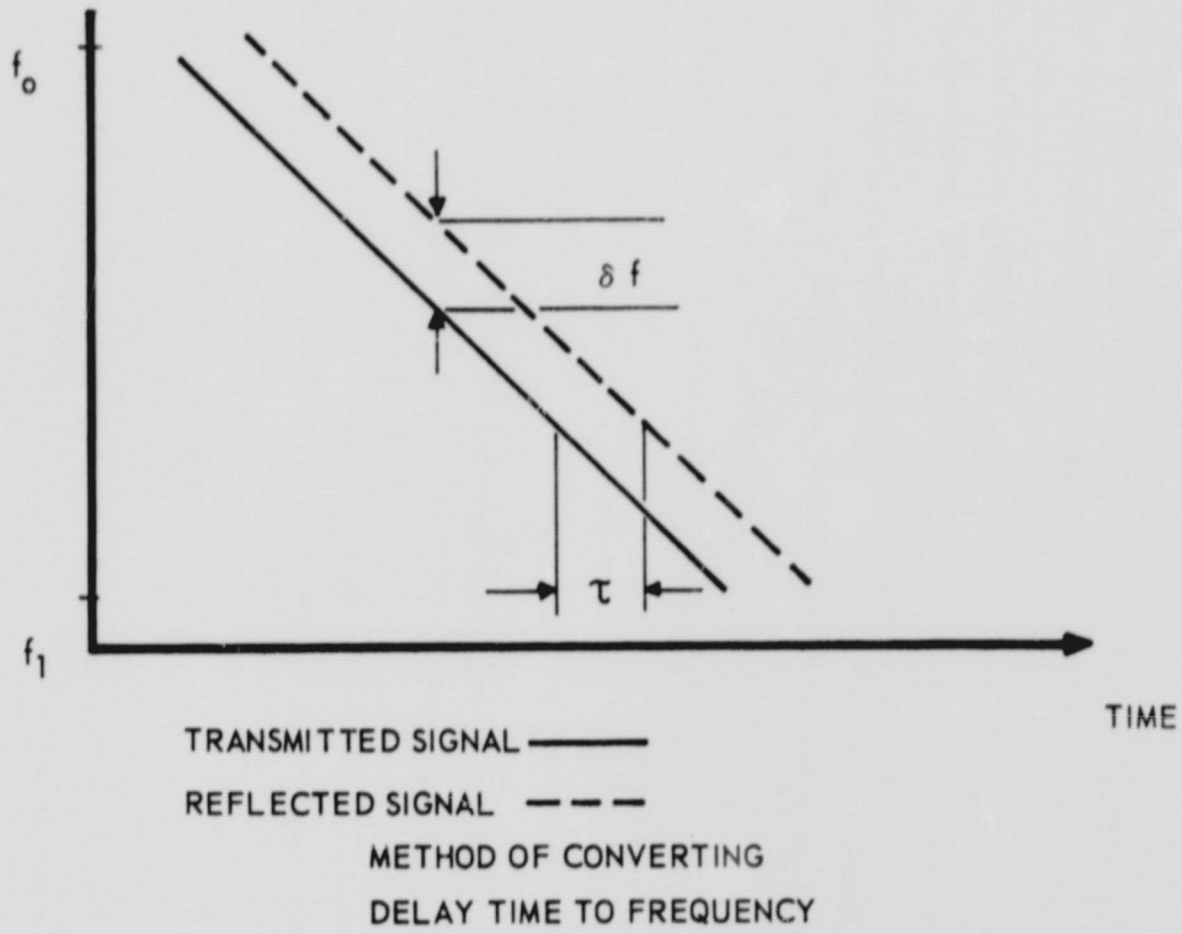

Method of Converting Delay Time to Frequency

Figure 2

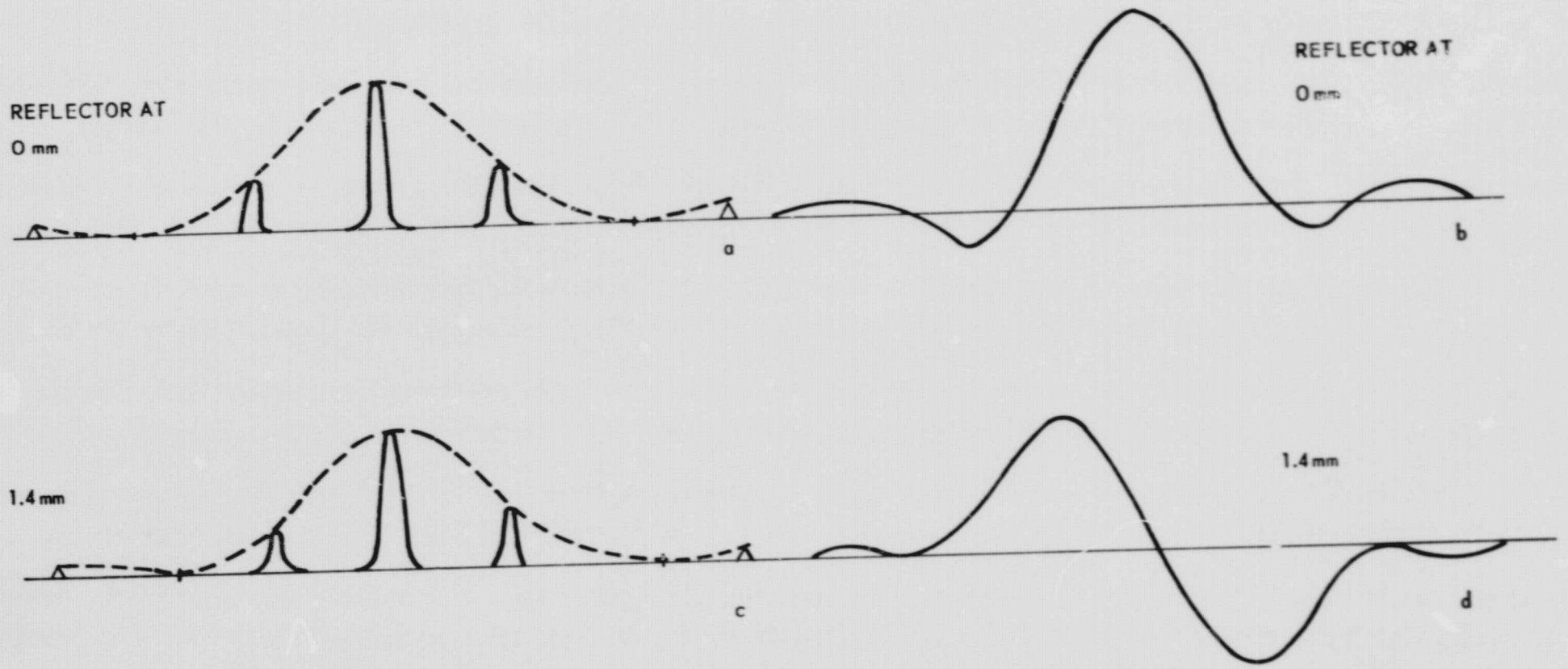

Figure 3

Spectrum Analyzer

APPENDIX A

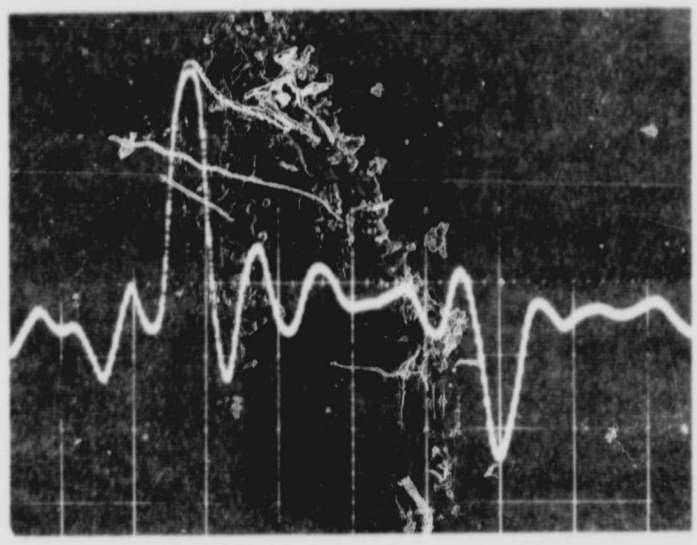

a. FRONT AND BACK REFLECTION OF 2 IN. AT PLEXIGLAS IN Ku BAND

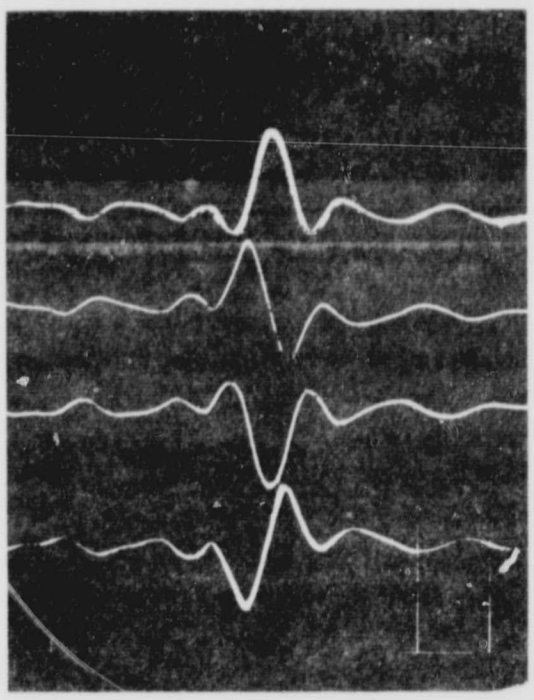

b. DISPLAY WITH PHASE CONTROL ROTATED IN 90° INCREMENTS

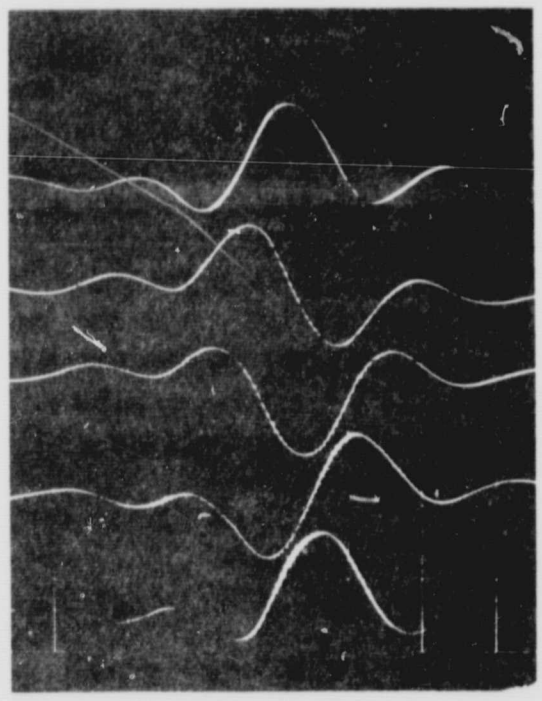

c. DISPLAY WITH REFLECTOR MOVED IN 2.7 mm INCREMENTS

Typical Displays

Figure 4